TENMAK BOR ARAŞTIRMA ENSTİTÜSÜ
TENMAK BORON RESEARCH INSTITUTE

ISSN: 2149-9020
e-ISSN: 2667-8438

BOR DERGİSİ
JOURNAL OF BORON

CİLT/VOL 06 | SAYI/ISSUE 03 | YIL/YEAR 2021

boren

ISSN: 2149-9020
e-ISSN: 2667-8438

BOR DERGİSİ
JOURNAL OF BORON

CİLT VOL **06** **SAYI** ISSUE **03** **YIL** YEAR **2021**

Türkiye Enerji Nükleer Maden Araştırma Kurumu (TENMAK) Adına İmtiyaz Sahibi
Owner on Behalf of TENMAK
Başkan/President
Dr. Abdulkadir Balıkçı

Baş Editör/Editor in Chief
Dr. Zafer Evis (Ankara, Türkiye)

Editörler/Editors
Dr. Abdulkerim Yörükoğlu (Ankara, Türkiye)
Dr. Fatih Akkurt (Ankara, Türkiye)
Dr. Sedat Sürdem (Ankara, Türkiye)

Sorumlu Yazı İşleri Müdürü
Manager of Publication
Dr. Sedat Sürdem
Ar-Ge Uzmanı
e-mail: sedat.surdem@tenmak.gov.tr

Editoryal Teknik Personel/Editorial Technical Staff
Dr. Abdulkadir Solak
Sema Akbaba
Sinem Erdemir Guran

Yayıncı/Publisher
TENMAK Bor Araştırma Enstitüsü (BOREN)

Yayın İdare Adresi/Adress of Publication Manager
Dumlupınar Bulvarı (Eskişehir Yolu 7. km), No:166, D Blok,
06530, Ankara, Türkiye
Tel: (0312) 201 36 00
Fax: (0312) 219 80 55
boren.journal@tenmak.gov.tr
https://dergipark.org.tr/boron

Yayın Türü/Type of Publication: Yaygın süreli yayın
Yayın Aralığı/Range of Publication: 3 Aylık
Basım Tarihi/Publication Date: 30/09/2021

Bor Dergisi uluslararası hakemli bir dergidir. Dergi, ULAKBİM TR Dizin ve Google Scholar tarafından indekslenmekte olup yılda dört defa yayımlanmaktadır. Derginin yazım kılavuzuna, telif hakkı devir formuna ve yayınlanan makalelere https://dergipark.org.tr/boron adresinden ulaşılabilir. / Journal of Boron is International refereed journal. Journal of Boron is indexed by ULAKBIM TR Indexed and Google Scholar, published quarterly a year. Please visit the Journal website https://dergipark.org.tr/boron for writing rules, copyright form and published articles.

ANKARA
EYLÜL 2021 / SEPTEMBER 2021

BOR DERGİSİ
JOURNAL OF BORON
https://dergipark.org.tr/boron

İÇİNDEKİLER/CONTENTS

BORON 6(3), 316 - 325, 2021

BOR DERGİSİ
JOURNAL OF BORON
https://dergipark.org.tr/boron

Effect of geothermal water composition and pretreatment on the product water for boron-sensitive crops

Enver Güler[1*]

[1]**Atılım University, Faculty of Engineering, Department of Chemical Engineering, Ankara, 06836, Turkey**
ORCID orcid.org/0000-0001-9175-0920

ARTICLE INFO

Article History:
Received December 19, 2020
Accepted June 28, 2021
Available online September 30, 2021

Research Article

DOI: 10.30728/boron.843259

Keywords:
Boron
Boron-sensitive crops
Geothermal water
Irrigation water
Membrane filtration

ABSTRACT

The membrane filtration is an effective way to produce water for human consumption, industrial use, or irrigation purpose. In this study, a brackish water reverse osmosis (BWRO) membrane was practically investigated to obtain irrigation water from geothermal water. The quality of the produced water was analyzed to understand the potential in agricultural use for boron-sensitive crops. The effects of the feed solution composition and pretreatment by microfiltration were studied. Results showed that the ionic content was effective in reduction of permeate flux. However, the rejections of salt and silica did not change significantly by the change in the feed water composition and they were successfully removed from the geothermal water by more than 95% rejection. Pretreatment of the geothermal water with a microfiltration (MF) membrane having a pore-size of 0.8 µm provided higher flux than the one having a pore size of 5 µm. The higher rejections of boron were only achieved with increased pH in the pretreatment. The pH of 9.5 in the geothermal water provided a rejection of boron as 75% with a permeate boron concentration of 2.4 mg/L when 15 bar of operating pressure was employed. This level of boron concentration in the irrigation water was found to be allowable only for some boron resistant crops (e.g. beans, lettuce, onion) and semi-sensitive crops (e.g. sunflower, potato, tomato).

1. Introduction

Increasing demand related to agricultural production is directly proportional to living standards and global growth of population. This demand has been increased significantly specifically towards horticultural crops for a healthy lifestyle. Thus, the importance of irrigation water is felt deeply for arid and semi-arid areas where the water shortage is becoming an issue [1].

Irrigation water is vital for sustainable agriculture and should have some specific quality, such as lack of colloids, low salt content, and also low content of some trace elements like boron that may have severe adverse effects on horticultural productivity in the short and long term. This limits the direct use of natural water resources for irrigation purposes. Therefore, production of irrigation water or its treatment should be carefully performed to get rid of undesired contaminants.

In general, to obtain stream waters that can be directly used for irrigation is quite challenging in most of the areas in the world. Thus, brackish water becomes one of the most abundant supplies of irrigation water. Nevertheless, its treatment for irrigation is comparatively new in agriculture. The utilization of geothermal water as brackish water has taken excessive attention recently [2-6]. The mineral content of those resources may vary widely from 1 g/L up to 200 g/L, which limits their direct use [7]. In the past, there have been several methodologies applied for the treatment and production of irrigation water from geothermal water. Most are task-specific techniques focusing on removal of particular species [5]. For instance, some include reverse osmosis (RO) and evaporation (for removal of dissolved solids [8]), oxidation and precipitation (for arsenic removal [9,10]), ion exchange (especially for boron removal/recovery [11-13]) and desilication by cooling ponds and soda ash (silica removal by soda ash or lime [14,15]). In addition, some integrated processes have been developed combining both ion exchange and membrane filtration for removal of boron and arsenic [16,17]. Each method has its own advantage considering the specific objective they have. However, RO, widely-used membrane process, have recently gained lots of attention due to the recently

*Corresponding author: enver.guler@atilim.edu.tr

developed, cost-effective membranes and continuous mode of operations in both single and hybrid processes. Therefore, as an energy-efficient and easy to scale-up technology, the membrane processes such as RO are quite promising to provide product water with desired quality.

RO is the most widely studied membrane technology among all other alternatives [18,19]. Although up-to-date RO membranes now can provide more than 99% of ionic rejection, retention of small and uncharged species is still a concern. At low pH values (lower than the dissociation constant of boron, pKa of 9.2), boron remains as very small uncharged species in aqueous media [20-24]. Thus, RO membranes perform less well and elevated pH is usually required in industrial desalination which is often limited by inorganic scaling (due to precipitation of calcium and magnesium compounds) as well. Moreover, when it is realized that the maximum allowable limit of boron in irrigation water is as low as 1 mg/L, boron removal turns into a great challenge [25].

It is known that boron is a vital element for plant growth. The deficiency of boron in plants directly affects the stem and root systems and reduces metabolic activities. On the other hand, high boron concentrations cause toxicity presenting some signs especially in leaves such as discoloring and distortion [4]. The tolerance of crops usually varies up to 4 mg/L in irrigation water. Thus, available data on boron tolerances are recommended to be referenced when the use of irrigation water is the case for boron-sensitive crops. It is realized that most of the crops that have commercial value and also the ones required for a healthy lifestyle has some certain level of boron sensitivity. Very sensitive crops are citrus plants and some others like walnut, apple, and cherry, and can tolerate only up to 1 mg/L of boron in irrigation water. On the other hand, some crops have high resistance towards boron content in irrigation water (up to 4 mg/L) such as beans, carrot, lettuce, and onion. Semi-sensitive crops which can tolerate 2 mg/L of boron concentration can be referred as sunflower, potato, tomato, wheat and corn.

One other issue on top of high boron content is the silica-containing water sources when it is considered for irrigation purposes. As silicon is very abundant element in the earth's crust, natural water sources usually contain silicon up to 40 mg/L, even in some terrestrial regions its concentration can extent up to 100 mg/L [26-30]. The concentration of silica (SiO_2) and its removal trend should be carefully monitored in RO systems. Hence, its concentration certainly affects the removal performance of boron as well. A certain level of silica naturally found in water streams such as in geothermal water may cause deposits or metal combinations on membrane surface. This is later inducted into silica fouling which is very difficult to remove. The existence of divalent cations such as calcium and magnesium promotes the precipitation of silica [31]. Silica fouling on RO membranes then results in significant flux decline reducing the water production capacity [32]. Therefore, not only the solution chemistry but also pretreatment or certain silica mitigation techniques should be realized before RO implementation.

In this work, the potential of a geothermal water source to be utilized for irrigation of boron-sensitive crops has been investigated. As operation parameters, the impacts of feed solution composition and pretreatment with microfiltration (MF) on the performance of a flat-sheet RO membrane were studied for removal efficiency of boron and silica by a commercial BWRO membrane.

2. Materials and Methods

2.1. Materials and Chemicals

2.1.1. BWRO membrane

The BWRO membrane commercialized by GE Osmonics is selected in this work due to high level of salt rejection properties. It is a thin-film polyamide-based membrane and represents a standard type of BWRO membrane in the industry. Specifications of the BWRO membrane employed were shown in Table 1.

Table 1. Specifications of the BWRO membrane [33].

Parameter	Specification
Manufacturer	GE Osmonics
Material	Thin Film Material
Typical Operating Pressure	1.379 kPa
Typical Operating Flux	15-35 LMH
Maximum Operating Pressure	3.103 kPa
Maximum Operating Temperature	50°C
Operating Range pH	4.0-11
Maximum Pressure Drop Over an element	83 kPa
Chlorine Tolerance	1,000 + mg/L-hours
Feed water	NTU< 1, SDI< 5
Salt rejection minimum (NaCl)[1,2]	98.5%

[1]Average salt rejection after 24 h operation
[2]Testing conditions: 2,000 mg/L NaCl solution at 1.551 kPa operating pressure, 25°C, pH 7.5 and 15% recovery.

2.1.2. MF membranes

For pre-filtration of geothermal water, MF membranes with 5 and 0.8 µm of pore sizes (Millipore Durapore, USA) were used in lab-scale flask type (vacuum-assisted) filtration unit. MF membranes do not have specific selectivity or affinity towards boron, silica and any other species naturally found in geothermal waters.

Filtration is merely based on size exclusion. Specifications of MF membranes are shown in Table 2.

Table 2. Specifications of MF membranes.

Parameter	5 µm pore size	0.8 µm pore size
Wettability	Hydrophilic	Hydrophilic
Filter Diameter, mm	47	47
Water Flow Rate, mL/min cm²	190	190
Maximum Operating Temperature, °C	85	75

2.1.3. Chemicals

Determination of boron content in samples is performed by spectrophotometric Azomethine-H method. The chemicals used in this analytical method are Azomethine-H monosodium salt hydrate ($C_{17}H_{12}NNaO_8S_2$, Fluka), ascorbic acid (99%, Acros Organics), ethylenediamine tetraacetic acid disodium salt dehydrate (EDTA, AnalaR, analytical grade), ammonium acetate (CH_3COONH_4, Merck) and acetic acid (CH_3COOH, 99-100%, Merck). Boric acid (H_3BO_3, 99.8 %, Merck) and ultrapure water (Milli-Q) were used to prepare the standard solutions.

2.2. Membrane Filtration Test System and Related Tests

A lab-scale flat sheet membrane test unit (SEPA CF II GE Osmonics) has been employed for the filtration of the geothermal water. It allows the pre-simulation of industrial-scale membrane units. This cross-flow system is comprised of a membrane filtration cell equipped with a hydraulic assembly, high-pressure pump, and a feed tank. The pressure is controlled by a needle valve on the concentrate line and is measured by a manometer as a pressure indicator (PI). Figure 1 depicts the RO system employed.

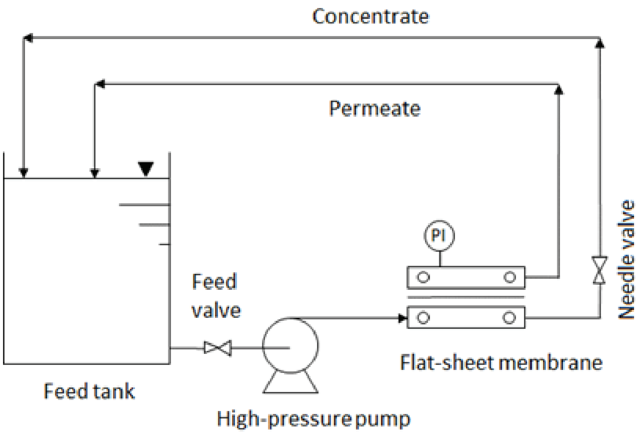

Figure 1. A representation diagram of the cross-flow flat-sheet membrane test system.

Before the RO operation, the membrane was immersed in the Milli-Q quality ultrapure water overnight. The membrane filtration was continued for 8 h. For each half an hour, flow rates, temperature, and total dissolved solids (TDS) were recorded, and samples were taken for the analyses of boron and silica at each one hour and two hours, respectively. In all tests, permeate and concentrate streams were re-circulated to the feed tank to maintain the feed content and volume constant to some extent.

2.3. Vacuum-Assisted MF System as Pretreatment

For pretreatment before the RO filtration of the geothermal water, a vacuum-assisted MF system was employed. A pressure/vacuum pump (Pall Life Sciences, USA) was used together with a glass-filter funnel (300 mL in capacity) where the geothermal water was fed. A flask with a capacity of 1 L was attached to a funnel where the filtrate was collected. The attachment was done with an aluminum clamp. Active filtration area was 9.6 cm² that can be provided by 47 mm-in-diameter filter.

2.4. Analytical Measurements

A portable conductivity meter (Mettler Toledo, Switzerland) was used to measure TDS, conductivity, salinity, and temperature of water samples. A digital pH meter (WTW pH 315i/SET, Germany) was used for pH measurements.

A spectrophotometer (JASCO V-530 UV/VIS, Japan) was used for spectrophotometric boron analysis by Azomethine-H method. Analyses of silica concentrations were performed by Spectroquant Nova 60 (Germany) test kit using a spectrophotometer.

2.5. Solute Rejection and Flux Calculations

2.5.1. Salt rejection

Solute rejection, i.e. salt rejection, is defined as the ratio of solute (i.e. salt referred to as TDS in this work) that remains in the concentrate stream over the solute content in feed:

$$SR = \left(1 - \frac{C_p}{C_f}\right) \times 100 \quad (1)$$

In Eq. 2, SR is salt rejection in percent, C_p and C_f are solute concentrations (TDS) in permeate and feed side in mg/L, respectively. Boron and silica rejections are calculated in the same fashion using the concentrations that are analytically determined [34].

2.5.2. Permeate Flux

Permeate flux (J) is calculated to observe any possible changes in filtration capacity of membranes. It is defined as volumetric flow per unit area [35]. Where V_p is the permeate volume, A_m is the membrane area used for filtration and t is the filtration time.

$$J = \frac{v_p}{A_m \cdot t} \quad (2)$$

2.6. Parameters Affecting the Performance of RO Membrane

2.6.1. Effect of the composition of the geothermal water

Two different geothermal water samples, namely Sample-A and Sample-B, having different specifications were used as feed solution in the membrane filtration tests (Table 3). Ion content of sample waters was given in Table 4. Only major species were provided in tables eliminating the other trace ions that are naturally present. Cations were determined by atomic absorption spectroscopy (AAS), and anions were determined by ion chromatography (IC) except bicarbonate ion measured by titrimetric method. Boron and silica were measured by Azomethine-H and colorimetric methods, respectively. To protect the filtration system and membranes from the adverse fouling/scaling effects of natural geothermal water, filtration with a rough filter paper was employed. Then, using BWRO membrane, cross-flow RO filtration was performed at 15 bar providing an 800 mL/min of feed flow.

Table 3. Characteristics of geothermal waters with different compositions.

Parameters	Sample-A	Sample-B
pH	8.60	8.50
Conductivity (µS/cm)	1770	1854
TDS (mg/L)	885	926
Salinity (‰)	0.700	0.930
Turbidity (NTU)	0.150	0.640
Si (mg/L)	56.0-65.0	65.0-72.0
B (mg/L)	10.3-11.0	10.2-10.9

2.6.2. Effect of MF pretreatment

To investigate the effect of pretreatment with MF, two different MF membranes were employed with 5 and 0.8 µm of pore-sizes for coarse and fine filtrations, respectively. After that, RO filtration with BWRO membrane was performed at 15 bar using 800 mL/min of geothermal water as feed flow rate. For these set of experiments, the geothermal water named as Sample-B, which has higher TDS than Sample-A, was used at its natural pH (8.5). Later, adjusted pH of 9.5 to realize the pH effect on microfiltration pretreatment was investigated for Sample-B as well. Vacuum-assistant filtration set up was used to investigate the effect of MF pretreatment.

Table 4. Ion content (mg/L) of geothermal water samples.

Parameters	Sample-A	Sample-B
Na^+	366	364
K^+	26.3	34.1
Ca^{2+}	26.2	12.1
Mg^{2+}	3.70	1.11
Cl^-	188	160
SO_4^{2-}	109	185
F^-	4.45	2.55
HCO_3^-	622	635

3. Results and Discussion

3.1. Effect of feed water characteristics on RO performance

Feed water specification is certainly a vital factor that affects the performance of the RO process. To investigate this impact, two different geothermal waters with different characteristics were selected. Tables 3 and 4 provide the brief data about these geothermal water sources that were filtered with a simple filter paper prior to RO filtration. Flux of the product water (permeate), rejections of boron and silica are calculated using a flat-sheet brackish water RO membrane. The applied pressure was 15 bar.

Permeate flux values calculated by Eq. 2 were calculated for two natural geothermal water samples during 8 h of the filtration test. Although pH of both samples was almost identical, their ionic compositions were different.

The similar trend of permeate fluxes was observed for both types of feed waters although the levels were different (Figure 2). It was possible to obtain a higher flux when Sample-A was used as feed. Although the presence of divalent cations in Sample-A is higher and

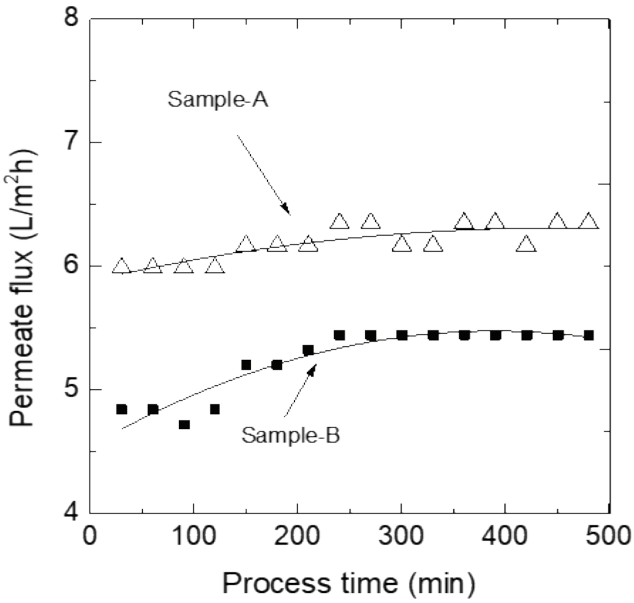

Figure 2. Impact of feed water characteristics on permeate flux.

elevation of membrane scaling might be expected to rise, it was not an issue that affects the permeate flux. There is another hypothesis that these divalent ions contribute to neutralization of the membrane charge density and allow the rapid deposition of macromolecules which reduces the permeate flux through the membrane [36]. However, it was not the case either. The lower flux of Sample-B can only be attributed to the higher level of TDS (or high conductivity). Silica in Sample-B was also higher. Thus, total hardness (calcium and magnesium) might promote the deposition of silica on the membrane surface [37]. Therefore, silica fouling has great potential to be the basis to obtain lower levels of permeate flux.

In Figure 3, influence of feed water characteristics on salt, boron, and silica rejections was shown. Satisfying rejection levels of more than 95% for both feed samples were obtained for salt and silica. Nevertheless, the rejections of boron were lower (around 50%). This was due to the relatively low pH of geothermal water samples at their natural state (Table 3). The acid dissociation constant of boric acid (pKa) is around 9.2 and higher pH levels can contribute to the existence of charged boron species and thus their retentions by membranes become easier. Boron at pH 8 in groundwater is mostly found in the form of boric acid ($B(OH)_3$). It is a small, polar and uncharged molecule like water molecule. Elevation of pH above pKa promoted the transformation of boric acid to its negatively charged form, so-called borate ($B(OH)_4^-$). Since most RO membranes today rely on charge and size based retention mechanisms to remove undesired species, increasing pH levels can certainly provide borate rejections as high as 99% [21,23,38].

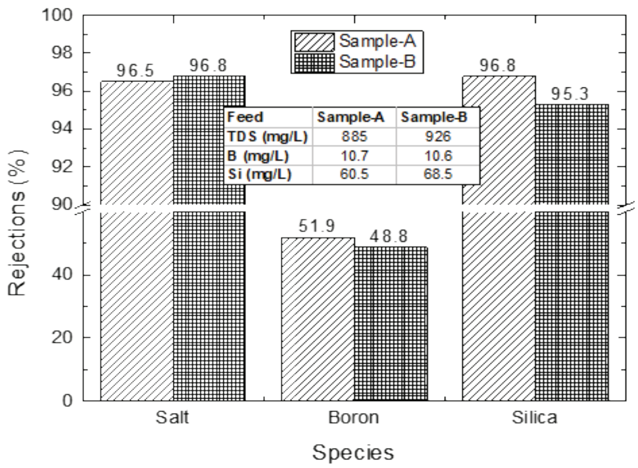

Figure 3. Impact of feed water characteristics on salt rejection.

Although the rejection values had minor differences when using two different geothermal water samples, it was observed that permeate of Sample-B had higher TDS value than that of Sample-A (Figure 4). The permeate TDS at the end of the operation was found as 35.3 mg/L from the geothermal water having TDS of 926 mg/L (Sample-B). For Sample-A, the permeate TDS was found as 30.9 mg/L from the geothermal water containing TDS of 885 mg/L. This shows that high TDS in the feed increases the dissolved solute level in permeate.

Even though the boron rejection for Sample-A was slightly higher than that for Sample-B, this difference did not contribute to a significant difference in the boron levels of the permeate samples at the end of operation. Boron concentrations in permeates of Sample-A and Sample-B were similar as 5.2 and 5.5, respectively (Figure 4).

Comparable retention behavior of silica like boron was observed when using Sample-A and Sample-B as feed waters. Nevertheless, silica was removed at high levels as more than 95% due to being less reliant on pH, unlike boron (Figure 3). Thus, the silica concentrations in permeates of Sample-A and Sample-B were 2.2 and 2.6 mg/L, respectively (Figure 4).

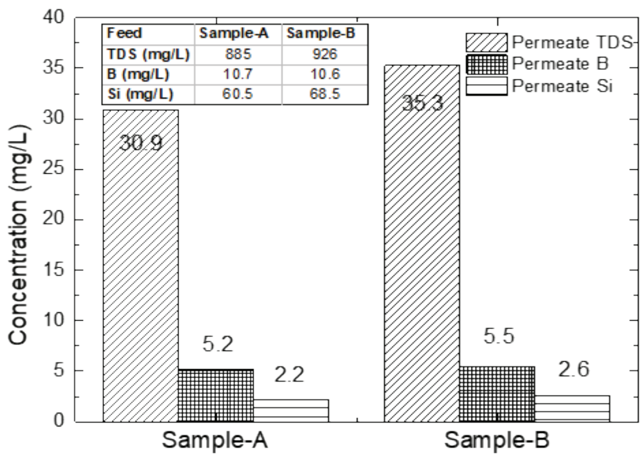

Figure 4. TDS, boron and silica concentrations in the RO permeates of different feeds at the end of operation.

Using RO membrane with 15 bar of filtration pressure provided permeates containing more than 5 mg/L of boron, which is not proper when considered as irrigation water for sensitive crops such as orange, lemon, apple, or grape. Standards for irrigation waters should be carefully checked when employing the RO permeate for agricultural irrigation because the level of boron is recommended as low as 1 mg/L in the irrigation water [25].

3.2. Effect of MF Pretreatment on RO Performance at Natural pH of Geothermal Water

MF is a physical pretreatment method of feed waters prior to the RO application. To investigate the effect of different filtration levels at natural pH of geothermal water, the feed geothermal water was filtered through *coarse* (5 µm pore size) and *fine* (0.8 µm pore size) MF membrane filters.

When the geothermal water was filtered by 0.8 µm of MF filter, the RO membranes provided higher permeate fluxes (Figure 5). An average of approximately 7 LMH of a stabilized permeate flux was obtained during RO run after a fine pre-filtration whereas the respective value was 6 LMH when a coarse pre-filtration was employed. The MF membrane was able to remove fine solids, silt, and some other particles. However, coarse filtration can be effective for removal of only coarser solids and suspended solids. Thus, those unrejected substances may deposit on the surface of the RO membrane, and reduce its efficiency resulting in a lower permeate flux. It was observed that the flux decline was not continuous during 480 min of operation. Yet there was a visible offset of flux levels between two RO tests due to coarse-and fine-filtered feeds prior to RO. It is also important to note that it took some time to level off the permeate flux for both feeds. This stabilization time was longer (up to 200 min) when the coarse filtered feed was used for the RO system (Figure 4). This is a characteristic behavior for most membranes, thus membranes were soaked in ultrapure water beforehand to reduce this time,

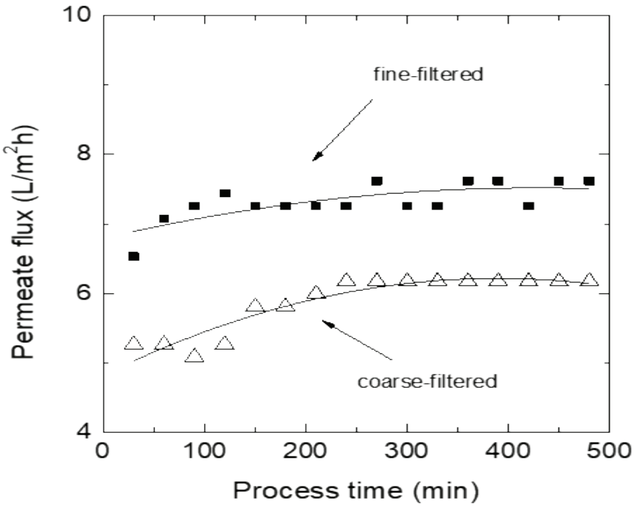

Figure 5. Effect of pre-filtration on permeate flux obtained by RO membrane at natural pH 8.5.

When salt, boron, and silica rejections were calculated, it was found that fine-filtered feeds provided higher retention of salt and silica by the RO membrane (Figure 6). This may be attributed to the high efficiency of RO membrane with reduced fouling materials using fine filtering with a smaller pore size (i.e. 0.8 µm). However, this behavior was reversed in the case of boron removal. Slightly lower boron removal was obtained for fine-filtered feed. This may possibly be due to the colloidal matter remained after coarse filtration, which may promote adsorption of boron compounds or agglomerations resulting in easier removal by RO [39,40]. It was also realized that boron removals were significantly lower than salt and silica rejections at natural pH of geothermal water. This shows that natural

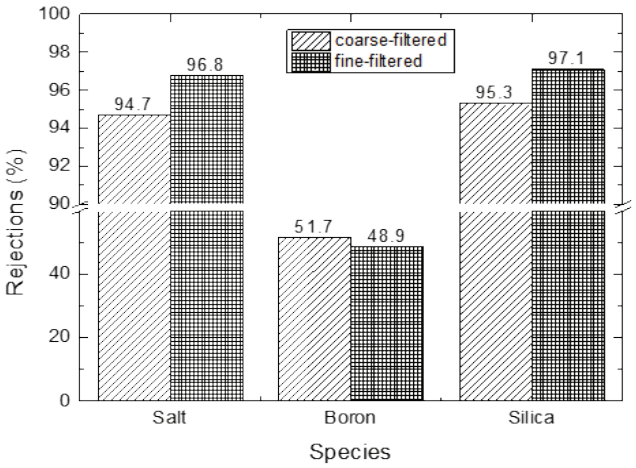

Figure 6. Effect of pre-filtration on salt, boron and silica rejections by RO membrane at pH 8.5.

pH 8.5 is low for efficient removal of boron.

Higher rejection levels of salt and silica for fine-filtered geothermal water provided lower concentrations of TDS and silica in the RO permeate samples as expected. In contrast, boron concentration in the RO permeate was higher for fine-filtered feed due to its lower rejection as indicated previously (Figure 7).

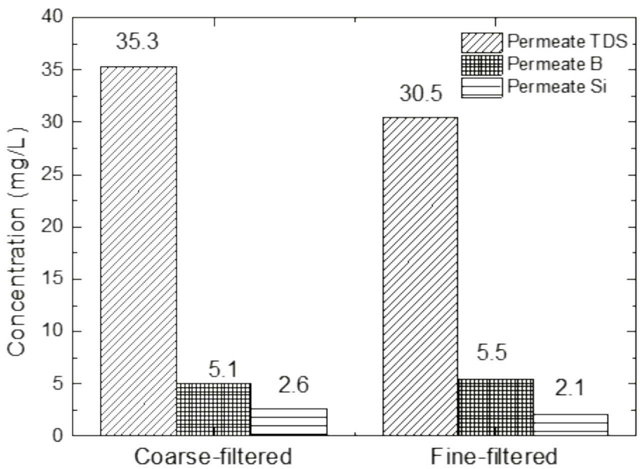

Figure 7. TDS, boron and silica concentrations of RO permeates at the end of RO operation using coarse-filtered and fine-filtered geothermal water samples at natural pH.

Boron concentrations in the range of 5.1-5.5 mg/L are already much higher for irrigation of horticultural crops with high boron sensitivity (Figure 6). On the other hand, these boron levels may be acceptable for boron resistant crops although 4 mg/L is recommended as the uppermost concentration in irrigation water. This result recalls again the necessity of some process design towards the enhancement of removal efficiencies such as integration of RO with hybrid systems such as adsorption with membrane filtration or an effective pH adjustment. Effects of those parameters were previously shown [41, 42].

3.3. Effect of MF Pretreatment on RO Performance at Adjusted pH 9.5

In certain cases, pH of the feed may be the issue in MF pretreatment before the RO operation. The pH of feed may vary or pH adjustment may be executed in some specific industrial RO systems. To better understand the effect of pH change before the MF pretreatment, NaOH solution was used to raise the pH of geothermal water (Sample-B) to 9.5. Then, the feed was filtered through *coarse* and *fine* MF membrane filters as discussed previously. After MF, cross-flow membrane set-up installed with BWRO membranes was operated at the same conditions (pressure: 15 bar; feed flow rate: 800 mL/min).

Both coarse-and fine-filtered feeds provided similar level of permeate flux of about 6 LMH on average (Figure 8). However, flux stabilization behaviors were different: coarse-filtered feed provided fluctuating flux over 8 h whereas fine-filtered feed provided conventional stabilization trend as previously described. Fluctuating random flux values during operation might be the indication of initial scaling or fouling because higher levels of pH promote the calcium and magnesium-based scaling. This will later become the reason for flux decline for the prolonged RO operations. Nevertheless, averaged flux values were relatively lower when compared to the ones with natural pH reported in Figure 5.

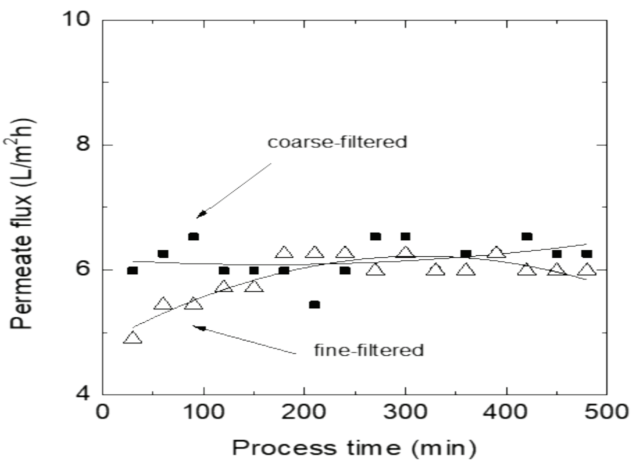

Figure 8. Impact of filtration on permeate flux at pH 9.5.

It is also worth noticing that significant flux decline was not observed for both cases during 8 h of operation. This shows that the scaling issue was not yet critical, but longer operation periods may be required to observe the high pH effect on permeate flux. It was realized that hardness and alkalinity are two vital indicators of scaling. As calcium represents most of the total hardness, its concentration has to be monitored in feed water. Calcium concentrations in the geothermal waters used in this work were low compared to the concentration level where scaling concentrations typically occur, i.e., 100 ppm hardness [43]. On the other hand, carbonate and hydroxide precipitations became pronounced at pH values of 9.3 and 10.5, respectively [44]. In this case, high pH in the feed waters might be an issue. Although the kinetics of carbonate precipitation is assumed to be instantaneous, its deposition on membrane surface did not become severe to affect permeate flux within 8 hours as seen in Figure 8.

Increasing pH to 9.5 did not change the range of salt and silica rejections compared to natural pH of geothermal water (Figure 9). Besides, coarse and fine filtrations provided very similar salt and silica rejections at pH 9.5. Scaling at elevated pH of 9.5 was not the issue affecting any change. However, boron rejections increased from 50% to more than 70% due to high pH dependency. Similar to the situation at natural pH, coarse-filtered feed delivered higher boron rejections compared to fine-filtration. This situation may be attributed to denser membrane surface due to particulate matter deposition that has potential for scaling, and boron-containing ionic compounds [45].

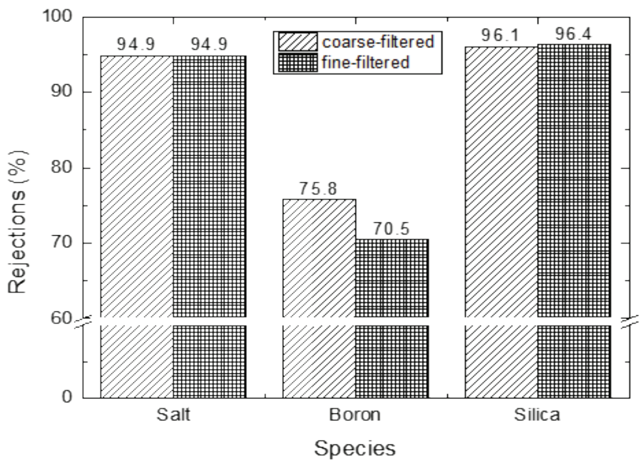

Figure 9. Effect of filtration on salt, boron and silica rejections at pH 9.5.

At pH 9.5, the RO membrane performed stable rejections throughout the study lasting for 8 h. Although salt and silica rejections were fairly in the same range, their concentrations in permeates obtained from both fine and coarse filtrated feeds were higher than the ones obtained at natural pH (Figure 10). Relatively high TDS in permeate was also a consequence of the NaOH added to the feed for pH adjustment. That means increasing pH slightly lowered membrane performance towards TDS and silica removals. The MF pretreatment can only help as mitigation of scaling factors to some extent, especially at elevated pH of feed waters. It was also good to realize that coarse filtration provided slightly better silica rejections thus lower permeate silica concentrations in permeate. This may be due the fact that silica probably polymerizes easily at the existence of Mg^{2+} and Ca^{2+} ions, thus not primarily removed by coarse filtration but subsequently better removed by the RO membrane afterward [31].

On the other hand, increasing pH increased boron removals resulting in lower boron concentrations in permeates (Figure 10). It was possible to obtain boron concentrations as low as 2.4 mg/L. When irrigation water standards are considered, this concentration is still high but resistant or even some semi-sensitive crops can tolerate this level of boron. Conversely, the RO process should be developed further to produce appropriate irrigation water for sensitive crops at this stage. Increasing pH higher than 9.5 or implementation of hybrid processes (e.g. adsorption-membrane filtration systems) could help to provide lower boron concentrations [41,46,47].

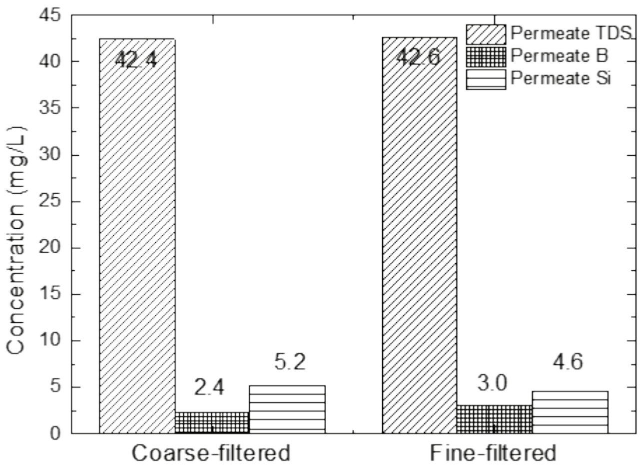

Figure 10. TDS, boron and silica concentrations of RO permeates at the end of operation using coarse-filtered and micro-filtered geothermal water samples at pH 9.5.

4. Conclusions

The performance of a flat-sheet BWRO membrane to produce irrigation water from geothermal water for boron-sensitive crops has been investigated by analyzing the impacts of feed solution composition and MF pretreatment. The results showed that relatively high levels of TDS and silica in the feed was effective in lowering the permeate flux. The BWRO membrane was successful in retaining salt and silica but not boron at natural pH. Also, different salt contents of the feeds used in this work did not change the boron concentrations in permeates significantly. It was also seen that choice of MF pretreatment filters is crucial. The choice of a smaller average pore size of 0.8 µm (i.e. *fine* filtration) in the pretreatment promoted higher permeate flux in the RO membrane, and also higher rejections of salt and silica although boron rejection was not affected by the pore size of MF membrane. On the other hand, at elevated pH of 9.5, *coarse* filtration (with 5 µm pore size) provided improved rejections of boron resulting in 2.4 mg/L boron concentration in the RO permeate. The results suggest that the current experimental set-up operating at 15 bar with BWRO membrane can provide irrigation water for semi-sensitive and resistant crops only. Nevertheless, there is still room for the development of advanced RO processes either with hybrid assembly containing adsorption systems or with optimized process conditions.

Acknowledgment

The author is grateful to Prof. Dr. Nalan Kabay, Ege University for her valuable help to use the laboratory facilities and run the membrane tests. Furthermore, the author would like to acknowledge Izmir Geothermal Energy Co. for providing geothermal water samples.

References

[1] Lew, B., Tarnapolski, O., Afgin, Y., Portal, Y., Ignat, T., Yudachev, V. & Bick, A. (2020). Irrigation with permeates to upgrade the quality of red pepper: a case study in Arava region, Israel. *Environmental Technology*, 1-11.

[2] Samatya, S., Köseoğlu, P., Kabay, N., Tuncel, A. & Yüksel, M. (2015). Utilization of geothermal water as irrigation water after boron removal by monodisperse nanoporous polymers containing NMDG in sorption-ultrafiltration hybrid process. *Desalination, 364*, 62-67.

[3] Koseoglu, H., Harman, B. I. I., Yigit, N. O. O., Guler, E., Kabay, N. & Kitis, M. (2010). The effects of operating conditions on boron removal from geothermal waters by membrane processes. *Desalination, 258*(1-3), 72-78.

[4] Yilmaz, A. E., Boncukcuoğlu, R., Kocakerim, M. M., Yilmaz, M. T. & Paluluoğlu, C. (2008). Boron removal from geothermal waters by electrocoagulation. *Journal of Hazardous Materials, 153*(1-2), 146-151.

[5] Gallup, D. L. (2007). Treatment of geothermal waters for production of industrial, agricultural or drinking water. *Geothermics, 36*(5), 473-483.

[6] Öner, Ş. G., Kabay, N., Güler, E., Kitiş, M. & Yüksel, M. (2011). A comparative study for the removal of boron and silica from geothermal water by cross-flow flat sheet reverse osmosis method. *Desalination, 283*, 10-15.

[7] Tomaszewska, B. & Szczepański, A. (2014). Possibilities for the efficient utilisation of spent geothermal waters. *Environmental Science and Pollution Research, 21*(19), 11409-11417.

[8] Bourcier, W., Ralph, W., Johnson, M., Bruton, C. & Gutierrez, P. (2006). Silica Extraction at Mammoth Lakes, California. *International Mineral Extraction from Geothermal Brine Conference*, Tiscon AZ, US, 1-6.

[9] Simmons, M., Gallup, D. & Harden, D. (2002). Photo-oxidation, removal and stabilization of arsenic residuals in drinking water, wastewater and process water systems. *Trends in Geochemistry, 2*, 73-84.

[10] Yoshizuka, K., Kabay, N., & Bryjak, M. (2016). Arsenic and boron in geothermal water and their removal, *The Global Arsenic Problem* (pp. 131-148). CRC Press.

[11] Recepoğlu, O. & Beker, Ü. (1991). A preliminary study on boron removal from Kizildere/Turkey geothermal

waste water. *Geothermics, 20*(1-2), 83-89.

[12] Gallup, D. L. (1995). Agricultural uses of excess steam condensate: Salton Sea geothermal field. *Geothermal Science and Technology, 4*(3), 175-187.

[13] Badruk, M., Kabay, N., Demircioglu, M., Mordogan, H. & Ipekoglu, U. (1999). Removal of boron from wastewater of geothermal power plant by selective ion-exchange resins. I. Batch sorption-elution studies. *Separation Science and Technology, 34*(13), 2553-2567.

[14] Gallup, D. K. & Glanzman, R. K. (2003). Method for synthesizing crystalline magnesium silicates from geothermal brine (U.S. Patent No. US6761865B1). U.S. Patent and Trademark Office.

[15] Gallup, D. L., Sugiaman, F., Capuno, V. & Manceau, A. (2003). Laboratory investigation of silica removal from geothermal brines to control silica scaling and produce usable silicates. *Applied Geochemistry, 18*(10), 1597-1612.

[16] Yanar, P. (2015). *Investigation the lithium, boron and arsenic levels in Aegean region geothermal waters and selective seperation of these elements* [M.Sc. thesis, Ege University] Council of Higher Education Thesis Center (Thesis Number 405320).

[17] Kabay, N., Yilmaz-Ipek, I., Soroko, I., Makowski, M., Kirmizisakal, O., Yag, S., Bryjak, M. & Yuksel, M. (2009). Removal of boron from Balcova geothermal water by ion exchange-microfiltration hybrid process. *Desalination, 241*(1-3), 167-173.

[18] Bick, A., Gillerman, L., Manor, Y. & Oron, G. (2012). Economic Assessment of an Integrated Membrane System for Secondary Effluent Polishing for Unrestricted Reuse. *Water, 4*(1), 219-236.

[19] Ozturk, O. F., Shukla, M. K., Stringam, B., Picchioni, G. A. & Gard, C. (2018). Irrigation with brackish water changes evapotranspiration, growth and ion uptake of halophytes. *Agricultural Water Management, 195*, 142-153.

[20] Teychene, B., Collet, G., Gallard, H. &Croue, J. P. (2013). A comparative study of boron and arsenic (III) rejection from brackish water by reverse osmosis membranes. *Desalination, 310*, 109-114.

[21] Jung, B., Kim, C. Y., Jiao, S., Rao, U., Dudchenko, A. V., Tester, J. & Jassby, D. (2020). Enhancing boron rejection on electrically conducting reverse osmosis membranes through local electrochemical pH modification. *Desalination, 476*, 114212.

[22] Oo, M. H. & Ong, S. L. (2012). Boron removal and zeta potential of RO membranes: impact of pH and salinity. *Desalination and Water Treatment, 39*, 83-87.

[23] Oo, M. H. & Song, L. (2009). Effect of pH and ionic strength on boron removal by RO membranes. *Desalination, 246*(1-3), 605-612.

[24] Ipek, I. Y., Guler, E., Kabay, N. &Yuksel, M. (2016). Removal of Boron from Water by Ion Exchange and Hybrid Processes. In *Ion Exchange and Solvent Extraction* (pp. 33-63). CRC Press.

[25] Al-Shammiri, M., Al-Saffar, A., Bohamad, S. &Ahmed, M. (2005). Waste water quality and reuse in irrigation in Kuwait using microfiltration technology in treatment. *Desalination, 185*(1-3), 213-225.

[26] Al-Rehaili, A. M. (2003). Comparative chemical clarification for silica removal from RO groundwater feed. *Desalination, 159*(1), 21-31.

[27] Gorzalski, A. S. & Coronell, O. (2014). Fouling of nanofiltration membranes in full-and bench-scale systems treating groundwater containing silica. *Journal of Membrane Science, 468*, 349-359.

[28] Sheikholeslami, R. & Bright, J. (2002). Silica and metals removal by pretreatment to prevent fouling of reverse osmosis membranes. *Desalination, 143*(3), 255-267.

[29] Neofotistou, E. & Demadis, K. D. (2004). Use of antiscalants for mitigation of silica (SiO2) fouling and deposition: Fundamentals and applications in desalination systems. *Desalination, 167*(1-3), 257-272.

[30] Ning, R. Y. (2003). Discussion of silica speciation, fouling, control and maximum reduction. *Desalination, 151*(1), 67-73.

[31] Park, Y. M., Yeon, K. M. & Park, C. (2020). Silica treatment technologies in reverse osmosis for industrial desalination: A review. *Environmental Engineering Research, 25*(6), 819-829.

[32] Piyadasa, C., Ridgway, H. F., Yeager, T. R., Stewart, M. B., Pelekani, C., Gray, S. R. & Orbell, J. D. (2017). The application of electromagnetic fields to the control of the scaling and biofouling of reverse osmosis membranes - A review. *Desalination, 418*, 9-34.

[33] *SUEZ eStore for Water Technologies & Solutions* (n.d.). Retrieved December 13, 2020, from https://estore.suezwatertechnologies.com/

[34] Singh, R. (2005). Hybrid Membrane System design and operation. *Hybrid Membrane Systems for Water Purification*. (pp-197-242), Elsevier.

[35] Mulder, M., & Mulder, J. (1996). Basic principles of membrane technology. Springer Science & Business Media.

[36] Wang, Y. N. & Tang, C. Y. (2011). Protein fouling of nanofiltration, reverse osmosis, and ultrafiltration membranes-The role of hydrodynamic conditions, solution chemistry, and membrane properties. *Journal of Membrane Science, 376*(1-2), 275-282.

[37] Koo, T., Lee, Y. J. & Sheikholeslami, R. (2001). Silica fouling and cleaning of reverse osmosis membranes. *Desalination, 139*(1-3), 43-56.

[38] Cengeloglu, Y., Arslan, G., Tor, A., Kocak, I. & Dursun, N. (2008). Removal of boron from water by using reverse osmosis. *Separation and Purification Technology, 64*(2), 141-146.

[39] Yilmaz, A. E., Boncukcuoğlu, R. & Kocakerim, M. M. (2007). A quantitative comparison between electrocoagulation and chemical coagulation for boron removal from boron-containing solution. *Journal of Hazardous*

Materials, 149(2), 475-481.

[40] Pokrovsky, O. S. & Schott, J. (2002). Iron colloids/organic matter associated transport of major and trace elements in small boreal rivers and their estuaries (NW Russia). *Chemical Geology, 190*(1-4), 141-179.

[41] Güler, E., Kabay, N., Yüksel, M., Yiğit, N. Ö., Kitiş, M. & Bryjak, M. (2011). Integrated solution for boron removal from seawater using RO process and sorption-membrane filtration hybrid method. *Journal of Membrane Science, 375*(1-2), 249-257.

[42] Kabay, N., Güler, E. & Bryjak, M. (2010). Boron in seawater and methods for its separation - A review. *Desalination, 261*(3), 212-217.

[43] Geothermal Communities (n. d.). *Chapter 4 - Chemistry of Thermal Fluids*, Retrieved December 13, 2020, from https://geothermalcommunities.eu/elearning/chapters

[44] Ayoub, G. M., Zayyat, R. M. & Al-Hindi, M. (2014). Precipitation softening: A pretreatment process for seawater desalination. *Environmental Science and Pollution Research, 21*(4), 2876-2887.

[45] Chen, B., Li, F. & Zhao, X. (2020). Boron removal with modified polyamide RO modules by cross-linked glutaric dialdehyde grafting. *Journal of Chemical Technology & Biotechnology, 96*, 465-473.

[46] Güler, E., Kabay, N., Yüksel, M., Yavuz, E. & Yüksel, Ü. (2011). A comparative study for boron removal from seawater by two types of polyamide thin film composite SWRO membranes. *Desalination, 273*(1), 81-84.

[47] Güler, E., Öner, Ş. G., Kabay, N. & Yüksel, M. (2019). Effect of operational parameters for boron removal from geothermal water by reverse osmosis (RO) membranes. *International Symposium on Boron-BORON2019*, 885-890.

boren

BOR DERGİSİ
JOURNAL OF BORON
https://dergipark.org.tr/boron

Kalsiyum floroborat sentezi, kinetik ve alev geciktirici özelliklerinin belirlenmesi

Metin Gürü[1], Gülden Güngör[2], Duygu Y. Aydın[3*], Çetin Çakanyıldırım[4]

[1]Gazi Üniversitesi, Mühendislik Fakültesi, Kimya Mühendisliği Bölümü, Ankara, 06570, Türkiye
ORCID orcid.org/0000-0002-7335-7583
[2]TENMAK Bor Araştırma Enstitüsü, Ankara, 06530, Türkiye ORCID orcid.org/0000-0003-1517-7821
[3]Malatya Turgut Özal Üniversitesi, Mühendislik ve Doğa Bilimleri Fakültesi, Biyomühendislik Bölümü, Malatya, 44210, Türkiye
ORCID orcid.org/0000-0003-0557-5279
[4]Hitit Üniversitesi, Mühendislik Fakültesi, Kimya Mühendisliği Bölümü, Çorum, 19030, Türkiye
ORCID orcid.org/0000-0001-7040-1369

MAKALE BİLGİSİ

Makale Geçmişi:
İlk gönderi 14 Şubat 2021
Kabul 28 Haziran 2021
Online 30 Eylül 2021

Araştırma Makalesi

DOI: 10.30728/boron.880116

Anahtar kelimeler:
Alev geciktirici
Floroborik asit
Kalsiyum floroborat
LOI

ÖZET

Bu çalışmada özel bor bileşiklerinden olan kalsiyum floroboratın sentez parametreleri belirlenmiş ve pamuklu kumaştaki alev geciktirici özelliği incelenmiştir. Ayrıca kinetik çalışmalar yapılarak reaksiyon mertebesi ve aktivasyon enerjisi hesaplanmıştır. Kalsiyum floroborat, reaktant olarak kalsiyum oksit ve floroborik asit kullanılarak yaş yöntemle sentezlenmiştir. İncelenen parametreler; reaktant mol oranı ($nCaO/nHBF_4$), sıcaklık ve reaksiyon süresidir. Karakterizasyon çalışmaları için FT-IR, XRD ve BF_4^- iyon seçici elektrot kullanılmıştır. Termal davranışın karakterize edilmesinde termogravimetrik-diferansiyel termal analiz (TG-DTA) kullanılmıştır. Kalsiyum floroborat, 1:4 reaktant mol oranı, 90°C sıcaklık ve 100 dakika reaksiyon süresinde %97 verimle sentezlenmiştir. Ayrıca yapılan kinetik çalışmada reaksiyonun birinci mertebeden olduğu belirlenmiş ve reaksiyonun aktivasyon enerjisi 19,14 kJ/mol olarak bulunmuştur. Sentezlenen kalsiyum floroboratın alev geciktirici özelliğini tespit etmek için LOI testinden yararlanılmıştır. Testler sonucunda kalsiyum floroboratın çok iyi alev geciktirici özellik gösterdiği gözlemlenmiştir.

Calcium fluoroborate synthesis, determination of kinetics and flame retardant properties

ARTICLE INFO

Article history:
Received February 14, 2021
Accepted June 28, 2021
Available online September 30, 2021

Research Article

DOI: 10.30728/boron.880116

Keywords:
Flame retardant
Calcium fluoroborate
Fluoroboric acid
LOI

ABSTRACT

In this study, the synthesis parameters of calcium fluoroborate, one of the special boron compounds, were determined and its flame retardant properties in cotton fabric were investigated. In addition, kinetic studies were carried out to calculate the reaction order and activation energy. Calcium fluoroborate was synthesized by wet method using calcium oxide and fluoroboric acid as reactants. The parameters examined were reactant mole ratio ($nCaO/nHBF_4$), temperature and reaction time. FT-IR, XRD and BF_4^- ion selective electrode were used for characterization studies. Thermogravimetric-differential thermal analysis (TG-DTA) was used to characterize the thermal behavior. Calcium fluoroborate was synthesized with 97% yield when molar ratio of reactants, temperature and reaction time are set as 1:4, 90°C and 100 minutes, respectively. In addition, kinetic experiments reveal that the reaction order obeys to first order kinetics and the activation energy was found as 19.14 kJ/mol. LOI tests were used to determine the flame retardant properties of synthesized calcium fluoroborate. Tests proved that the calcium fluoroborate has very good flame retardant properties.

1. Giriş (Introduction)

Dünyada ticari olarak üretilip değişik alanlarda kullanılan ve nihai ürün olarak sınıflandırılabilen birçok özel bor bileşiği mevcuttur. Bu bileşiklerin her biri farklı amaçlar için değişik sektörlerde kullanılmaktadır. Bu ürünlerden kullanım alanı en yaygın olanları; potasyum borhidrür, sodyum borhidrür, boranlar, susuz bo-

*Corresponding author: duygu.aydin@ozal.edu.tr

rik asit (bor oksit), metal borürler, disodyum oktaborat tetrahidrat, çinko borat, bor triklorür, bor karbür, ferrobor, bor fiberleri, metalik (elementel) bor ve bor nitrür olarak sıralanabilir [1]. Özel bor bileşiklerinden birisi olan floroboratlar, floroborik asidin tuzları olup ilk bilimsel çalışmalar Berzelius tarafından yapılmıştır [2]. Bu gruptaki bileşikler, alkali metal floroboratlar, amonyum floroborat ve geçiş element floroboratlarıdır [3]. Metal floroboratlar; floroborik asit ve metal tuzlarından veya borik asit ya da hidroflorik asidin metal tuzları ile reaksiyonundan elde edilir [4]. Ayrıca floroboratlar; metal florür ve elementel borun katı faz reaksiyonu ile elde edilebilmektedirler [5,6].

Floroboratlar endüstrinin çeşitli alanlarında farklı kullanım alanları bulmaktadırlar. Kalsiyum floroborat, nadir toprak elementleriyle birlikte camlarda kullanıldıklarında fiziksel parametreleri iyileştirirler ve devitrifikasyona karşı termal kararlılık sağlarlar [7-9]. Ayrıca lityum iyon pillerinde ve kalsiyum kaplamalarda elektrolit olarak kullanılmaktadırlar [10,11]. Metal floboratlardan biri olan çinko floroborat, çeşitli reaksiyonlarda katalizör olarak, tekstil endüstrisinde buruşmazlık apresi reçinelerinde kür kimyasalı olarak kullanılmaktadır [12-14]. Lityum floroborat, lityum sülfür pillerinde elektrolit olarak kullanılmaktadır. Lityum floroborat bazlı elektrolit kullanan Li-iyon hücresi neme karşı daha az duyarlıdır ve yüksek sıcaklıkta elektrolitte çok daha iyi performans göstermektedir [15]. Potasyum floroboratın elektrolizi ile yüksek saflıkta elementel bor elde edilebilmektedir [16]. Kalay floroborat, kaplamalarda kullanılmaktadır. Yüksek çözünürlüğü ve iyi elektrik iletkenliği sayesinde, yüksek akım yoğunluğu uygulanabilmektedir [17]. Floroborat banyoları, yüksek akım verimlilikleri olmasının yanında düşük gerilime sahip, katkı maddeleri gerektirmeyen ve safsızlıklara karşı çok az bir hassasiyet sağlayan katmanlar sağlamaktadırlar [18].

Diğer yandan floroboratlar malzemelerin alev direncini artırırlar. Floroboratlar; sentetik liflerde, polimerlerde [19] ve tekstil malzemelerinde [20-24] alev geciktirici olarak kullanılmaktadırlar. Alev geciktiricilerin kullanımı gün geçtikçe artmaktadır dolayısıyla yeni alev geciktiriciler geliştirmek önemli bir araştırma konusu haline gelmiştir. Alev geciktiriciler kimyasal veya fiziksel mekanizmalar yoluyla buhar fazında veya yoğun fazda hareket etmek suretiyle ısıtma, piroliz, ateşleme veya alev yayılması sırasında yanmaya müdahale eder. Borlu bileşikler, CO veya CO_2 oluşumu yerine karbon ayrışma sürecini lehine yeniden yönlendirerek yoğun fazda hareket ederler. Borlu bileşikler, karbon oksidasyonunu önleyen koruyucu camsı koruma tabakasının oluşmasını sağlarlar ve yanan malzemenin üzerini oksijenle temasını kesecek şekilde kaplayarak yanmayı bastırırlar [25]. Bor içeren alev geciktiriciler halojen içeren geleneksel alev geciktiricilere nazaran daha az toksiktirler [26]. Bor bileşikleri alev geciktirici olarak kullanıldıklarında çevre dostu olarak kabul edilirler [27,28]. Ayrıca duman bastırmada, yanmayı önlemede ve çok işlevli alev geciktiricilerde boya pigmenti olarak kullanılırlar [29]. Malzemelerin alev geciktiriciliğini analiz eden test metodlarından bazıları LOI analizi, UL-94 testi, termogravimetrik analiz, koni kalorimetre testidir [30].

Bu çalışmanın amacı, fonksiyonel ve yüksek katma değerli bor uç ürünlerinden biri olan kalsiyum floroboratın üretim parametrelerinin belirlenmesi, kinetik ve alev geciktirici özelliklerinin incelenmesidir. Literatürde kalsiyum floroboratın sentez parametrelerinin belirlendiği ve reaksiyon kinetiğinin çalışıldığı ve ayrıca kalsiyum floroboratın pamuklu kumaşta alev geciktirici etkisinin incelendiği bir çalışma bulunmamaktadır.

2. Malzemeler ve Yöntemler (Materials and Methods)

Yapılan çalışmada yaş metot yöntemi ile kalsiyum oksit (%99 saflıkta Sigma-Aldrich) ve floroborik asit (%50 saflıkta ACROS Organics) reaktant olarak kullanılarak kalsiyum floroborat sentezlenmiştir. Reaksiyon Eş. 1’de verilmiştir.

$$CaO + 2HBF_4 \rightarrow Ca(BF_4)_2 + H_2O \quad (1)$$

Deneyler, floroborik asitin camlarda korozif etki göstermesinden dolayı teflon reaktörler içerisinde gerçekleştirilmiştir. Çalışılan parametreler; reaktant mol oranı (2:1, 3:1, 4:1, 5:1), sıcaklık (30°C, 50°C, 70°C, 90°C, 100°C) ve reaksiyon süresidir. Deneylerde karıştırma hızı 400 rpm (rotation per minute) olarak sabit tutulmuştur. Eş. 1’de verilen reaksiyon denklemine göre oluşabilecek maksimum kalsiyum floroborat miktarı hesaplanıp üretilen madde miktarından verime geçilmiştir. Sentezlenen kalsiyum floroboratın karakterizasyon çalışmalarında FT-IR (Jasco FT-IR-480), XRD (Bruker D8 Advance) ve BF_4^- iyon seçici elektrot (Mettler Toledo DX287) kullanılmıştır. Numunenin termal davranışı, TG-DTA (NETZSCH5) cihazı ile argon atmosferinde 10°C/dakika hızla oda sıcaklığından 800°C’ye kadar gözlemlenmiştir. Kinetik çalışmada reaksiyonun mertebesi belirlenmiş ve aktivasyon enerjisi hesaplanmıştır. Kalsiyum floroboratın alev geciktirici özelliğinin incelenmesinde limit oksijen indeksi testi (LOI) kullanılmış ve testler ASTM D2863 standardına göre yapılmıştır. Optimum koşullarda sentezlenen kalsiyum floroborat farklı derişimlerde (%20 ve %50) hazırlanarak pamuklu kumaşlara emdirilmiş ve kumaşlar oda sıcaklığında kurutulmuştur. Deneylerde kullanılan kumaşın özellikleri Tablo 1’de verilmiştir.

Tablo 1. LOI testinde kullanılan kumaşın özellikleri (Properties of the fabric used in the LOI test).

Lif Cinsi	%100 Pamuk Ring İpliği
Dokuma biçimi	2x2
Alanın yoğunluğu	437 g/m^2
İp sıklığı	Atkı yönünde 15 adet/cm Çözgü yönünde 23 adet/cm

3. Sonuçlar ve Tartışma (Results and Discussion)

Yapılan deneysel çalışmanın ilk aşamasında farklı parametrelerin reaksiyon verimi üzerine etkisi incelenmiştir. Eş.1'de verilen reaksiyon denklemine göre reaktant mol oranının ($nHBF_4/nCaO$) 2:1, 3:1, 4:1, 5:1 olduğu durumlarda reaksiyon verim değerleri hesaplanmıştır. Sabit sıcaklık ve karıştırma hızında (50°C ve 400 rpm) 120 dakika boyunca gerçekleşen reaksiyonlarda elde edilen maddeler süzülüp kurutulmuştur. Reaktant mol oranının verim üzerine olan etkisi Şekil 1'de verilmiştir. Şekil 1'de görüldüğü üzere kalsiyum floroboratın en uygun şartlarda %74 verimle ile 4:1 reaktant mol oranında elde edildiği gözlemlenmiştir. Reaktant mol oranı arttıkça seyreltme etkisinden kaynaklı verimin azaldığı belirlenmiştir.

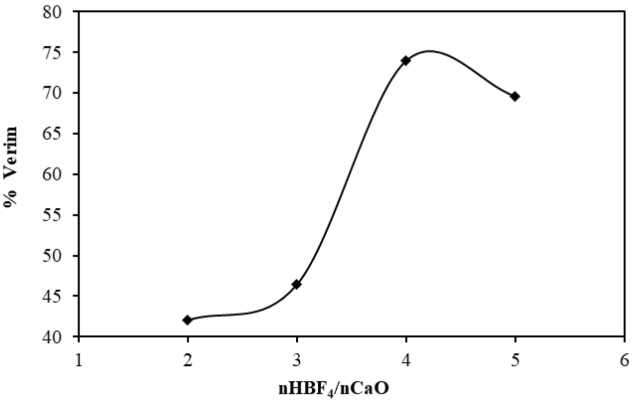

Şekil 1. Reaktant mol oranının ($nHBF_4/nCaO$) reaksiyon verimi üzerine etkisi (50°C ve 400 rpm) (Effect of reactant mole ratio ($nHBF_4/nCaO$) on reaction efficiency (50°C ve 400 rpm)).

Reaksiyonun mol oranı ($nHBF_4/nCaO$=4:1) ve karıştırma hızı (400 rpm) sabit tutularak farklı sıcaklıklarda (30°C, 50°C, 70°C, 90°C, 100°C) deneylere devam edilmiş, sıcaklığın reaksiyon verimi üzerine etkisi belirlenmiştir. Farklı sıcaklık değerlerinde elde edilen verim değerleri Şekil 2'de verilmiştir. Şekil 2'de görüldüğü gibi, sıcaklık arttıkça reaksiyon veriminin arttığı gözlemlenmiştir. 90°C ve 100°C'de elde edilen verim değerlerinin yaklaşık aynı olduğu görülmüştür. Enerji maliyetleri göz önünde bulundurulduğunda reaksiyon için en uygun sıcaklık 90°C olarak belirlenmiştir. 4:1 reaktant mol oranında ve 90°C'de kalsiyum floroborat %97 verim ile sentezlenmiştir.

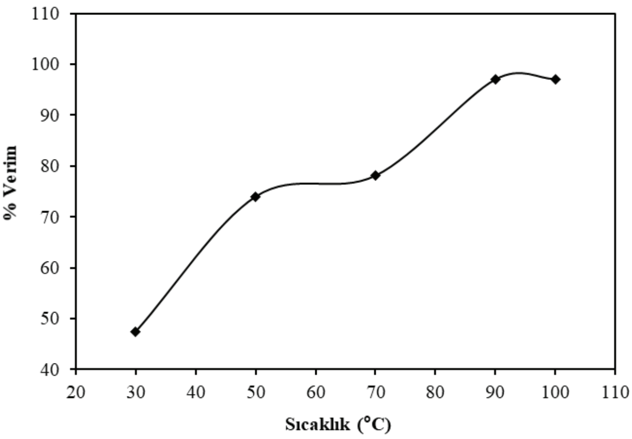

Şekil 2. Sıcaklığın reaksiyon verimi üzerine etkisi ($nHBF_4/nCaO$=4:1, 400 rpm) (Effect of temperature on reaction efficiency ($nHBF_4/nCaO$=4:1, 400 rpm)).

Çalışmanın bir sonraki basamağında reaksiyon süresinin incelenmesi maksadı ile 4:1 reaktant mol oranı ve 90°C sabit sıcaklık şartlarında reaksiyon ortamından 1'er mL numune alınarak 100 mL'ye seyreltilmiştir. BF_4^- iyon seçici elektrot kullanılarak BF_4^- konsantrasyonu iyon metrede okunmuştur. BF_4^- konsantrasyonunun zamana bağlı değişimi Şekil 3'te verilmiştir. BF_4^- konsantrasyonunun zamanla arttığı fakat 100. dakikadan sonra yaklaşık aynı değerde kaldığı gözlemlenmiştir. Dolayısı ile reaksiyon süresi 100 dakika olarak belirlenmiştir.

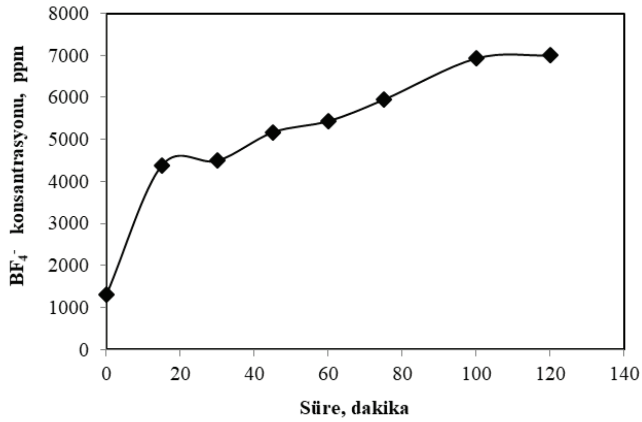

Şekil 3. Reaksiyon süresinin BF_4^- konsantrasyonu üzerine etkisi ($nHBF_4/nCaO$=4:1, 90°C) (Effect of reaction time on BF_4^- concentration ($nHBF_4/nCaO$=4:1, 90°C)).

Yaş yöntem ile en uygun koşullarda sentezlenen kalsiyum floroboratın saflaştırma işlemi için kalsiyum floroboratın suda çözünürlüğünden yararlanılmıştır. Elde edilen ürün 40°C sıcaklıktaki suda çözülmüş, süzülmüş ve kurutulmuştur. Daha sonra sentezlenen kalsiyum florobarattan 0,03 g alınmış ve 0,47 g KBr ile karıştırılarak pellet oluşturulmuş ve FT-IR cihazında analiz edilmiştir. FT-IR spektrumunda B-F bağı karakteristik piki 1000-1100 cm^{-1} aralığında görülmektedir [31]. Sentezlenen numunenin FT-IR spektrumu Şekil 4'te verilmiştir. Şekil 4'te verilen FT-IR spektrumunda literatür verisiyle örtüşecek şekilde 1000-1100 cm^{-1} aralığında B-F bağı piki görülmektedir. 541 cm^{-1} dalga

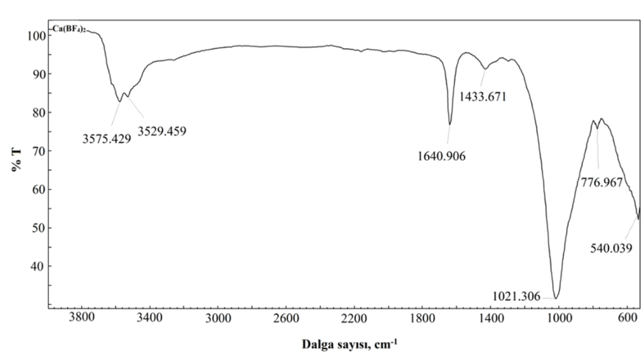

Şekil 4. Sentezlenen kalsiyum floroboratın FTIR spektrumu (FTIR spectrum of synthesized calcium fluoroborate).

sayısında B-F geriliminden kaynaklanan titreşim mevcuttur. 3500-3600 cm^{-1} dalga sayısı aralığında ise O-H pikleri belirmiştir.

Şekil 5'te sentezlenen kalsiyum floroboratın kristal yapısını gösteren XRD analizi grafiği verilmiştir (ICSD/98-000-1839). 12,6°, 13,2° ve 19,1° değerlerinde gözlemlenen piklerin literatür verileriyle örtüştüğü görülmektedir [11]. Bu durum reaksiyonun başarılı bir şekilde gerçekleştiğini göstermektedir.

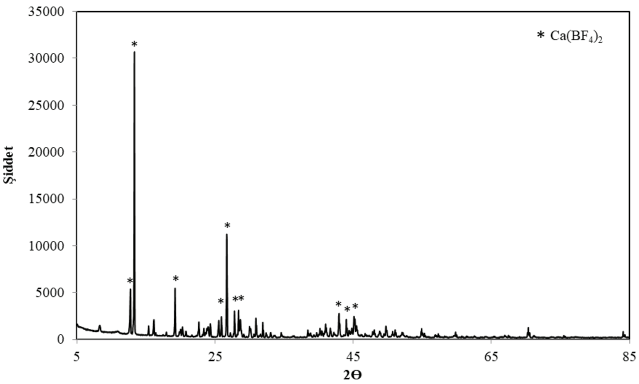

Şekil 5. Sentezlenen kalsiyum floroboratın XRD analiz grafiği (XRD analysis graph of synthesized calcium fluoroborate).

Sentezlenen kalsiyum floroboratın TG-DTA grafiği Şekil 6'da verilmiştir. İlk olarak yapıdan su buharlaşmıştır. 300°C'de bağların parçalanması ve gaz çıkışından dolayı yapıda %61 kütle kaybı olmuştur. Yüksek sıcaklıklarda borlu yapı, camsı tabaka oluşturmaktadır. İnorganik bor bileşikleri yanma esnasında malzeme yüzeyinde camsı koruyucu tabaka oluşturarak, yanma için gerekli oksijen ve ısıya karşı koruma görevi yapmaktadırlar [32].

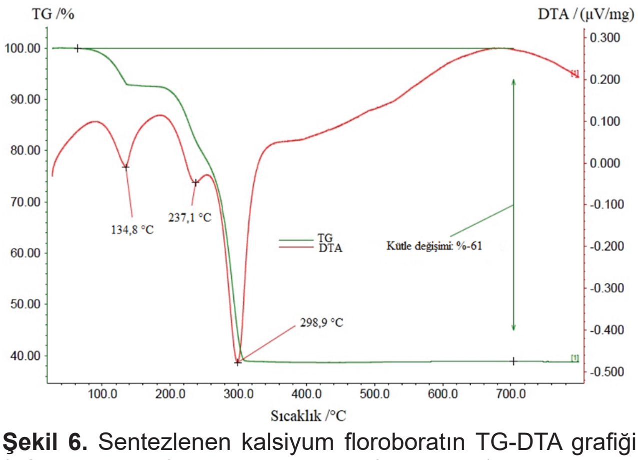

Şekil 6. Sentezlenen kalsiyum floroboratın TG-DTA grafiği (TG-DTA graph of synthesized calcium fluoroborate).

Yapılan kinetik çalışmada reaksiyonun mertebesini belirlemek için her bir sıcaklıkta $ln(C_A/C_{A0})$'a karşı T grafiği çizilmiş ve reaksiyon mertebesinin birinci dereceden olduğu bulunmuştur. $ln(C_A/C_{A0})$'a karşı T grafiklerinin eğimlerinden k değerleri bulunmuştur. Aktivasyon enerjisinin belirlenmesinde beş farklı sıcaklık için lnk' ya karşı 1/T değerleri grafiğe geçirilerek doğrusal bir çizgi elde edilmiştir. Kalsiyum floroboratın lnk'ya karşı 1/T Arrhenius grafiği Şekil 7'de verilmiştir. Bu doğrunun eğiminden $-E_a/R$ elde edilmiş ve aktivasyon enerjisi (E_a) değeri bulunmuştur.

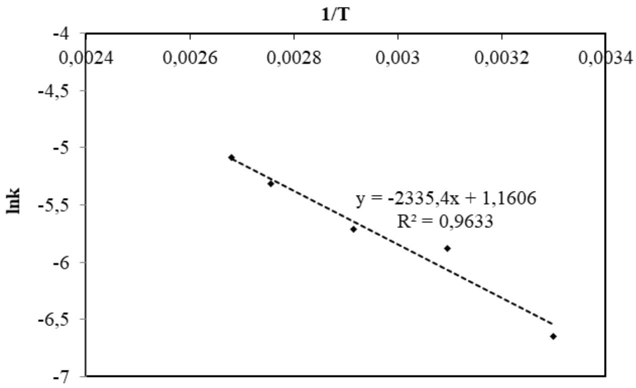

Şekil 7. Kalsiyum floroborat Arrhenius grafiği (Arrhenius plot of calcium fluoroborate).

Yapılan kinetik çalışma sonucunda reaksiyonun aktivasyon enerjisi 19,14 kJ/mol olarak bulunmuştur. Bu sonuç elde edilen kalsiyum floroboratın üretim sürecinin enerji tüketimi bakımından ekonomik olduğunu göstermektedir. Ayrıca üretim aşamasında yüksek sıcaklığa ihtiyaç yoktur. Zira düşük aktivasyon enerjisine sahip süreçler sıcaklığa çok duyarlı değildir. Kinetik çalışma ve diğer sonuçlar birlikte değerlendirildiğinde reaksiyonun teknolojik olarak uygulanabilir olduğu anlaşılmaktadır.

Kalsiyum floroboratın alev geciktirici özelliğini incelemek için sentezlenen kalsiyum floroborat kristallerinin farklı derişimlerde (%20 ve %50) çözeltileri hazırlanmış ve %100 pamuklu kumaşlara emdirilmiştir. Ardından katkısız kumaşın ve kalsiyum floroborat çözeltisi emdirilmiş kumaşların LOI değerleri belirlenmiştir. Bir malzemeyi alev geciktirici olarak nitelendirilebilmek için, limit oksijen indeks değerinin %28'in üzerinde olması gerektiği belirtilmiştir [33]. Limit oksijen indeksi, malzemenin havada yanmaya devam etmesi için gerekli olan % oksijen miktarı olarak tanımlanabilmektedir. LOI değeri yüksek olan malzeme standart atmosfer şartları altında daha zor yanma karakteristiğine sahiptir.

ASTM D 2863 standardına göre yapılan testlerde fazla güçlü olmayan sabit miktardaki alev, malzemenin uç kısmına gerekirse üst yüzeyini kaplayacak şekilde sürekli hareket ettirilmek sureti ile 30 saniye kadar uygulanmış ve her 5 saniyede bir uzaklaştırılarak numunenin kendiliğinden yanmaya devam edip etmeyeceği gözlemlenmiştir. LOI testi sonucunda elde edilen sonuçlar Tablo 2'de verilmiştir. Tablo 2'de görüldüğü üzere katkısız pamuklu kumaşının LOI değeri 16 iken, %20'lik kalsiyum floroborat çözeltisi emdirilen kumaşın LOI değeri 23, %50'lik kalsiyum floroborat çözeltisi emdirilen kumaşın LOI değeri ise 32'dir. Literatürde %50 derişimdeki amonyum floroborat çözeltisinin katkısız kumaşın LOI değerini %22 arttırdığı görülmüştür [24]. %20 derişimdeki bakır floroborat çözeltisinin katkısız

Tablo 2. Farklı derişimlerde kalsiyum floroborat çözeltisi emdirilen kumaşların LOI değerleri (LOI values of fabrics impregnated with calcium fluoroborate solution at different concentrations).

Numune Adı	Katkısız Kumaş	%20'lik $Ca(BF_4)_2$ Çözeltisi Emdirilmiş Kumaş	%50'lik $Ca(BF_4)_2$ Çözeltisi Emdirilmiş Kumaş
LOI değeri	16	23	32

kumaşın LOI değerini %75 arttırdığı, %30 derişimdeki kobalt floroborat çözeltisinin ise katkısız kumaşın LOI değerini iki katından fazla arttırdığı görülmüştür [34,35]. Kalsiyum floroboratın pamuklu kumaşın LOI değerini yani alevin devam edebilmesi için gerekli olan oksijen miktarını iki katı kadar yükselttiği ve kumaşa alev geciktirici özellik kazandırdığı görülmüştür.

4. Sonuçlar (Conclusions)

Yapılan çalışmada kalsiyum oksit ile floroborik asit reaktant olarak kullanılarak kalsiyum floroborat yaş yöntem ile sentezlenmiştir. Reaktant mol oranı, sıcaklık ve reaksiyon süresinin verim üzerine etkisi incelenmiştir. 4:1 reaktant mol oranı, 90°C sıcaklık ve 100 dakika reaksiyon süresinde %97 verimle kalsiyum floroborat sentezlenmiştir. Kinetik çalışmada reaksiyon derecesinin birinci dereceden kinetiğe sahip olduğu belirlenmiş ve aktivasyon enerjisinin (E_a) 19,14 kJ/mol olarak hesaplanmıştır. Bu sonuçlar reaksiyonun ekonomik olduğunu göstermektedir. Teknolojik açıdan uygulanabilirliği ve fizibilitesi yüksektir. LOI testi maddelerin alev geciktirici karakteristiğini ortaya koyan önemli testlerden biridir. Kalsiyum floroborat emdirilmiş kumaşlara LOI testi uygulanmış, alev geciktirici özellikleri incelenmiştir. Katkısız kumaşın LOI değeri 16 bulunurken; %20 ve %50 kalsiyum floroborat içeren çözeltiler emdirilip kurutulmuş kumaşların LOI değerleri sırasıyla 23 ve 32 olarak bulunmuştur. LOI testi sonuçları kalsiyum floroboratın alev geciktirici özelliğe sahip olduğunu göstermektedir. Yüksek katma değerli özel bor ürünlerinden olan kalsiyum floroboratın tekstil kumaşlarında alev geciktirici olarak kullanımının yaygınlaştırılması önerilmektedir.

Teşekkür (Acknowledgement)

Bu çalışma, TENMAK Bor Araştırma Enstitüsü (BOREN) tarafından desteklenmiştir. Proje No: 2017-30-06-30-002.

Kaynaklar (References)

[1] Türk Mühendisler Mimarlar Odaları Birliği. (2016). *Bor Raporu.* [Boron Report]. ISBN 978-605-01-0883-5.

[2] Booth, H. S., & Martin, D. R. (1949). *Boron Trifluoride and Its Derivatives*. Wiley, Newyork. DOI: 10.1021/ed028p56.

[3] Yünlü, K. (2019). *Bor: Bileşikleri, Sentez Yöntemleri, Özellikleri, Uygulamaları.* [Boron: Its Compounds, Synthesis Methods, Properties and Applications] (2nd Ed.). Aydili Advertising Agency. ISBN 978-605-5310-93-6.

[4] Achilonu, M. C., & Umesiobi, D. O. (2010). The formation of carbon-carbon and carbon–heteroatom bonds using silver tetrafluoroborate as a promoter. *Arabian Journal of Chemistry, 9*(2), 1984-2003.

[5] Aydın, Y. D., Gürü, M., İpek, D., & Özyürek, D. (2019). Obtainment of copper(II) fluoroborate by high-energy impacted ball-milling. *Acta Physica Polonica A*, *135*, 888-891.

[6] Aydın, D. Y., Gürü, M., Ipek, D., & Özyürek, D. (2017). Synthesis and characterization of zinc fluoroborate from zinc fluoride and boron by mechanochemical reaction. *Arabian Journal for Science and Engineering, 42*(10), 4409-4416.

[7] Krishnapuram, P., Jakka, S. K., Thummala, C., & Lalapeta, R. M. (2012). Photoluminescence characteristics of Eu2O3 doped calcium fluoroborate glasses. *Journal of Molecular Structure, 1028*, 170-175.

[8] Kumar, J. S., Pavani, K., Babu, A. M., Giri, N. K., Rai, S.B., & Moorthy, L. R. (2010). Fluorescence characteristics of Dy3+ ions in calcium fluoroborate glasses. *Journal of Luminescence, 130* (10), 1916-1923.

[9] Kumar, J. S., Babu, A. M., Sasikala, T., Moorthy, & L. R. (2010). NIR fluorescence and visible upconversion studies of Nd3+ ions in calcium fluoroborate glasses. *Chemical Physics Letters, 484*(4-6), 207-213.

[10] Prabakar, S. J. R., Sohn, K.S., & Pyo, M. (2019). Enhancement in high-rate performance of graphite anodes via interface modification utilizing Ca(BF4)2 as an electrolyte additive in lithium ion batteries. *Journal of The Electrochemical Society, 166*, A591.

[11] Forero-Saboya, J. D., Lozinšek, M., & Ponrouch, A. (2020). Towards dry and contaminant free Ca(BF4)2-based electrolytes for Ca plating. *Journal of Power Sources Advances, 6*, 100032.

[12] Sarkar, A., Santra, S., Kundu, S. K., Ghosal, N. C., Hajra, A., & Majee, A. (2015). Zinc tetrafluoroborate: a versatile and robust catalyst for various organic reactions and transformations. *Synthesis, 47*,1379-1386.

[13] Pujala, B., Rana, S., & Chakraborti, A. K. (2011). Zinc tetrafluoroborate hydrate as a mild catalyst for epoxide ring opening with amines: scope and limitations of metal tetrafluoroborates and applications in the synthesis of antihypertensive drugs (RS)/(R)/(S)-metoprolols. *The Journal of Organic Chemistry, 76*(21), 8768-8780.

[14] Ranu, B. C., Jana, U., & Majee, A. (1999). A simple and efficient method for selective deprotection of t-butyldimethylsilyl ethers by zinc tetrafluoroborate in water. *Tetrahedron Letters, 40*(10), 1985-1988.

[15] Zhang, S. S., Xu, K., & Jow, T. R. (2002). Study of LiBF4 as an electrolyte salt for a li-ion battery. *Journal of The Electrochemical Society, 149*(5), A586–A590.

[16] Tressaud, A. (2010). *Functionalized Inorganic Fluorides: Synthesis, Characterization and Properties of Nanostructured Solids*. John Wiley & Sons. ISBN 978-0-470-74050-7.

[17] Hashmi S. (Ed.) (2014). *Comprehensive Materials Processing*, Elsevier. ISBN 978-0-08-096533-8

[18] Menz, W., Mohr, J., & Paul, O. (2008). *Microsystem Technology*. John Wiley & Sons. ISBN 9783527296347.

[19] Wilkie, C. A., & Morgan, A. B. (Eds.). (2009). *Fire Retardancy of Polymeric Materials*. CRC Press.

[20] Aydın, D. Y. (2015) *Çinko floroborat sentezi ve alev geciktirici olarak kullanılabilirliği [Synthesis of zinc fluoroborate and usability as flame retardant]*. Yüksek Lisans Tezi, Gazi Üniversitesi, [M. Sc. Thesis, Gazi University]. Council of Higher Education Thesis Center (Thesis Number 395758)..

[21] Aydın, D. Y., Patlar, K., Gürü, & M., Akkurt, F. (2017). Synthesis of antimony fluoroborate and usability as flame retardant, 8th International Advanced Technologies Symposium (IATS'17), Elazığ, Turkey.

[22] Aydın, D. Y., Kurt, H., Kandemir, E. B., & Gürü, M. (2017) Synthesis of lead fluoroborate and usability as flame retardant, *8th International Advanced Technologies Symposium (IATS'17)*, Elazığ, Turkey.

[23] Aydın, D. Y., Biberoğlu, R., Kümbetlioğlu, F., Gürü, M., Akkurt F., & Kuru, F. (2018) Kobalt floroborat sentezi ve alev geciktirici olarak kullanılabilirliği [Synthesis of cobalt fluoroborate and its usability as a flame retardant] *1st International Eurasion Conference on Science, Engineering and Technology*, Ankara, Turkey.

[24] Ceyhan, A. A., Bağcı, S., Baytar, O., & Şahin, Ö. (2020). Amonyum floroborat üretimi ve üretim parametrelerinin belirlenmesi [Ammonium fluoroborate production and determination of production parameters]. *Journal of Boron, 5*(2), 63-72.

[25] Aydın, D. Y., Gürü, M., Ayar, B., & Çakanyıldırım, Ç. (2016). Bor bileşiklerinin alev geciktirici ve yüksek sıcaklığa dayanıklı pigment olarak uygulanabilirliği. [Applicability of boron compounds as flame retardant and high temperature resistant pigments]. *Journal of Boron, 1*(1), 33-39.

[26] Lu, S. Y., & Hamerton I. (2002) Recent developments in the chemistry of halogen-free flame retardant polymers. *Progress in Polymer Science, 27*(8), 1661-1712.

[27] Dogan, M., & Unlu, M. (2014). Flame retardant effect of boron compounds on red phosphorus containing epoxy resins. Polymer Degradation and Stability, 99, 12-17.

[28] Wang, X, Song, Y., & Bao, J. (2010). Synergistic effects of ZrO2 or B2O3 on flame-retarded poly (butyl methacrylate) with tricresylphosphate. *Fire and Materials, 34*(7), 357-366.

[29] Ayar, B., Gürü, M., & Çakanyıldırım, Ç. (2014). Solid phase synthesis of anhydrous zinc borate from zinc and boron oxide and utilization as a flame retardant in dye and textile. *Gazi University Journal of Science, 27*(3), 987-991.

[30] Bourbigot, S., Bras, M. L., Leeuwendal, R., Shenc, K. K., & Schubertc, D. (1999). Recent advances in the use of zinc borates in flame retardancy of EVA. *Polymer Degradation and Stability, 64*(3), 419-425.

[31] Leoni, P., Sommovigo, M., Pasqualli, M., Midollini, S., Braga, D., & Sabatino, P. (1991). Coordinated water/anion hydrogen bonds and Pd-H bond acidity in cationic palladium(II) aquo hydrides and the x-ray crystal and molecular structures of trans-[(Cy3P)2Pd(H)(H2O)]BF4 (Cy=cyclohexyl). *Organometallics, 10*(4), 1038-1044.

[32] Bozacı, E. (2018). Borlu bileşiklerin çevre dostu yöntemlerle poliakrilnitril kumaşlara uygulanması [Application of boron compounds to polyacrylonitrile fabrics by environmentally friendly methods]. *Journal of Boron, 3*(1), 17-23.

[33] Friedrich, K., Breuer, U. (2015) *Multifunctionality of Polymer Composites: Challenges and New Solutions.* (1st Ed.), Elsevier, ISBN 978-0-323-26434-1.

[34] İpek, D., (2018). *Bakır floroborat sentezi ve alev geciktirici olarak kullanılabilirliği [*Synthesis of copper fluoroborate and usability as flame retardant]. Yüksek Lisans Tezi, Gazi Üniversitesi, [M. Sc. Thesis, Gazi University]. Council of Higher Education Thesis Center (Thesis Number 493623).

[35] Biberoğlu, R. (2020). *Kobalt floroborat sentezi ve alev geciktirici olarak kullanılabilirliği* [Synthesis of cobalt fluoroborate and usability as flame retardant]. [M. Sc. Thesis, Gazi University]. Council of Higher Education Thesis Center (Thesis Number 634601).

BOR DERGİSİ
JOURNAL OF BORON
https://dergipark.org.tr/boron

Çeliklerin korozyonuna boraksın etkisi

Gülden Asan[1,*], Abdurrahman Asan[2]

[1]Hitit Üniversitesi, Teknik Bilimler Meslek Yüksekokulu, Çorum, 19030, Türkiye
ORCID orcid.org/0000-0002-6075-159X
[2]Hitit Üniversitesi, Mühendislik Fakültesi, Kimya Mühendisliği Bölümü, Çorum, 19030, Türkiye
ORCID orcid.org/0000-0002-1010-3981

MAKALE BİLGİSİ

Makale Geçmişi:
İlk gönderi 1 Mart 2021
Kabul 8 Ağustos 2021
Online 30 Eylül 2021

Araştırma Makalesi

DOI: 10.30728/boron.889110

Anahtar kelimeler:
Boraks
Çelik
Korozyon
Tafel polarizasyon metodu

ÖZET

Bu çalışmada Ç 1010, Ç 304 ve Ç 316 çeliklerin korozyonuna boraksın ($Na_2B_4O_7$) etkisi araştırılmıştır. Bu amaçla farklı derişimlerde (0,0125 M, 0,025 M, 0,050 M ve 0,100 M) borakslı çözeltiler hazırlanmıştır. Çeliklerin bu ortamdaki elektrokimyasal davranışını belirlemek için Dönüşümlü Voltametri (CV) tekniği, korozyon hızlarını ölçmek için ise Tafel Polarizasyon Yöntemi uygulanmıştır. Deneyler sonucunda boraks derişiminin artması ile her üç çelikte korozyon hızının azaldığı ve korozyon potansiyelinin arttığı tespit edilmiştir. En yüksek boraks derişiminde en düşük korozyon hızı Ç 316 çeliğinde belirlenmiştir. Ç 1010, Ç 304 ve Ç 316 çeliklerin 0,100 M boraks derişiminde korozyon hızları sırasıyla; 0,251, 0,132 ve 0,071 mm/yıl olarak ölçülmüştür. Boraks anodik inhibitör davranışı göstererek çelikleri korozyondan korumuştur. Çeliklerin borakslı çözeltilerde güvenle kullanılabileceği sonucuna varılmıştır.

The effect of borax on corrosion of low carbon steels

ARTICLE INFO

Article History:
Received March 1, 2021
Accepted August 8, 2021
Available online September 30, 2021

Research Article

DOI: 10.30728/boron.889110

Keywords:
Borax
Steel
Corrosion
Tafel polarization method

ABSTRACT

In this study, the effect of borax ($Na_2B_4O_7$) on the corrosion of Ç 1010, Ç 304 and Ç 316 steels was investigated. For this purpose, solutions with borax at different concentrations (0.0125 M, 0.025 M, 0.050 M and 0.100 M) were prepared. Cycling Voltammetry (CV) technique was used to determine the electrochemical behavior of steels in this environment, and Tafel Polarization Method was used to measure corrosion rates. As a result of the experiments, it was determined that the corrosion rate decreased and the corrosion potential increased in all three steels with increasing borax concentrations. Lowest corrosion rate at higest borax concentration was obtained from Ç 316. Corrosion rates of Ç 1010, Ç 304 and Ç 316 steels at 0,100 M borax concentration have been measured respectively as 0.251, 0.132 and 0.071 mm/year. Borax protected steels from corrosion by showing anodic inhibitory behaviour. It is concluded that the steels can be used safely in borax solutions.

1. Giriş (Introduction)

Korozyon, gelişmiş ve gelişmekte olan ülkelerde büyük ekonomik ve güvenlik zararlarına neden olan evrensel bir sorundur. Korozyon, ekonomik ve güvenlik kayıplarının yanı sıra, zehirli kimyasalların ve solventlerin paslanmış metal ekipmanlardan sızması nedeniyle çevre sorunlarına da neden olur [1,2]. Çelikler, yüksek mekanik güç ve maliyet etkinliği nedeniyle en yaygın olarak inşaat ve yapı malzemeleri olarak kullanılmaktadır. Demir alaşımları, petrol ve gaz endüstrilerinde depolama tankı, işleme ekipmanları ve nakliye boru hatları olarak yaygın bir şekilde kullanılmaktadır. Malzeme kayıplarını azaltmak için korozyona karşı birçok yöntem uygulanmakla birlikte, organik bileşiklerin kullanımı, etkili ve kolay sentezleri, yüksek inhibisyon etkinliği ve maliyet etkinliği nedeniyle en yaygın ve en sık olanıdır. Genel olarak organik bileşikler, metal ve çevre (elektrolit) ara yüzünde koruyucu bir film oluşturarak korozyonu etkili bir şekilde inhibe ederler [3].

Ülkemizde bol miktarda bulunan bor, ekonomik olması ve stratejik olması nedeniyle birçok endüstride kullanım alanı bulmuştur. Bor, tepkimelerde katalizör [4],

*Corresponding author: guldenasan19@gmail.com

Tablo 1. Çelik malzemelerin kimyasal bileşimleri (Chemical compositions of steel materials).

	C	Mn	Si	P	S	Cr	Ni	Mo	Cu
Ç 1010	0,07	0,55	0,01	<0,01	<0,01	<0,01	0,11	0,01	0,09
Ç 304	0,07	1,91	0,77	0,047	0,03	18,25	8,20	0,08	0,25
Ç 316	0,05	1,22	0,45	0,40	0,02	16,10	10,09	2,01	0,42

nükleer teknolojide, yakıt olarak roket motorlarında, ısıya dayanıklı polimerlerde, kimyasal termokimyasal depolamada [5], cam, ilaç, boyar madde, kozmetik, alev geciktiricilerde, gıda koruyucularda, hafif antiseptiklerde, seramik ve refrakter gibi ısıya dayanımlı malzeme üretiminde, yüksek kalitede çelik, sabun, deterjan, antifriz, dezenfektan ve gübre üretimlerinde kullanılmaktadır [6,7]. Son zamanlarda yapılan bir araştırmada çelik yüzeyinde oluşturulan Ni-B kaplamaların, herhangi bir yağlayıcı takviye elemanı kullanılmadan aşınma ortamına dayanıklı olduğunu göstermiştir [8]. Korozyona karşı inhibitör olarak kullanımı ile ilgili çok sınırlı sayıda çalışma yapılmıştır [9,10].

Metalleri korozyondan korumak için; metal kaplama, ortamı değiştirme, katodik koruma, anodik koruma, metali değiştirme vb. birçok yöntem kullanılmaktadır. Günümüz endüstrisinde çeliklerin çok yaygın kullanımı vardır. Ancak korozif ortamlarda özellikle asidik ve klorürlü ortamlarda korozyona uğrarlar[11]. Çeliklerin korozyonunu önlemek için çözeltilere katılan nitritler, kromatlar ve fosfatlar gibi anodik inhibitörler çevreye olan toksik etkisi nedeniyle birçok ülkede kullanımları kısıtlanmış veya yasaklanmıştır [12-14]. Bu nedenle son zamanlarda daha çevreci metal tuzlarının inhibitör olarak kullanımı için birçok çalışma yapılmaktadır [15-17]. İnhibitörler, metal yüzeyinde adsorplanır veya metalleri (çelik, alüminyum, titanyum) pasifleştirerek ya da çözelti ortamındaki hidrojenin indirgenmesini önleyerek korozyonu önlerler [18,19]. Korozyonun önlenmesinde inhibitörün molekül yapısı kadar çözeltinin bileşimi ve metal yüzeyi de oldukça önemlidir [20,21].

Bor bileşiklerin üretim sürecinde büyük oranda düşük karbonlu çelikler kullanılmaktadır. Ayrıca evlerde ve sanayide kullanılan temizlik maddelerin bileşiminde boraks yer almaktadır. Özellikle de çamaşır ve bulaşık makinalarında kullanılan deterjan bileşiminde bulunan boraksın makine aksamının korozyonuna ne kadar etki yaptığı konusunda daha önce bir çalışma yapılmadığı bilinmemektedir. Bu çalışma, bu amaca yönelik olarak boraksın, bor bileşiklerinin üretimi sürecinde kullanılan düşük karbonlu çelikten imal edilen ekipmanlara ve üretim sonrasında boraks ve boraks içeren kimyasalların kullanıldığı çelik malzemelere olan inhibitör etkisini tespit etmek için yapılmıştır.

2. Malzemeler ve Yöntemler (Materials and Methods)

Deneylerde, 250 ml'lik üç boyunlu korozyon hücresi kullanılmıştır. Çözeltiler deiyonize su içinde boraks çözülerek hazırlanmıştır. Kimyasal bileşimi Tablo 1'de verilen çalışma elektrotları, çelikler polyester reçineye gömülmüş ve 1 cm^2'lik yüzey alanı çözeltiyle temas edecek şekilde açıkta bırakılacak şekilde hazırlanmıştır. Her deneyden önce çalışma elektrotunun yüzeyi su altında 4000 meshlik zımpara kâğıdı ile parlatıldıktan sonra saf su ile yıkanmıştır. Yağ ve kirlerden arındırmak için de etanolden geçirilmiştir. Karşı elektrot olarak 1 cm^2'lik yüzey alanına sahip platin levha kullanılmıştır. Potansiyel ölçümleri için referans elektrot olarak da doygun kalomel elektrot (DKE) kullanılmıştır. Ölçülen potansiyeller bu elektroda göre verilmiştir. Tafel polarizasyon ölçümleri, bilgisayar kontrollü İvium Technologies De Regent 178 5611 HW Eindhoven model Potansiyostat/Galvanostat cihazı ile elde edilmiştir.

Çeliklerin elektrokimyasal davranışını belirlemek amacıyla elde edilen dönüşümlü voltamogramlar, en derişik ortam olan 0,100 M borakslı çözeltilerde elde edilmiştir. Dönüşümlü Voltametri tekniği, -1,50 V ile +1,00 V aralığında 0,2 V tarama hızı ile uygulanmıştır. Korozyon hızının belirlenmesi için Tafel Polarizasyon yöntemi uygulanmıştır [22]. Bu amaçla; 0,0125 M, 0,025 M, 0,050 M ve 0,100M boraks içeren çözeltilerde, -2,00 V ile 0,20 V potansiyel aralığında 0,002 V/s tarama hızı ile çeliklerin polarizasyon eğrileri elde edilmiştir.

3. Sonuçlar ve Tartışma (Results and Discussion)

Çeliklerin elektrokimyasal davranışlarının belirlenmesi amacıyla boraks derişiminin en fazla olduğu 0,100 M da Dönüşümlü Voltamogramları alındı. Şekil 1 de Ç 1010 çeliğin bu ortamdaki eğrisi görülmektedir. Ç 1010 çeliğinin ileri yöndeki anodik taramasında ileri yöndeki taramada -1,0 civarında anodik akımın başladığı ve

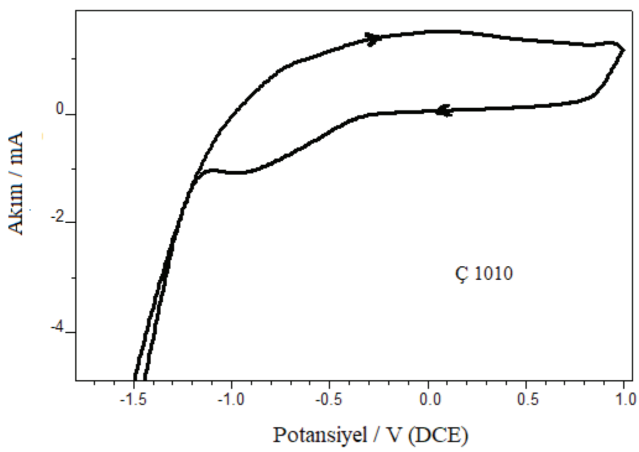

Şekil 1. Ç 1010 çeliğin 0,100 M boraks içeren çözeltideki dönüşümlü voltamogram (Cyclic voltammogram of Ç 1010 steel in solution containing 0.100 M borax).

1,0 V a kadar pasifliğini koruduğu görülmektedir. Anodik akımın en fazla yaklaşık olarak 0,0 V da 1,5 mA olduğu anlaşılmaktadır. Geri yöndeki katodik taramada ise korozyon akımının azaldığı ve çukurcuk korozyonunun oluşmadığı anlaşılmaktadır [23].

Şekil 2 ve Şekil 3'de Ç 304 ve Ç 316 çeliklerin, -0,5 V ve 0,8 V'da iki pasifleşme pikinin oluştuğu görülmektedir. Ancak Şekil 1'de verilen Ç 1010 çeliğinde bu pikler belirgin değildir. Birinci pik oluşumunda Fe → Fe^{2+} + 2 e^- reaksiyonu ile Fe, Fe^{2+} iyonlarına, ikinci pik oluşumunda Fe → Fe^{3+} + 3 e^- reaksiyonu ile Fe, Fe^{3+} iyonlarına ayrışmaktadır. Pasifleşmeye ise alaşım içindeki krom ve nikelin etkisi olduğu bilinmektedir [24]. Ç 1010 çeliğinde En yüksek anodik akım 1,5 mA olarak oluşurken, Ç 304 çeliğinde yaklaşık 1,0 mA olarak oluşmuştur. Ç 316 çeliğinde ise en yüksek potansiyelde (1,0 V) dahi akım 0,6 mA olarak okunmaktadır (Şekil 3). Üç çelik için geri yöndeki akım, ileri yöndeki taramada elde edilen akımdan küçük olduğundan, çukurcuk korozyonunun oluşmadığı anlaşılmaktadır.

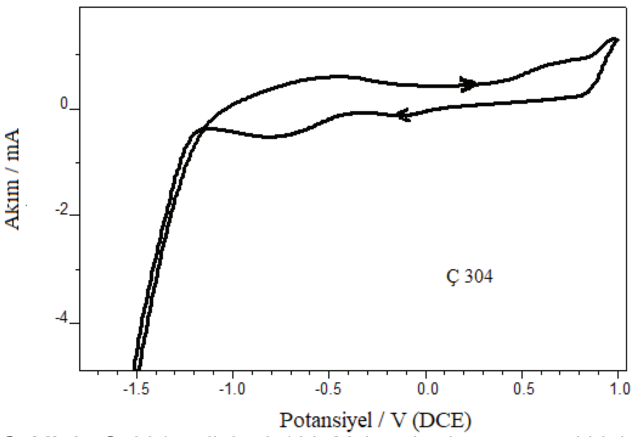

Şekil 2. Ç 304 çeliğin 0,100 M boraks içeren çözeltideki dönüşümlü voltamogram (Cyclic voltammogram of Ç 304 steel in solution containing 0.100 M borax).

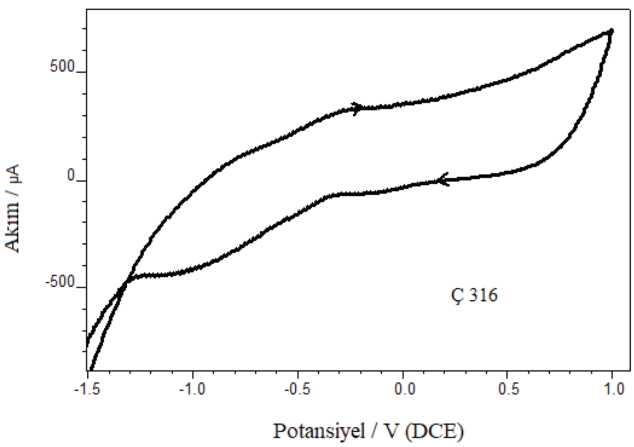

Şekil 3. Ç 316 çeliğin 0,100 M boraks içeren çözeltideki dönüşümlü voltamogram (Cyclic voltammogram of Ç 316 steel in solution containing 0.100 M borax).

Çeliklerin yükseltgenmesine karşı gösterilen direnci ifade eden polarizasyon direnci (Rp) her üç çelik için, boraks derişimin artması ile artış göstermiştir. Bu durum ölçülen korozyon hızının derişim artışıyla düşmesi sonucunu desteklemektedir. Korozyon hızı, Tafel polarizasyon metodu ile elde edilen eğrilerden anodik ve katodik eğrilerin eğim çizgilerin kesişmesi ile elde edilen akım yoğunluğunun bulunması ile belirlenmektedir [25]. Cihaza yüklü proğram, çeliklerin yoğunluğu ve eşdeğer gram ağırlığının programa girilmesi ile belirlenen bu akım yoğunluğunu Faraday yasalarını kullanarak mm/yıl olarak hesaplayarak vermektedir.

Boraks derişiminin etkisini belirlemek amacıyla dört farklı boraks derişimde (0,0125 M, 0,025 M, 0,050 M ve 0,100 M) Ç 1010 çeliğinin korozyon hızı ölçüldü. Elde edilen Tafel polarizasyon eğriler Şekil 4'de çakıştırılmış haliyle verilmiştir. Bu eğrilerden elde edilen korozyon parametreleri Tablo 2'de özet olarak verilmiştir. Boraks derişiminin artmasıyla, korozyon potansiyeli daha pozitif değerlere kayarken, korozyon hızı düşmüştür. Korozyon hızı artan boraks derişimi ile sırasıyla 0,293, 0,278, 0,263 ve 0,251 mm/yıl olarak azalmıştır. Bu durum boraksın anodik bir inhibitör gibi davrandığını göstermektedir. Literatürde anodik inhibitör metal yüzeyinde bir film tabakası oluşturup pasifliği sağlayarak anodik reaksiyonu engelleyen kimyasal madde olarak tanımlanmaktadır. İnhibitör derişiminin artması ile korozyon hızında azalma ile birlikte korozyon potansiyelindeki pozitif artış anodik inhibitöre kanıt olarak gösterilmektedir [26,27].

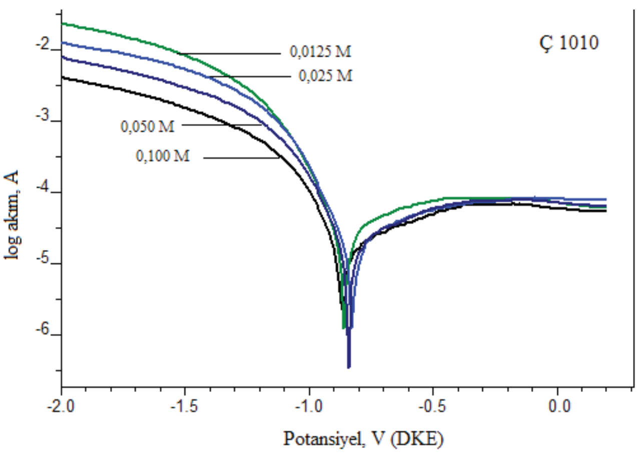

Şekil 4. Ç 1010 Çeliğin farklı boraks derişimi içeren çözeltilerde elde edilen Tafel Polarizasyon Eğrileri (Tafel Polarization Curves of Ç 1010 Steel in solutions with different borax concentrations).

Şekil 5'de Ç 304 çeliğin farklı boraks derişimlerde elde edilen Tafel Polarizasyon eğrilerinin çakıştırılmış hali görülmektedir. Ç 304 çeliğinde anodik ve katodik dallar Ç 1010 çeliğine benzemekle beraber, korozyon akımı daha düşük ölçülmüştür. Korozyon hızı boraks derişimi ile azalma göstermiştir. Korozyon hızı artan derişimle sırasıyla, 0,162, 0,145, 0,138 ve 0,132 mm/yıl olarak ölçülmüştür.

Şekil 6'da Ç 316 çeliğin dört farklı derişimdeki boraks çözeltisinde elde edilen çakıştırılmış Tafel polarizas-

Tablo 2. Farklı boraks derişimlerinde çeliklerin korozyon parametreleri (Corrosion parameters of steels obtained in different borax concentrations).

	Boraks Derişimi (M) (Borax Concentration (M))	Ecor (V)	βa	βc	Rp (ohm)	Korozyon Hızı (mm/yıl) (Corrosion Rate (mm/year))
Ç 1010	0,0125	-0,843	0,458	0,198	1836	0,293
	0,025	-0,836	0,463	0,207	1849	0,278
	0,050	-0,825	0,476	0,212	1892	0263
	0,100	-0,817	0,487	0,223	1910	0,251
Ç 304	0,0125	-0,896	0,602	0,205	3980	0,162
	0,025	-0,888	0,605	0,235	4209	0,145
	0,050	-0,822	0,612	0,242	4222	0,138
	0,100	-0,813	0,620	0,257	4241	0,132
Ç 316	0,0125	-0,905	0,683	0,251	8452	0,090
	0,025	-0,882	0,698	0,263	8546	0,082
	0,050	-0,852	0,710	0,260	8651	0,079
	0,100	-0,803	0,729	0,263	9028	0,071

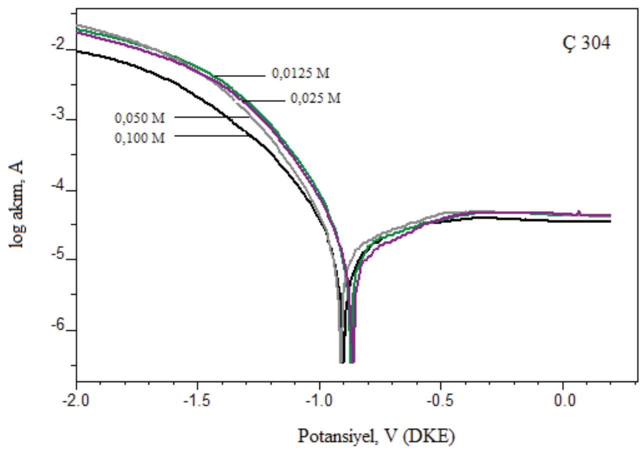

Şekil 5. Ç 304 Çeliğin farklı boraks derişimi içeren çözeltilerde elde edilen Tafel Polarizasyon Eğrileri (Tafel Polarization Curves of Ç 304 Steel in solutions with different borax concentrations).

yon eğrileri verilmektedir. Tüm çeliklerde, Tafel polarizasyon yöntemi ile elde edilen βa, βc den oldukça yüksek çıkmıştır. Bu durum boraksın çeliği anodik olarak koruduğunun bir başka göstergesi olarak değerlendirilmektedir [18]. Korozyon hızında da önemli oranda azalma görülmektedir. Korozyon hızı 0,0125, 0,025, 0,050 ve 0,100 M boraks derişimin artışı ile sırasıyla; 0,090, 0,082, 0,079 ve 0,071 olarak ölçülmüştür. Korozyon potansiyelinde, 0,1 M boraks çözeltinde -0,803 V değerine kadar anodik yönde artış olmuştur.

Şekil 7'de çalışılan en derişik ortam olan 0,100 M boraks çözeltisinde elde edilen, çeliklerin çakışık Tafel polarizasyon eğrileri verilmiştir. Çeliklerin genel olarak boraks çözeltilerinde oldukça korunaklı olduğu anlaşılmaktadır. Boraks çözeltilerinde korozyona karşı en iyi dayanım Ç 316 çeliğinde, daha sonra Ç 304 ve Ç 1010 da tespit edilmiştir. 0,100 M boraks çözeltisindeki korozyon hızları sırasıyla; 0,251, 0,132 ve 0,071 mm/yıl olarak ölçülmüştür. Ç 304 ve Ç 316 çeliklerin, Ç 1010 a göre daha korunaklı olması her iki çeliğin bileşiminde bulunan krom ve nikel alaşım elementinden kaynaklanmıştır. Ç 316 çeliğin Ç 304 çeliğinden daha dayanıklı olması ise Ç 316 bileşiminde bulunan

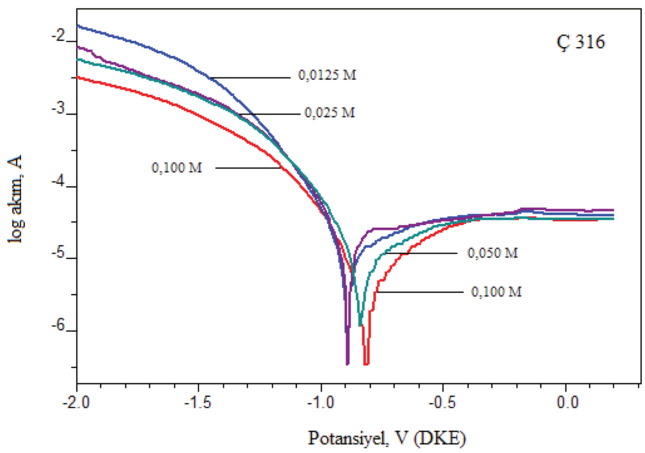

Şekil 6. Ç 316 Çeliğin farklı boraks derişimi içeren çözeltilerde elde edilen Tafel Polarizasyon Eğrileri (Tafel Polarization Curves of Ç 316 Steel in solutions with different borax concentrations).

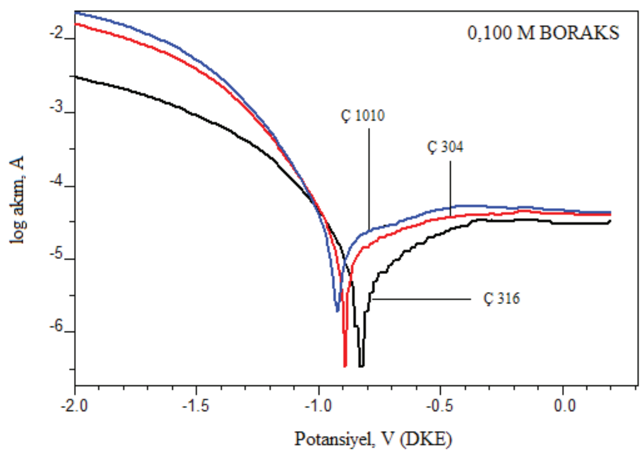

Şekil 7. Çeliklerin 0,100 M boraks içeren çözeltilerde elde edilen Tafel Polarizasyon eğrileri (Tafel Polarization curves of steels obtained in solutions containing 0.100 M borax).

Mo alaşım elementinden kaynaklanmış olabilir. Ingle ve arkadaşları çalışmalarında, 316 L çeliği içine katılan Mo alaşım elementinin, çelik bileşimi içinde yer alan kromun pasifleştirme özelliğine katkı sağladığı ve çelik yüzeyindeki aktif bölgeleri önleyerek çeliği korozyondan koruduğu sonucuna vardılar [28].

Tablo 2 incelendiğinde, tüm verilerde Tafel anodik sabitinin (βa), Tafel katodik sabitinden (βc) büyük olduğu görülmektedir. Bu durum korozyon mekanizmasının anodik reaksiyon kontrolünde olduğunu göstermektedir. Bu durum boraksın anodik inhibitör davranış gösterdiği tezini desteklemektedir [28].

Boraks derişiminin artması ile düşük karbonlu çeliklerde korozyon hızı azalmaktadır. En yüksek boraks derişime (0,100 M) ile en düşük boraks derişime (0,0125M) sahip boraks çözeltilerde, Ç 1010 çeliğinde %14,3, Ç 304 çeliğinde %18,5 ve Ç 316 çeliğinde %21,1 koruma sağlandığı anlaşılmaktadır. Bu durum boraksın inhibitör olma potansiyeli olduğunu ve bu çeliklerin borakslı ortamlarda güvenle kullanılabileceğini göstermektedir.

4. Sonuçlar (Conclusions)

Sonuç olarak; borakslı çözeltilerde, Ç 1010, Ç 304 ve Ç 316 çelikleri korozyona karşı oldukça dirençlidir. Artan boraks derişimlerinde tüm çeliklerde korozyon hızı azalmıştır. Boraks, çeliklerde anodik inhibitör davranışı göstermiştir. Kimyasal bileşiminde bulundurduğu Cr, Ni ve Mo alaşım elementleri sayesinde Ç 316 çeliği korozyona karşı en dayanıklı malzeme olarak tespit edilmiştir. Ç 1010 çeliği Ç 304 ve Ç 316 çeliklerine kıyasla daha düşük dayanım göstermekle birlikte, bu ortamda pasifleşme özelliği nedeniyle korozyona karşı direnç göstermiştir. Ç 304 çeliğin korozyona dayanımı Ç 316 dan düşük, Ç 1010 çeliğinden yüksek olarak bulunmuştur.

Kaynaklar (References)

[1] Perumal, K. E. (2014). Corrosion risk analysis, risk-based inspection and a case study concerning a condensate pipeline. *Procedia Engineering, 86*, 597-605.

[2] Loto, R. T. & Oluwatobilola, O. (2018). Corrosion inhibition properties of the combined admixture of essential oil extracts on mild steel in the presence of SO4 anions, *South African Journal of Chemical Engineering, 26*, 35-41.

[3] David, A.W.(2017). Predicting the performance of organic corrosion inhibitors. *Metals, 7*(12), 553-559.

[4] Yilmaz, A. E. Boncukcuoğlu, R., Kocakerm, M. M., & Kocadağistan, E. (2008). An empirical model for kinetics of boron removal from boroncontaining wastewaters by the electrocoagulation method in a batch reactor. *Desalination, 230*(1-3), 288-297.

[5] Abu-Hamed, T., Karni, J., & Epstein, M. (2007). The use of boron for thermochemical storage and distribution of solar energy. *Solar Energy, 81*(1), 93-101.

[6] Obut, A., Ehsani, İ., Aktosun, Z., Yörükoğlu, A., Girgin, İ., & Temel, A. (2020). Leaching behaviour of lithium from a clay sample of Kırka borate deposit in sulfuric acid solutions. *Journal of Boron, 5*(4), 170-175.

[7] Ezechi, E. H., Isa, M. H., Kutty, S. R., & Sapari, N. B. (2011, September). Boron recovery, application and economic significance: A review. In 2011 *National Postgraduate Conference* (pp. 1-6). IEEE.

[8] Doğan, F., Duru E., Uysal,M., Akbulut, H. & Arslan, S. (2021). Investigation of mechanical and tribological characteristics of Ni-B coatings deposited on steel. *Journal of Boron, 6*(1), 209-215.

[9] Mohana, K.N. & Badiea, A.M. (2008). Effect of sodium nitrite-borax blend on the corrosion rate of low carbon steel in industrial water medium. *Corrosion Science, 50*(10), 2939-2947.

[10] Graham, M. J., Bardwell, J. A., Sproule, G. I., Mitchell, D. F., & MacDougall, B. R. (1993). The growth and stability of passive films. *Corrosion Science, 35*(1-4), 13-18.

[11] Sılku, P., Özkinalı, S., Öztürk, Z., Asan, A., & Köse, D.A. (2016). Synthesis of novel Schiff Bases containing acryloyl moiety and the investigation of spectroscopic and electrochemical properties. *Journal of Molecular Structure, 1116*, 72-83.

[12] Tran, M., Mohammedi, D., Fiaud, C., & Sutter, E. M. M. (2006). Corrosion behaviour of steel in the presence of Y(III) salts: Kinetic and mechanistic studies. *Corrosion Science, 48*(12), 4257-4273.

[13] Igual Muñoz, A., García Antón, J., Guiñón, J. L., & Pérez Herranz, V. (2006). The effect of chromate in the corrosion behavior of duplex stainless steel in LiBr solutions. *Corrosion Science, 48*(12), 4127-4151.

[14] Bethencourt, M., Botana, F. J., Calvino, J. J., Marcos, M., & Rodríguez-Chacón, M. A. (1998). Lanthanide compounds as environmentally-friendly corrosion inhibitors of aluminium alloys: A review. *Corrosion Science, 40*(11), 1803-1819.

[15] Sruthi, R., Rampradheep, G. S., & Raja, K. (2020). A review on natural plant extract as a green inhibitor for steel corrosion resistance. *International Journal of Advanced Science and Technology, 29*(3), 3529-3550.

[16] Paul, S., & Koley, I. (2016). Corrosion inhibition of carbon steel in acidic environment by papayaseed as green inhibitor. *Journal of Bio-and Tribo-Corrosion, 2*(2) 1-9.

[17] Abbas, A. S., Fazakas, É., & Török, T. I. (2018). Corrosion studies of steel rebar samples in neutral sodium chloride solution also in the presence of a bio-based (green) inhibitor. *International Journal of Corrosion and Scale Inhibition, 7*(1), 38-47.

[18] Bakirhan, N. K., Asan, A., Colak, N., & Sanli, S. (2016). The inhibition of steel corrosion in acidic solutions by a new Schiff base. *Journal of the Chilean Chemical Society, 61*(3), 3066-3070 .

[19] Olefjord, I., & Clayton, C. R. (1991). Surface composition of stainless steel during active dissolution and passivation. ISIJ International, 31(2), 134-141.

[20] Alibakhshi, E., Ramezanzadeh, M. Bahlakeh, G.,

Ramezanzadeh, B., Mahdavian, M., & Motamedi, M. (2018). Glycyrrhiza glabra leaves extract as a green corrosion inhibitor for mild steel in 1 M hydrochloric acid solution: Experimental, molecular dynamics, Monte Carlo and quantum mechanics study. *Journal of Molecular Liquids, 255*, 185-198.

[21] Salhi, A., Tighadouini, S., El-Massaoudi, M., Elbelghiti, M., Bouyanzer, A., Radi, S., ... & Zarrouk, A. (2017). Keto-enol heterocycles as new compounds of corrosion inhibitors for carbon steel in 1 M HCl: weight loss, electrochemical and quantum chemical investigation. Journal of Molecular Liquids, 248, 340-349.

[22] McCafferty, E. (2005). Validation of corrosion rates measured by the Tafel extrapolation method. *Corrosion Science, 47*(12), 3202-3215.

[23] Pardo, A., Merino, M. C., Coy, A. E., Viejo, F., Arrabal, R., & Matykina, E. (2008). Pitting corrosion behaviour of austenitic stainless steels - combining effects of Mn and Mo additions. *Corrosion Science, 50*(6), 1796-1806.

[24] Olsson, C. O. A., & Landolt, D. (2003). Passive films on stainless steels - Chemistry, structure and growth. *Electrochimica Acta, 48*(9), 1093-1104.

[25] Mansfeld, F. (1973). Tafel slopes and corrosion rates from polarization resistance measurement. *Corrosion, 29*(10), 397-402.

[26] Oguzie, E. E., Li, Y., & Wang, F. H. (2007). Corrosion inhibition and adsorption behavior of methionine on mild steel in sulfuric acid and synergistic effect of iodide ion. *Journal of Colloid and Interface Science, 310*(1), 90-98.

[27] Aliofkhazraei, M. (Ed.). (2014). *Devolepments in Corrosion Protection*. Intech Open. ISBN: 978-953-51-6359-6.

[28] Ingle, A. V., Raja, V.S., Mishra, P., & Rangarajan, J.(2020). Effect of Mo Addition on the corrosion behavior of Al-40Cr-xMo coatings on type 316L stainless steel. *Metallurgical and Materials Transactions A: Physical Metallurgy and Materials Science, 51*(4), 1933-1944.

BOR DERGİSİ
JOURNAL OF BORON
https://dergipark.org.tr/boron

Lubricants having zinc borate by homogeneous precipitation and Span 60 in spindle oil

Sevdiye Atakul Savrik[1], Burcu Alp[2], Mehmet Gönen[3], Devrim Balkose[4,*]

[1]**Akzo Nobel, Izmir, 35410 Turkey,**
ORCID orcid.org/0000-0002-1402-0569
[2]**Süleyman Demirel University, Department of Chemical Engineering, Isparta, 32260, Turkey**
ORCID orcid.org/0000-0002-0380-2020
[3]**Süleyman Demirel University, Department of Chemical Engineering, Isparta, 32260, Turkey**
ORCID orcid.org/0000-0001-5780-4622
[4]**Izmir Institute of Technology, Department of Chemical Engineering, Izmir, 35430, Turkey**
ORCID orcid.org/0000-0002-1117-9486

ARTICLE INFO

Article history:
Received June 12, 2021
Accepted August 11, 2021
Available online September 30, 2021

Research Article

DOI: 10.30728/boron.951463

Keywords:
Four ball tests
Homogeneous precipitation
Lubricants
Span 60
Zinc borate

ABSTRACT

Nano particles of zinc borate were obtained by homogeneous precipitation method which is based on dissolving zinc borate in ammonia and precipitating it as nano particles by slow evaporation of ammonia. The synthesized zinc borates were characterized by advanced analytical techniques. Zinc borate nano particles were used as a lubricant additive to spindle oil having Span 60 dispersant. The particles were well dispersed in spindle oil as shown by optical microscopy of the oils. Four ball tests of the lubricants indicated zinc borate lowered (61.8%) the wear scar diameter significantly. The hardness of wear surfaces of test balls was reduced from 688 HV to 618 HV and presence of zinc borate particles embedded on the surface indicated a flexible skin was formed. Therefore the pressure was decreased due to increase of the contact area of the balls. The surface roughness was also decreased from 35.63 nm to 27.60 nm by the addition of zinc borate to spindle oil having Span 60. Zinc borate prepared by homogeneous precipitation technique lowered the wear of the surfaces that rub to each other.

1. Introduction

Nano particles of zinc borate hydrates can be obtained using different methods. $4ZnO \cdot B_2O_3 \cdot H_2O$ nanoparticles can be synthesized by dissolving the precipitate obtained from borax decahydrate and zinc nitrate solution [1] or by dissolving $2ZnO \cdot 3B_2O_3 \cdot 3.0\text{-}3.5H_2O$ [2] in ammonia and then reprecipitating it with the help of evaporation of ammonia by heating the solution. Forming zinc borate nano particles in mineral oil allows the use of the mixture as lubricating oil [3]. Hydrophobic zinc borate nanoparticles could be obtained from zinc oxide, boric acid and oleic acid in water [4]. Saffari et al. prepared nano-sized zinc borates at 200°C and 15 bar pressure from aqueous borax and zinc nitrate solutions [5]. The surfactants are added to the mixture in order to obtain nano zinc borate particles with different geometries [6-9]. Agglomerates of nano zinc borate platelets were obtained from nano zinc oxide and boric acid at 85°C with surfactants or without surfactants. Either $2ZnO \cdot 3B_2O_3 \cdot 7H_2O$, $2ZnO \cdot 3B_2O_3 \cdot 3.5H_2O$ or $3ZnO \cdot 3B_2O_3 \cdot 5H_2O$ were obtained by mixing aqueous borax and sodium nitrate solutions in different proportions by controlling the temperature (80°C-90°C) and pH [10]. The effects of temperature (45°C-85°C), mixing rate (400-500 rpm) and reactant feed rate (300-900 cm^3 hr^{-1}) on zinc borate particle size were investigated by Polat and Sayan [11]. Zinc sulfate hydroxide ($Zn_4SO_4(OH)_6$) and boric acid in aqueous solution were used in zinc borate preparation [12]. The morphology of zinc borates ($2ZnO \cdot 3B_2O_3 \cdot 3H_2O$) changed from platelet to polyhedron at the reaction temperature of 90°C with increasing the water content in the reaction solution [12].

Zinc borates had flame retarding effect in epoxy resin [1], polyvinyl chloride [2], polyethylene [4], polyurethane [10], polyvinyl alcohol [12] and cellulose [13]. Cotton fabric that was dried after immersing in a suspension of nano particles of zinc borate had flame retardant properties [13].

Many studies were made using zinc borate nanoparticles as lubricant additives [3]. Zinc borate nanoparticles by inverse emulsion method in mineral oil using Span 60 lowered friction coefficient and wear scar diameter in four ball tests compared to that of pristine mineral oil [3]. Nano zinc borate with 40 nm size dispersed in mineral oil lowered the wear scar diameter by 50% and friction coefficient by 20% [14]. Nano zinc

*Corresponding author: devrimbalkose@iyte.edu.tr

borates with 600 nm size improved the tribological properties of water-based drilling fluids [5]. Sunflower oil containing zinc borate with a particle size of 500-800 nm lowered the friction and wear, as well [15]. The tribological capacity of zinc borate ultrafine powders modified with hexadecyltrimethoxysilane or oleic acid in mineral oil can be explained by the formation of continuous tribo-film on the worn surface which improves the friction and wear properties [16].

The present study aims the synthesis of zinc borate nano particles which are used as a lubricant additive in order to reduce the wear of the metal machine parts that rub to each other. For this purpose, the aqueous zinc nitrate and borax solutions were mixed and the precipitate was dissolved with ammonia. Nano particles of zinc borate were formed as the ammonia was evaporated by heating. The nano particles were characterized by advanced analytical methods. The effect of nano zinc borate on tribological behavior of spindle oil was investigated. Both the state of dispersion of particles in lubricants and tribological behavior of the lubricants were determined and the worn test surfaces were characterized by elemental analysis, atomic force microscopy (AFM), scanning electron microscopy (SEM) and Vickers hardness.

2. Materials and Methods

Borax decahydrate (99.9%, Eti Maden Inc.), zinc nitrate hexahydrate (99.9%, Fluka), Sorbitan monostearate (Span 60) from Sigma Aldrich, ethanol (99.8%) from Riedel were used in the experiments. Light neutral oil called as spindle oil (SN 150) (TÜPRAŞ A.Ş) was used as a base oil for lubricant preparation.

2.1. Synthesis of Zinc Borate

The precipitation of zinc borate in the bulk phase was carried out by homogeneous precipitation method [2,6,17]. 20 cm^3 1.25 mol dm^{-3} zinc nitrate and 30 cm^3 0.08 mol dm^{-3} borax solution were mixed at 45°C. The formed white precipitate was dissolved by addition of 12.5 cm^3 25% ammonia. The mixture was added to 75 cm^3 water and mixed at 600 rpm by magnetic stirring at 45°C in an 8 cm diameter open container. During the mixing the pH of the solution was monitored by a pH meter. Nano zinc borate precipitated while ammonia was slowly evaporated. The experiments were repeated for different heating periods of 3, 5, 6,12 and 15 hours in order to reveal the effect of heating time on the tribological properties of the lubricants The volume of each solution was measured at the end of the heating period. The white sediment for each heating period was separated by centrifuging at 9000 rpm for 10 minutes, washed with ethanol and water and recentrifuged. The sediments were dried at 40°C under vacuum for 12 hours. A lower drying temperature (40°C) was applied rather than that of the previous investigators [2,17] drying temperature (70°C) to avoid further reaction and growth of particles during drying.

2.2. Characterization of Zinc Borate

The Fourier Transform Infrared (FTIR) spectra of the samples were attained by KBr transmission method in Shimadzu FTIR 8601. For thermal characterization, the samples (10-15 mg) were heated from room temperature to 600°C at 10°C min^{-1} under N_2 flow of 40 cm^3 min^{-1} in alumina sample holder in Thermogravimetric (TG) analysis and in aluminum pan for Differential Scanning Calorimetric (DSC) analysis in Shimadzu TGA 51 and Shimadzu DSC 50, respectively. X ray diffraction diagrams (XRD) of the samples were obtained with CuK_α radiation with 0.154 nm wavelength in Philips Xpert-Pro. SEM micrographs of gold sputtered samples fixed to a double sided tape were achieved using Philips XL30 SFEG. C, H, N, S content of the samples were determined in CHNS analyzer (Leco). The experiments run in dublicate and the average results were reported. The particle size distribution of samples dispersed in water using 1% calgon was measured by Malvern Mastersizer 2000. An analytical titration method described by Savrik [14] was used for determination of B and Zn contents of the samples. The titration experiments were run in triplicate and their average was reported.

2.3. Preparation of Lubricants

The lubricants were prepared using sorbitan monostearate as a surfactant. Firstly, 1 g sorbitan monostearate was dissolved in 100 cm^3 spindle oil and heated up to 70°C, secondly, 1 g zinc borate prepared at different heating periods during its preparation was dispersed in the spindle oil. The lubricants are coded as L1: spindle oil, L2: spindle oil with surfactant, L3: spindle oil with surfactant and zinc borate heated for 6 hours, L4: spindle oil with surfactant and zinc borate heated for 12 hours and L5: spindle oil with surfactant and zinc borate heated for 15 hours. The lubricants were mixed at 150°C at 20000 rpm for 2 minutes using a 700 Watt homogenizer (OMNI GLH) with 10 mm diameter rotor-stator generator prob. The samples were further stirred for 2 hours using a magnetic stirrer (Yellowline MSH Basic) at 600 rpm.

2.4. Characterization of Lubricants

The microphotographs of lubricants at room temperature were taken with an optical microscope (Olympus BX60M) fitted with a digital camera (Olympus DP25). The avarege diameters of particles in oil were measured by Olympus DP2-BSW program.

A four-ball wear test machine (Falex Corp.) was used for measurement of the friction coefficient and wear scar diameter of test balls for the lubricants L1-L5. The test was performed according to ASTM D 4172-94.

2.5. Characterization of Balls After Four Ball Tests

2.5.1. Cutting of fixed balls

Fixed balls used for four ball tests for spindle oil (L1), spindle oil with dispersant (L2) and spindle oil with dispersant and zinc borate heated for 15 hours (L5) during its preparation were cut into half with a microcutter (Metkon Microcut Precision Cutter) operating at 2000 rpm using water as coolant. Thus worn surfaces of the balls could further be examined by SEM, EDX, AFM and microhardness testing.

2.5.2. Microhardness tests

Microhardness of the unworn and worn surfaces of the fixed balls was measured with digital microhardness tester (TIME HVS-1000) operating at 4.9 N load and 20 s indentation time. Average of the measurements at three points was reported as the hardness of the ball surface in Vicker's Hardness (VH).

2.5.3. Atomic force microscopy

Multimode Atomic Force Microscope (Digital Instrument, Nanoscope IV) was used for measurement of roughness of the wear scars of the fixed balls.

2.5.4. EDX

EDX analysis of the uncoated samples was achieved using Philips XL30 SFEG.

3. Results and Discussion

3.1. Synthesis of Zinc Borate

Nano-sized zinc borate particles were produced according to homogeneous precipitation technique described by Mergen et al [2], İpek [6] and Ting et al. [17]. The mechanism of this method is explained as the following. Firstly, zinc nitrate to Zn^{2+} cations and NO_3^- anions and borax decahydrate dissociates to $[B_4O_5(OH)_4]^{2-}$ and Na^+ cation in the solutions. When these two solutions are mixed $Zn[B_4O_5(OH)_4]$ precipitates. The precipitate dissolves forming $Zn(NH_3)_4^{2+}$ complex as ammonia is added to the mixture. As the solution was heated at 45°C, ammonia and water are evaporated from the system. 17, 36, 93 and 116 cm^3 water was eliminated from total volume of 137.5 cm^3 solution for 3, 5, 6 and 15 hours of heating. The solution become concentrated at long periods of heating and by products such as sodium nitrate precipitates besides zinc borates. The by products were eliminated by washing the precipitates. The pH value of the ammonia added solution was 10 initially and it was lowered with time as it was heated at 45°C in the open container. At the end of 3, 6, 12 and 15 hours, pH values were measured as 8.8, 8.2, 6.6 and 5.3, respectively. The decrease in pH was due to the removal of ammonia by heating and reaction 1 as reported by Savrik [18].

$$Zn[B_4O_5(OH)_4]\cdot H_2O(s) + 2H_2O(l) \rightarrow Zn[B_3O_3(OH)_5]\ H_2O(s) + B(OH)_3(s) \quad (1)$$

$Zn[B_4O_5(OH)_4]\cdot H_2O$ precipitates when the zinc ion concentration satisfies its solubility parameter. The precipitation reaction of zinc cations and borate can only reach to molecular level due to small concentration of zinc ions. The growth of the crystals was inhibited owing to the presence of few Zn^{2+} ions in the solution. Thus nano-sized particles form. Further heating the mixture leads to the formation of $Zn[B_4O_5(OH)_4]\cdot H_2O$ and then $Zn[B_3O_3(OH)_5]$. However at higher pH values (10-12) Zn^{2+} ions reacts with OH^- and NO^{3-} ions to form zinc hydroxyl nitrate, $Zn_5(OH)_8(NO_3)_2\cdot 2H_2O$ as indicated by Savrik et al [14].

3.2. Characterization of Zinc Borates

The FTIR spectra of zinc borates prepared are shown in Figure 1a They exhibit the specific peaks of borate groups reported in the literature [17,19]. The band at 3300 cm^{-1} is due to hydrogen bonded O-H groups stretching vibration. The band at 1634 cm^{-1} belonged to H-O-H bending vibration indicating that the samples had crystal water. The stretching bands of B(3)-O and B(4)-O are observed at 1343 and 1050 cm^{-1} respectively. The peaks between 745-658 cm^{-1} belong to out-of-plane bending mode of B(3)-O. The peak intensities also do not increase with mixing time.

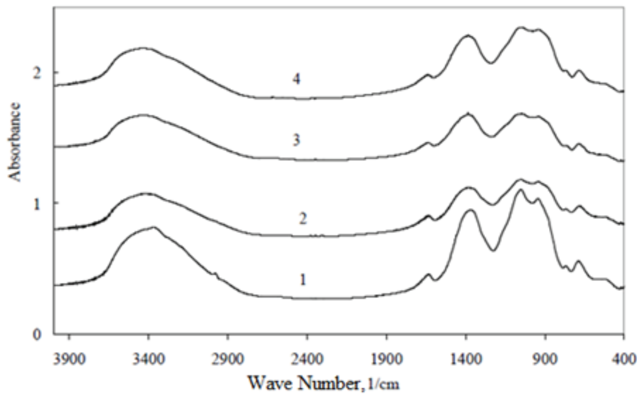

Figure 1. FTIR spectra of the samples obtained by heating 3 (Plot 1), 6 (Plot 2), 12 (Plot 3) and 15 (Plot 4) hours at 45°C during their preparation.

XRD diagrams of the zinc borates in Figure 2 have no sharp diffraction peaks. The line broadening due to nano-sized crystals formed and overlap of the broadened peaks results in a diffraction diagram similar to that of an amorphous substance. The precipitates obtained from dilute zinc nitrate and borax solutions at 25°C by Savrik et al [14] had similar x-ray diffraction diagrams of the samples obtained in the present study. On the other hand İpek [6] obtained sharp peaks at 2θ values of 13.2°, 17.5°, 19.8°, 21.2°, 23.4°, 26.5°, 28.5°, 30.9°, 33.4°, 35.3°, 37.4°, 40.2°, 41.1°, 43.3°, 44°, 47.2°, 50.3°, and 54.9° belonging to $2ZnO.3B_2O3\cdot 7H_2O$ (JCPDS 75-0766) for the nano particles with 211 nm mean size. The primary particle size of particles in the present study should have been much smaller since they had very large line broadening. According to Scherrer Equation.

$$L = k\lambda/(B \cos\theta) \qquad (2)$$

Where L is the size of the crystals perpendicular to diffraction plane with θ angle in nm, k=constant which is taken as 0.9, λ is the wavelength of the x-rays. For CuK_α radiation the wavelength is 0.1546 nm. B is the breadth of the diffraction line at half height at angle θ. For instance the breadths of the first two peaks at 2θ values of 13.2° and 17.7° of XRD diagram of $2ZnO.3B_2O_3{\cdot}7H_2O$ were found as 3.20° and 3.22° respectively for particle size of 5 nm using Scherer equation. The breadth increases to 4.02° and 4.04° as the particle size is reduced to 4 nm. This value is sufficient for the overlap of the first two peaks of the XRD diagram of $2ZnO.3B_2O_3{\cdot}7H_2O$ at 2θ value of 13.2° and 17.7°. The line broadening values of the x-ray peaks increases to 3.6° and 4.5° for 2θ value of 54.9° for 5 and 4 nm particle sizes respectively. Thus for 4 to 5 nm particle size all the x-ray diffraction peaks of $2ZnO.3B_2O_3{\cdot}7H_2O$ will be broadened and overlap with each other.

Ting et al. [17] indicated formation of crystalline phases with increased heating period. The diffraction diagrams obtained did not belong to any of the known zinc borates [17].

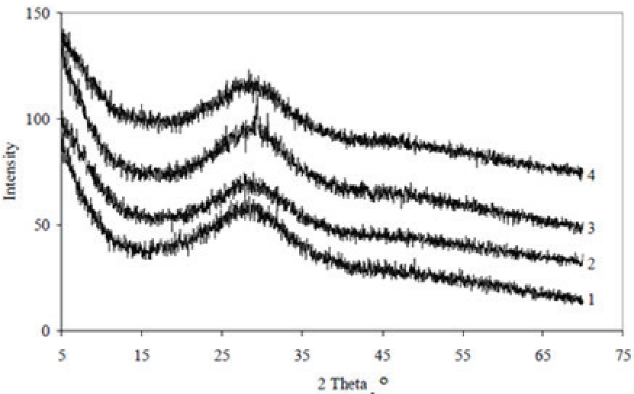

Figure 2. XRD diagrams of samples heated for 3 (Plot 1), 6 (Plot 2), 12 (Plot 3) and 15 (Plot 4) hours at 45°C during their preparation.

The TG curves of the samples are shown in Figure 3. Since all the samples were dried at 40°C further heating would eventually cause evaporation of remaining water. The onset of mass loss is 50°C for all samples. The first step of the mass loss was completed at 270°C for the sample heated for 3 hours and there was a small second step at 520°C. There was a second step of mass loss at 490°C for the sample heated for 6 hours. The sample heated for 9 hours completed its mass loss at 550°C. The sample heated for 15 hours had a second step of mass loss at 250°C.

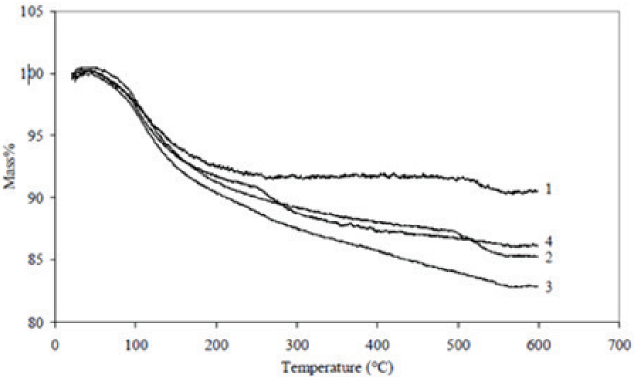

Figure 3. TG curves of samples heated for 3 (Plot 1), 6 (Plot 2), 12 (Plot 3) and 15 (Plot 4) hours at 45°C during their preparation.

Considering dehydration behavior of possible products that will be obtained in the precipitation reaction, their identification was attempted to be made in the present study.

Alp et al. [20] determined the onset of dehydration of zinc borate $2ZnO{\cdot}3B_2O_3{\cdot}7H_2O$, $2ZnO{\cdot}3B_2O_3{\cdot}3H_2O$ as 129°C and 320°C, respectively, at a 10°C min^{-1} heating rate. Therefore, the present samples could only be zinc borate with seven mols of water.

Formation of $Zn_5(OH)_8(NO_3)_2{\cdot}2H_2O$ was also possible in homogeneous precipitation reaction. The dehydration of $Zn_5(OH)_8(NO_3)_2{\cdot}2H_2O$ occurs in three steps. The first step at 120°C is due to crystal water loss, the second step is at 145-160°C because of the de-hydroxylation, whereasthe third step between about 160-230°C is owing to decomposition to ZnO and nitrogen- and oxygen-containing compounds [21]. On the other hand, $4ZnO{\cdot}B_2O_3{\cdot}H_2O$ was stable up to around 520°C and no considerable weight loss was detected up to this temperature. A sharp decrease in weight (4.4 wt%.) occurred between 520 and 560°C [2].

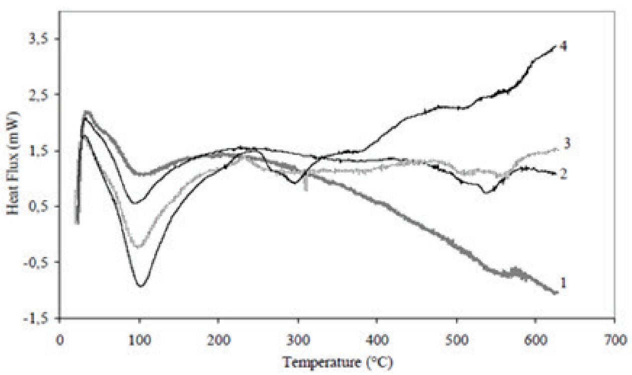

Figure 4. DSC curves of samples heated for 3 (Plot 1), 6 (Plot 2), 12 (Plot 3) and 15 (Plot 4) hours at 45°C during their preparation.

DSC curves of the samples shown in Figure 4 exhibit two endothermic peaks at around 100°C and 500°C that may be due to loss of free and bound water. Table 1 presents the dehydration behavior of the samples and the first endothermic peak of the samples is re-

Table 1. Dehydration temperatures and enthalpies of samples prepared by heating for different periods.

Heating Time	First Peak				Second Peak			
	Onset (°C)	Maximum (°C)	Endset (°C)	ΔH ($J\ g^{-1}$)	Onset (°C)	Maximum (°C)	Endset (°C)	ΔH ($J\ g^{-1}$)
3	33.1	100.6	204.7	-163.7	520.0	582.0	580.0	-10.7
6	31.0	94.6	230.4	-220.2	504.4	538.5	582.3	-61.6
12	48.9	98.2	162.3	-191.0	309.7	521.5	313.9	-1.7
15	40.4	102.2	233.3	-305.0	245.6	296.4	365.9	-43.0

lated to removal of free water from the samples and the second peak is linked to the removal of water formed by the condensation of OH groups. The enthalpy changes were calculated from the areas of the observed peaks. The high enthalpy change (ΔH) of the first peak than that of the second peak indicated the presence of higher amount of free water than bound water in the samples.

The elemental composition of the samples displayed in Table 2 were determined by CHNS elemental analyzer. The samples contained N and C elements besides H. The samples contained 1.19 to 2.02 %. N which might be present as NO_3^- ions. The presence of carbon (0.39-1.51 %) in the samples may be due to the CO_2 adsorption of the samples from the air.

Table 2. C, H, N element % of zinc borates obtained at different time of heating.

Time (h)	Average (wt %)		
	C	H	N
3	0.43±0.10	1.99±0.04	1.19±0.01
6	0.44±0.02	2.15±0.09	2.13±0.01
12	0.39±0.10	1.99±0.06	1.77±0.01
15	1.51±0.05	2.30±0.04	2.02±0.01

ZnO % and B_2O_3 %, CO_3^{2-} and NO_3^-, contents of the samples are shown in Table 3. B_2O_3/ZnO molar ratio of samples for different mixing periods is changing between 0.683 and 0.755 as seen in the Table 3. This results the empirical formula of the zinc borate obtained as $2ZnO.3B_2O_3.xH_2O$.

Water content of the samples were determined by three different methods. The first method is thermogravimetric analysis. The total mass loss at 600°C corresponds to elimination of water from the samples. The second method is CHNS analysis. It can be assumed that the H in the samples can only be present as H_2O or OH. The third method is related to the material balance of chemical analysis. The difference between 100 and the summation of B_2O_3 %, ZnO %, CO_3^{2-} % and NO_3^- % gives the water content by material balance. Mass losses of the samples are changing from 9.48% to 17.07% by to TG analysis, 17.91-20.7 % by CHNS elemental and 9.36% to 16.50% by material balance.

$2ZnO{\cdot}3B_2O_3{\cdot}3H_2O$ and $ZnO{\cdot}B_2O_3{\cdot}2H_2O$ contain 12.69% and 19.25% H_2O, respectively [22], [23]. The water content of $2ZnO{\cdot}3B_2O_3{\cdot}3H_2O$ is eliminated above 340°C [22], the samples prepared in the present study can not be $2ZnO{\cdot}3B_2O_3{\cdot}3H_2O$ since their maximum dehydration temperature is around 100°C as DSC analysis indicated.

Particle size distributions of samples are found as bidisperse as shown in Figure 5. There is a small peak being maximum around 600 nm, and a big peak around 20 μm. The mean particle diameter of zinc borate particles were increased with heating time from 16.78, 18.93, 18.22 and 22.36 μm for 3, 6, 12 and 15 hours heating time, respectively. These large particles were thought to be formed by the agglomeration of the nanoparticles formed by homogeneous precipitation.

SEM images of the sample heated for 3 hours are ex-

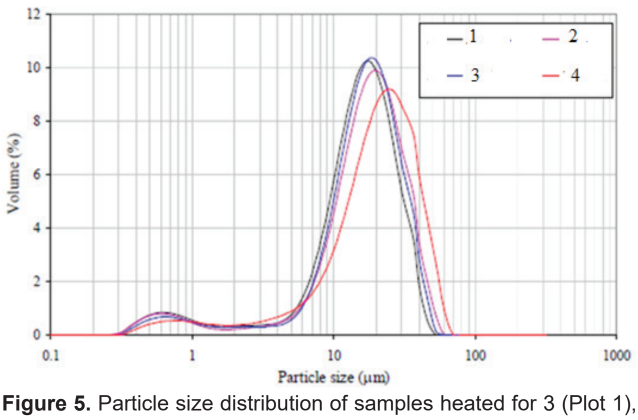

Figure 5. Particle size distribution of samples heated for 3 (Plot 1), 6 (Plot 2), 12 (Plot 3) and 15 (Plot 4) hours at 45°C during their preparation.

Table 3. ZnO, B_2O_3, CO_3^{2-} and NO_3^- weight % and B_2O_3/ZnO molar ratio and H_2O weight % of zinc borates.

Time (h)	Weight (%)				B_2O_3/ZnO	H_2O (%)		
	ZnO	B_2O_3	CO_3^{2-}	NO_3^-	mol ratio	TG	CHNS	Chem.
3	44.81	31.27	2.15	5.27	0.683	9.48	17.91	16.50
6	42.28	30.94	2.20	9.43	0.736	14.76	19.35	15.15
12	43.78	30.95	1.95	7.84	0.734	17.07	17.91	15.48
15	42.36	31.78	7.55	8.95	0.755	13.89	20.70	9.36

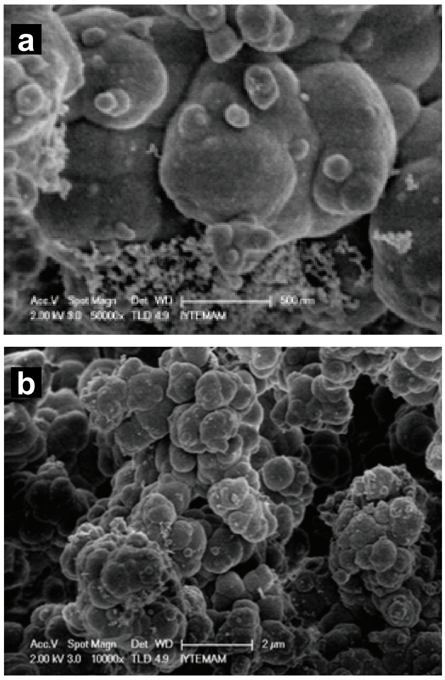

Figure 6. SEM micrographs of the sample heated for 3 hours at 45°C during its preparation. At a. 50000x, b. 10000x magnification. The scale is 500 nm and 2 µm for a and b, respectively.

hibited in Figure 6. Spherical agglomerates are with 100-500 nm size are observed in Figure 6a. The agglomerated particles were also sticked together to form larger particles as seen in Figure 6b. Since the particle size analysis indicated the presence of particles around 20 µm, these particles were also further agglomerated. It was thought that these agglomerates formed by continuous mixing of the precipitation medium at high rate, 600 rpm for long period. The decrease in stirring rate could solve the agglomeration problem. This problem of agglomeration were also observed by other investigators [7-9].

3.3. Characterization of Lubricants and Wear Surfaces

3.3.1. Optical microscopy of lubricants

The inorganic additives were used simultaneously with dispersants in lubricants. The surfactant, sorbitan monostearate (Span 60) was employed as dispersant in the present study. Figure 7 indicates the optical microphotographs of the spindle oil (L1), spindle l oil with dispersant (L2) and spindle oil with dispersant and zinc borate heated for 15 hours (L5). The microphotograph of the spindle oil (Figure 7a) has only an air bubble, whereas, the microphotographs of the oil with additives has the polydispersed particles. The spindle oil with Span 60 has rod-like shape particles with 5.55 µm average length (Figure 7b). When the zinc borate mixed for 15 hours is added into spindle oil, average diameter of the particles is 3.06 µm (Figure 7c). Span 60 covered the zinc borate particles and therefore rod like Span 60 particles are not present. The particle size of the samples differs than the values measured by particle size distribution analysis since the zinc borate particles are well dispersed in mineral oil. Besides, the homogenization process during lubricant preparation disperses the agglomerated zinc borate particles.

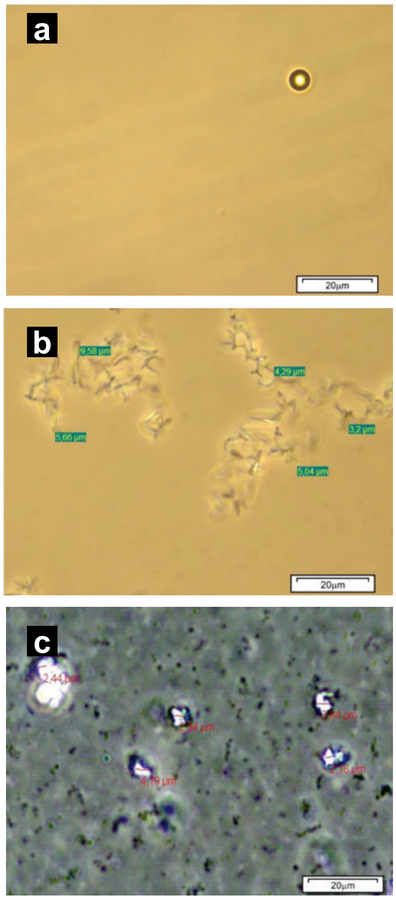

Figure 7. Optical micrographs of a. Spindle oil (L1), b. Spindle oil and dispersant (L2), c. Spindle oil with dispersant and zinc borate heated for 15 hours.

3.3.2. Tribological properties of the lubricants

Colloidal boron compounds are more effective extreme pressure and antiwear additives compared to sulfur and phosphorous containing additives which are considered causing damage to both engine and environment [24-27]. Zinc borate particles are added to spindle oil and four ball tests were applied to determine the tribological properties in the present study. Results of the four ball tests of the lubricants are reported in Table 4 for both the present study and previous studies.

At 75°C, the four ball test temperature, Span 60 dispersed in spindle oil is in liquid form since it melts at 50°C [18]. It has strong effect on reducing friction coefficient and wear scar diameter in four ball tests since it can be adsorbed on the surfaces of the balls with its polar ester groups. When Span 60 and zinc borate are added simultaneously to spindle oil, Span 60 ensures the even dispersion of zinc borate particles. On the other hand, Span 60 addition to spindle oil lowered the coefficient of friction from 0.1 to 0.07. The friction

Table 4. Tribological properties of lubricants.

Code	Lubricant	Friction coefficient	Wear scar diameter (mm)	Reference
L1	Spindle oil	0.10	1.40	Present study
L2	Spindle oil with Span 60	0.07	0.66	Present study
L3	Spindle oil with Span 60 and zinc borate 6 hour	0.09	0.56	Present study
L4	Spindle oil with Span 60 and zinc borate 12 hour	0.07	0.53	Present study
L5	Spindle oil with Span 60 and zinc borate 15 hour	0.08	0.53	Present study
-	Nano zinc borate and Span 60in mineral oil by inverse emulsion	0.09	0.60	[3]
-	Nano zinc borate and Span 60 in mineral oil	0.08	0.69	[14]

coefficient of spindle oil with Span 60 and zinc borate prepared by mixing 6, 12 and 9 hours had friction coefficients of 0.09, 0.07 and 0.08 respectively (Table 4). The wear scar diameter was reduced from 1.4 mm to 0.66 mm by addition of the sufactant Span 60. It was 0.56 mm, 0.53 mm and 0.53 mm for the lubricant with both surfactant and zinc borates prepared in 6, 12 and 15 hours respectively as seen in Table 4. Thus wear scar diameter of the lubricant with zinc borate heated for 12 hours was smaller than 61.8% than the spindle oil (L1). The zinc borates lowered the wear scar diameter compared to that of the spindle oil having only surfactant (L2) (Table 4). Lubricant with Span 60 and nano zinc borate prepared by heating for 12 hours had minimum coefficient of friction and wear scar diameter among the present and previous studies [3,14] as presented in Table 4. The decrease in the wear of the surfaces with lubricants with zinc borate particles is due to filling of the cavities created on the worn surface by them. Therefore, the smoother surfaces result in a decrease in shearing stress and tribological properties.

3.3.3. Surface topography and composition of the worn balls

The surface topography of unworn and worn surfaces of the test are shown in Figure 8 and their average surface roughness values measured by AFM are tabulated in Table 5. The images showed that no new phase was obtained on the rubbed surfaces of the test balls. The agglomeration of particles on the pit in Figure 8a might be the deposition film on the friction contacting area. Figure 8b exhibits much smoother surface. The surface roughness was also decreased from 35.63 nm to 27.60 nm by the addition of zinc borate to spindle oil having Span 60.

The fixed balls lubricated with spindle oil (L1), spindle oil and sorbitan monostearate (L2), the lubricant containing sorbitan monostearate and zinc borate (L5) were cut with a microcutter for closer examination of worn surfaces by SEM. The scars and pits observed by AFM on the surfaces are also visible in SEM micrographs of worn surfaces in Figure 9.

The elemental composition of unworn, worn and deformed surface of the fixed ball lubricated with the oil with Span 60 and zinc borate particles was determined by EDX (Figure 8c). The white, red and green frames in Figure 9c represent areas of pristine, worn and deformed surfaces. The EDX analysis results of these surfaces are listed in Table 6. The oxygen content is higher for the deformed and worn surfaces than that of pristine surface due to oxidation by cooling water used during cutting process. Boron content was also higher for the worn surface. While in previous stud-

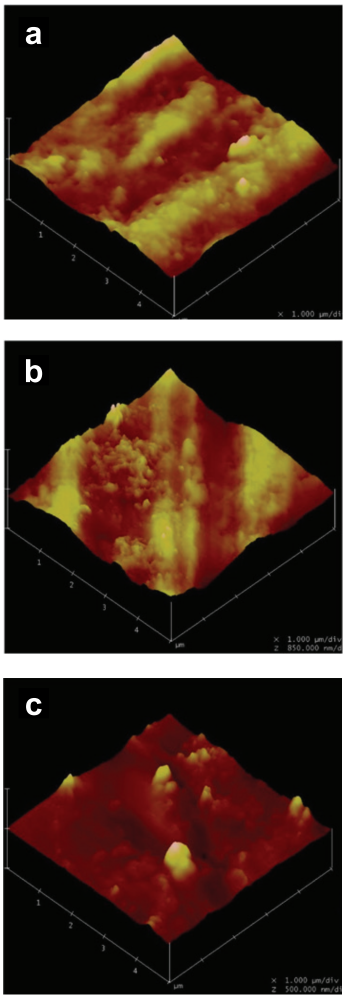

Figure 8. Three dimensional AFM view of 5μm x 5μm are of worn surfaces of balls after four ball tests. Surfaces of ball tested with a. Spindle oil, b. Spindle oil with Span 60 c. Spindle oil with Span 60 and zinc borate heated for 15 hours.

Table 5. Surface rougness and hardness of values unworn and worn surfaces of test balls after four ball tests.

Ball Surface	Surface Roughness R_a(nm)	Surface Hardness Vickers
Unworn	35.37	709
Worn with Spindle oil (L1)	27.10	677
Worn with Spindle oil with Span 60 (L2)	35.63	688
Worn with Spindle oil with Span 60 and zinc borate (L5)	27.60	618

ies either only B element [25] or Zn element [16] was found on the worn surface, both elements existed simultaneously in the present study. This indicated that zinc borate particles were embedded on the surface.

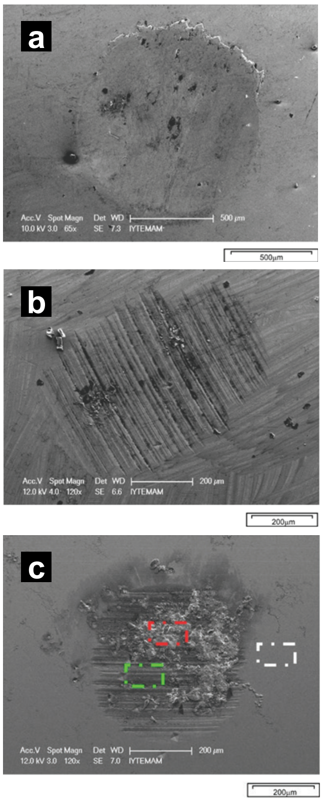

Figure 9. SEM micrographs of warn surfaces of balls after four ball tests with a. Spindle oil (L1) b. Spindle oil with Span 60 (L2), c. Spindle oil with Span 60 and zinc borate heated for 15 hours (L5) (white frame: Pristine surface, red frame: Worn surface, green frame. Deformed surface.

3.3.4. Surface hardness

The hardness of pristine and worn surfaces of four ball test balls was measured by indentation test and results are shown in Table 5. The average Vickers hardness value of the pristine ball surface was found as 709 HV (equivalent to 61 HRC). This value is consistent with literature value of 52100 steel which is 59-61 HRC. The average Vickers hardness values of the balls lubricated with spindle oil (L1), spindle oil with surfactant (L2) and the lubricant including zinc borate (L5) were measured as 677, 688 and 618 HV, respectively. The hardness of the worn surface with oil with Span 60 is higher than that of the worn surface with pure oil (L1). This can be explained by the migration of polar groups to the metal surface and formation of physical bonds with surfaces. However, the addition of zinc borate particles to spindle oil (L5) considerably decreases hardness of worn surface. A soft thin layer which candeform easily could be the cause of this behavior. Therefore the pressure is decreased due to the decrease of the contact area between the rubbing surfaces and the wear scar diameter is lowered, as well [15,28].

Table 6. Elemental composition of unworn, worn and deformed surfaces of the fixed ball after four ball test with lubricant with Span 60 and zinc borate.

Element	Mass (%)		
	Pristine Surface	Worn Surface	Deformed Surface
Carbon	4.8	18.5	38.4
Oxygen	1.7	8.4	13.5
Iron	80.3	56.2	21.0
Silicon	0.8	0.4	0.8
Chromium	1.4	1.3	0.6
Manganese	2.0	0.7	0.6
Sulfur	0.4	0.2	0.4
Phosphorous	0.6	0.1	0.2
Nickel	2.6	1.1	0.9
Calcium	0.2	0.2	0.6
Boron	5.4	10.8	21.4
Zinc	0.0	2.3	1.6

4. Conclusions

In this study, zinc borates were obtained from zinc nitrate and borax solutions. Dissolution of zinc borate with ammonia and reprecipitation by removing ammonia resulted in formation of nanoparticles of zinc borate. The FTIR spectra of the samples confirm the presence of borate groups. XRD of the samples appear as if they belong to amorphous substances. Spherical agglomerated particles were formed due to mixing of the precipitation medium at high rate for long periods. The mean particle diameter of zinc borate particles dispersed in water were measured as 16.78 μm, 18.93 μm, 18.22 μm and 22.36 μm for 3, 6, 12 and 15 hours heating at 45°C during preparation of zinc borates respectively.

The zinc borate particles were well dispersed in spindle oil with average diameter of 3.06 μm. In the lubricant large sized particles such as 22.36 μm was not detected which confirmed the homogenization process during lubricant preparation well dispersed the agglomerated zinc borate particles. The zinc borate particles also points their potential use as tribological additives. The wear scar diameter was reduced by 61.8% for lubricant containing zinc borate and Span 60 as compared to the spindle oil. The boron and zinc contents of the worn surfaces lubricated with oil with zinc borate were higher than that of the unworn surfaces. This may be caused by the presence of embedded zinc borate additive on the worn surface. The hardness of the worn surface lubricated with spindle oil containing surfactant was highest one compared to the surfaces lubricated with only oil and oil having both zinc borate and surfactant.

Acknowledgement

The authors thank to OPET Mineral Oil Factory for the measurement of tribological properties of the lubricants. Turkish Scientific and Technological Research Council is acknowledged for supporting this study with project number 105M358.

References

[1] Gao, P. Q., Song, W. H, & Wang X. (2013). Preparation and characterization of nano zinc borate/epoxide resin composite. *Key Engineering Materials, 567*, 87-90.

[2] Mergen, A., Ipek, Y., Bolek, H., & Oksuz, M. (2012). Production of nano zinc borate (4ZnO·B2O3·H2O) and its effect on PVC. *Journal of Europan Ceramic Society, 32*, 2001-2005.

[3] Savrık, S. A., Balköse, D., & Ülkü, S. (2011). Synthesis of zinc borate by inverse emulsion technique for lubrication. *Journal of Thermal Analysis and Calorimetry,104*(201), 605-612.

[4] Li, S., Long, B., Wang, Z., Tian, Y., Zheng, Y., & Zhang, Q. (2010). Synthesis of hydrophobic zinc borate nanoflakes and its effect on flame retardant properties of polyethylene. *Journal of Solid State Chemisty,183*, 957-962.

[5] Saffari, H. R. M., Soltani, R., Alaei, M., & Soleymani, M. (2018). Tribological properties of water-based drilling fluids with borate nanoparticles as lubricant additives, *Journal of Petroleum Science and Engineering, 171*, 253-259.

[6] Ipek, Y. (2020). Effect of surfactant types on particle size and morphology of flame retardant zinc borate powder, *Turkish Journal of Chemistry, 44*, 214-223.

[7] Baltacı B. (2010). *Synthesis and Characterizatıon of Nano Zinc Borate and Its Usage as A Flame Retardant for Polymers* [M. Sc. thesis, Middle East Technical Universitiy]. Council of Higher Education Thesis Center (Thesis Number 286210).

[8] Baltaci, B., Cakal, G. O., Bayram, G., Eroglu, I., Ozkar, S. (2013). Surfactant modified zinc borate synthesis and its effect on the properties of PET. *Powder Technology, 244*,38-44.

[9] Cakal, G. O., Baltaci, B., Bayram, G., Ozkar S., & Eroglu, I. (2020). Synthesis of zinc borate using water soluble additives: Kinetics and product characterization. *Journal of Crystal Growth, 533*, 125461.

[10] Cui, Y., Liu, X., Tian, Y., Ding, N., & Wang, Z. (2012). Controllable synthesis of three kinds of zinc borates and flame retardant properties in polyurethane foam. *Colloids and Surfaces A: Physicocheical and Engineering Aspects 414*, 274-280.

[11] Polat, S., & Sayan, P. (2020) Box-Behnken experimental design for zinc borate Zn2B6O11·7H2O. *Journal of Boron, 5*(3), 152-161.

[12] Gao, J., Yin, H., Wang, A., & Jiang, T. (2013). Preparation of zinc borates with different structures and morphologies and their effect on thermal and oxidative stability of polyvinyl alcohol. *Powder Technology, 237*, 537-542.

[13] Durrani, H., Sharma, V., Bamboria, D., Shukla, A., Basak, S., & Ali, W. (2020). Exploration of flame retardant efficacy of cellulosic fabric using in-situ synthesized zinc borate particles, *Cellulose, 27*, 9061-9073.

[14] Savrik, S. A., Alp, B., Ustun, F., & Balköse, D. (2018). Nano zinc Borate as a lubricant additive. *Journal of Turkish Chemical Society A, 5*(1), 45-52.

[15] Zhao, C., Jiao, Y., Chen, Y., & Ren, G. (2014). The Tri bological Properties of Zinc Borate Ultrafine Powder as a Lubricant Additive in Sunflower Oil. *Tribology Transactions, 57*, 425-434.

[16] Zhao, C., Chen, Y.K., Jiao, Y., Loya, A., & Ren, G. G., (2014). The preparation and tribological properties of surface modified zinc borate ultrafine powder as a lubricant additive in liquid paraffin. *Tribology International 70*, 155-164.

[17] Ting, C., Deng, J. C., Shuo, W. L., & Gang, F. (2009). Preparation and Characterization of Nano-Zinc Borate by a New Method. *Journal of Materials Processing Technology, 209*, 4076-4079.

[18] Savrik S. A. (2010). *Enhancement of Tribologıcal Properties of Mineral Oil by Addition of Sorbitan Monostearate and Zinc Borate* [PhD Thesis, İzmir Institute of Technology). Council of Higher Education Thesis Center (Thesis number 266584).

[19] Gao, Y. H., & Liu, Z. H. (2009). Synthesis and thermochemistry of two zinc borates, Zn2B6O11·7H2O and Zn3B10O18·14H2O. *Thermochimica Acta, 484*, 27-31.

[20] Alp, B., Gonen, M., Savrık, S. A., Balkose, D., & Ulku, S. (2012). Dehydration, Water Vapor Adsorption and Desorption Behavior of Zn[B3O3(OH)5]·H2O and Zn[B3O4(OH)3]. *Drying Technology, 30*, 1610-1620.

[21] Moezzi, A., Lee, P., McDonagh, A. M., Michael, B., & Cortie, M. B. (2020). On the thermal decomposition of zinc hydroxide nitrate, Zn5(OH)8(NO3)2·2H2O. *Journal of Solid State Chemisty, 286*, 121311.

[22] Schubert, D. M. (2019). Hydrated zinc borates and their industrial use. *Molecules, 24*, 2419.

[23] Briggs, M. (2001). Boron oxides, boric acid, and borates. *Kirk-Othmer Encyclopedia of Chemical Technology*, John Wiley & Sons, Inc.

[24] Zheng, Y., Tian, Y., Ma, H., Qu, Y., Wang, Z. ., An, D., ... & Gao, X. (2009). Synthesis and performance study of zinc borate nanowhiskers. *Colloids and Surfaces A. 339*,178-184.

[25] Dong, J. X., & Hu, Z. S. (1998). A Study of the antiwear and friction-reducing properties of the lubricant additive, nanometer zinc borate. *Tribology International, 31*, 219-223.

[26] Erdemir, A. (1995). U.S. Patent No. 5,431,830. Washington, DC: U.S. Patent and Trademark Office.

[27] Lingtong, K., Hua, H., Tianyou, W., Dinghai, H., & Jianjian F. (2011). Synthesis and surface modification of the nanoscale cerium borate as lubricant additive. *Journal of Rare Earths, 29*, 1095-1099.

[28] Yu, H., Xu, Y., Shi, P., Xu, B., & Wang, X. (2008). Tribological Properties and Lubricating Mechanisms of Cu Nanoparticles in Lubricant. *Transactions of Nonferrous Metals Society of China, 18*, 636-641.

BORON 6(3), 348 - 358, 2021

BOR DERGİSİ
JOURNAL OF BORON
https://dergipark.org.tr/boron

Ultrasound supported flocculation of borate tailings with differently charged flocculants

İsmail Demir[1], Can Güngören[2,*], Yasin Baktarhan[3], Melike Yücel[4], İlgin Kurşun Ünver[5], Kenan Çinku[6], Şafak Gökhan Özkan[7]

[1] İstanbul University-Cerrahpaşa, Engineering Faculty, Mining Engineering Department, Büyükçekmece, Istanbul, 34500, Turkey
ORCID orcid.org/0000-0003-0949-7706
[2] İstanbul University-Cerrahpaşa, Engineering Faculty, Mining Engineering Department, Büyükçekmece, Istanbul, 34500, Turkey
ORCID orcid.org/0000-0002-6664-1551
[3] İstanbul University-Cerrahpaşa, Engineering Faculty, Mining Engineering Department, Büyükçekmece, Istanbul, 34500, Turkey
ORCID orcid.org/0000-0001-7547-0785
[4] İstanbul University-Cerrahpaşa, Engineering Faculty, Mining Engineering Department, Büyükçekmece, Istanbul, 34500, Turkey
ORCID orcid.org/0000-0003-1731-4041
[5] İstanbul University-Cerrahpaşa, Engineering Faculty, Mining Engineering Department, Büyükçekmece, Istanbul, 34500, Turkey
ORCID orcid.org/0000-0001-7348-6054
[6] İstanbul University-Cerrahpaşa, Engineering Faculty, Mining Engineering Department, Büyükçekmece, Istanbul, 34500, Turkey
ORCID orcid.org/0000-0001-7523-8126
[7] Turkish-German University, The Institute of the Graduate Studies in Science and Engineering, Department of Robotics and Intelligent Systems, Beykoz, İstanbul, 34820, Turkey
ORCID orcid.org/0000-0002-7770-7480

ARTICLE INFO

Article history:
Received July 17, 2021
Accepted August 22, 2021
Available online September 30, 2021

Research Article

DOI: 10.30728/boron.971892

Keywords:
Boron tailings
Flocculation
Settling rate
Turbidity
Ultrasound

ABSTRACT

Mining activities are followed by mineral processing and wet beneficiation methods which generate a significant amount of tailings. Slime fractions are discharged to the tailing ponds with associated process water and this causes storage and disposal difficulties and creates severe environmental problems. Therefore, dewatering these tailings is necessary for both economic and environmental aspects. In this study, the flocculation behaviors of the boron tailings from Ağıldere and Hisarcık (Turkey) were studied in the presence of anionic, cationic, and non-ionic flocculants. The results showed that the free settling condition was optimum for the Ağıldere sample. On the contrary, the settling rate of the Hisarcık sample increased considerably by the use of flocculants with a significant decrease in the turbidity of the suspension. Flocculation experiments indicated that the effect of the flocculant type on the flocculation of the Hisarcık sample can be generally ordered as anionic>cationic>non-ionic>no-flocculant. Furthermore, ultrasound was used as a supporting application. The results indicated that although the ultrasound application decreased the settling rate of both samples, lower sediment bed heights were obtained for the Hisarcık sample with ultrasound because of the formation of a more compact sediment bed in the presence of ultrasound.

1. Introduction

Dewatering of suspensions is carried out by the separation of solids from a liquid by mechanical compression, air displacement under vacuum or pressure, and drainage in a gravitational or centrifugal system. When the products of these methods are considered, it can be seen that the solid/liquid separation usually needs a long time [1,2]. In order to accelerate and increase the efficiency of solid/liquid separation, long-chain polymers (flocculants) which adsorb to particle surfaces and form bridges between the finely dispersed particles can be employed [3-5]. The flocculation rate and efficiency dependent upon various parameters including the surface properties of the solid, the interactions between the flocculant and the particles, the water content of the suspension, and the dosage of the flocculant. Therefore, many optimization experiments should be carried out for these parameters including the various flocculant types [6,7].

As of the end of 2020, Turkey has 73.6% of the total world reserves [8]. Turkey has the biggest boron reserve in the world and a significant amount of the production of boron minerals [9]. Some methods including flotation [10,11], leaching [12], heat treatment [13], gravity separation [9], electrostatic separation [14] were tried for the beneficiation of boron minerals at a laboratory scale. However, the most economic and viable beneficiation method for boron minerals is

*Corresponding author: can@iuc.edu.tr

known as the removal of clay content by washing after mechanical attrition at the industrial scale [11,15]. As a result of the beneficiation processes, a significant amount of tailings are generated and the fine fractions typically less than 3 mm are discharged to the tailing ponds with associated process water, which causes important storage, disposal, and environmental problems [16]. Therefore, the dewatering of these tailings is very crucial in the economic and environmental aspects. However, only a few researchers studied the flocculation of boron ores and tailings. Çırak and Hoşten [2] emphasized that since the clay content of the boron tailings decreases the sedimentation rate, the sedimentation process in the tailing ponds can be increased up to ten days. In addition, it is reported that the treatment of borax tailings can be feasible if the parameters of the solid/liquid separation process are implemented properly [5].

The efficiency of mineral processing operations can be enhanced by ultrasound (US) applications [17]. Ultrasound is a soundwave above the human perception frequency limit (more than 20 kHz) [18]. The ultrasonic application causes acoustic streaming in a liquid medium [19]. In addition, ultrasound travels in a fluid as three-dimensional pressure waves consisting of alternating cycles of compression and rarefaction. If the negative pressure generated during the rarefaction cycle is sufficient to overcome the molecular forces binding the liquid, cavitation bubbles occurred [20]. These bubbles are collapsed in the immediate compressing phase with releasing a very large but localized burst of energy. This process is known as cavitation and some extremely high temperature (5000 K) and pressure (1000 atm) conditions can be obtained in the liquid medium via the cavitation process [21]. The level of cavitation is higher in the presence of solid particulate matter in the liquid. The cavitation bubbles formed at the solid surfaces can help the separation of solid and liquid via decreasing the surface energy.

Singh [22] used ultrasound in the solid/liquid separation of fine clean coal particles by vacuum filtration. His results indicated that ultrasound pretreatment has the potential for better cake moisture removal and enhanced filtration rate. Önal et al. [23] reported that the flocculant consumption is reduced with the use of ultrasound in the clay flocculation, decrease the settling time by half with an increased final pulp density. Burat et al. [24] investigated the effects of ultrasound on the dewatering of fine coal particles with a high frequency vibrating screen and they obtained a lower moisture content with ultrasound.

In this study, the flocculation behaviors of the tailings of two boron processing plants located in Ağıldere (Bandırma), and Hisarcık (Emet) were studied in the presence of differently charged (anionic, cationic, and non-ionic) flocculants and the effect of the use of ultrasound on the flocculation process was investigated.

2. Materials and Methods

2.1. Materials

Although boron is one of the rarest elements in the earth's crust (10 ppm) [25], there are also places where boron minerals are collected and economically exploited. These deposits are generally directly related to hydrothermal spring activity, closed basins and Cenozoic volcanism in arid climate conditions and occurs in a limited number of Neogene to Holocene non-marine evaporitic settings [26]. Hisarcık deposit was formed in Miocene lake environments contributed by volcanism [27].

The samples used in this study were obtained from the tailing ponds of two different boron processing plants, which produce various boron-containing compounds including boric acid, borax pentahydrate, borax decahydrate, dehydrated borax, disodium octaborate tetrahydrate, zinc borate, and amorphous boron oxide [28,29]. The representative samples were taken systematically from the different sites and depths of the tailing ponds. The plants are located in Ağıldere/Bandirma and Hisarcık/Emet regions in Turkey. The samples were coded as “Ağıldere” and “Hisarcık”, respectively related to the plants they were collected.

Although the composition of borate formations differs related to the deposit, they are generally found together with sandstone, tuff, marl, clay, conglomerate, and limestone [26]. The Hisarcık deposit is generally composed of colemanite, ulexite, hydroboracite, and meyerhofferite. Clays accompanying boron minerals are mainly composed of montmorillonite. There are also illite and chlorite present in the clay zone. In addition, there are plenty of zeolites in the tuffs [30]. Other accompanied minerals are calcite, dolomite, gypsum, celestine, realgar, orpiment, and sulfur [25].

The chemical analysis of the samples was carried out by the volumetric titration method and the results are given in Table 1.

The particle size analysis of the samples was carried out with a laser diffraction particle size analyzer (Mastersizer 3000, Malvern, UK) and the results are given

Table 1. Chemical analysis of the samples.

	B_2O_3 (%)	Na_2O (%)	SiO_2 (%)	SrO (%)	SO_4 (%)	MgO (%)	CaO (%)	Fe_2O_3 (%)	Al_2O_3 (%)	As_2O_3 (%)
Ağıldere	8.16	4.91	17.6	0.824	1.308	13.6	15.5	0.245	1.02	0.0038
Hisarcık	2.45	0.03	8.68	1.62	37.07	1.83	30.5	0.87	1.72	0.88

in Figure 1, in addition to the d_{10}, d_{50}, and d_{90} sizes seen in Table 2.

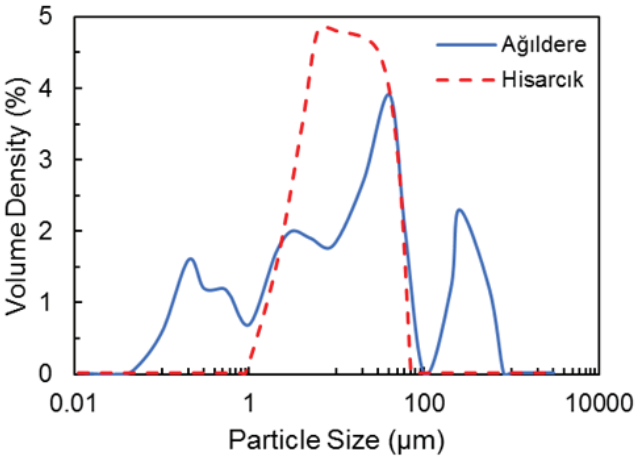

Figure 1. The particle size distribution of the samples.

Table 2. d_{10}, d_{50}, and d_{90} sizes of the samples.

	d_{10}	d_{50}	d_{90}
Ağıldere (μm)	0.3	20.6	256.0
Hisarcık (μm)	2.8	10.1	32.5

It is seen in Figure 2 and Table 2 that the Ağıldere sample shows a wide particle size distribution with a d_{90} size of 256 μm. On the contrary, the Hisarcık sample was comprised of finer particles (d_{90}=32.5 μm). Furthermore, although the tailings have consisted of various minerals, the zeta potential was measured for the characterization of the surface electrical properties of the tailings. The measurements were done twice with the electrophoresis method using a zeta meter (Zeta Plus, Brookhaven, UK) without and with ultrasound, and the average of two measurements were calculated.

It is seen in Figure 2 that since the samples have differences in their chemical compositions as shown in Table 1, they have different behaviors at various pH conditions. The changes in the zeta potential in the presence of ultrasound should be originated from the removal of clay particles from the surfaces. It is also clear from Figure 2 that both of the tailings had no point of zero charges (pzc) and the zeta potentials were always negative.

The flocculants used in this study were obtained from NCC Chemical Co. (Turkey) with the commercial names of Newfloc-123 (anionic flocculant), NewFloc-8243 (cationic flocculant), and Newfloc-101 (non-ionic flocculant). The flocculant solutions were prepared using de-ionized (DI) water (18.2 MΩ·cm at 25°C) (Millipore Milli-Q, Merck, Germany), freshly. All experiments were performed at room temperature (23 ± 1°C).

2.2. Methods

First, the effect of the solid-in-pulp ratio on the settling properties of the samples was investigated with free settling experiments in the absence of flocculant. For this purpose, suspensions at 3%, 5%, and 7% solid-in-pulp ratios were prepared in a 1 dm^3 glass beaker and stirred using a flocculator (jar test device) (Velp Scientifica, Italy) at 200 rpm for 10 min. Since the success of the flocculation process is dependent upon the stirring speed and time [31,32] these values were kept constant in further experimental studies to investigate the effect of ultrasound on the flocculation process properly. In addition, in order to mimic the plant conditions, the flocculation experiments were carried out at the natural pH of the suspensions, which were 9.0 ± 0.2 for the Ağıldere and 9.7 ± 0.1 for the Hisarcık samples.

Then, the suspensions were transferred to a graduated cylinder, separately and the height of the sediment bed was recorded as a function of time up to 240 min. The sediment bed heights as a function of settling time were used to obtain the settling rates.

Then, the effect of the flocculant type and dosage on the flocculation was studied using anionic, cationic,

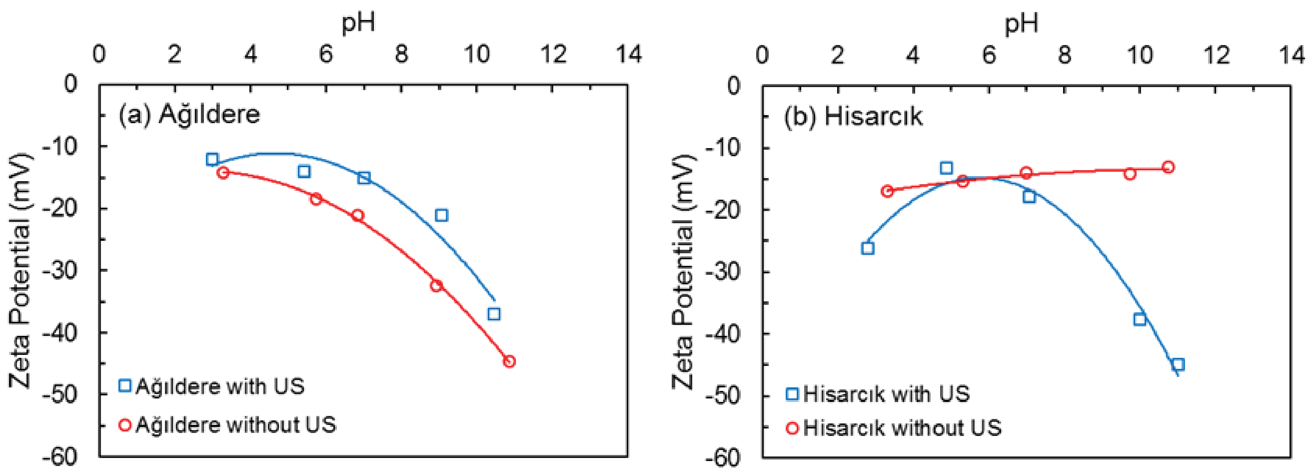

Figure 2. Zeta potential of Ağıldere (a) and Hisarcık samples (b).

and non-ionic flocculants, separately. The flocculant solutions were prepared at 0.1% concentration by weight and used in the flocculation experiments in the volumes of 2 cm^3 (67 g/t), 4 cm^3 (133 g/t), and 6 cm^3 (200 g/t).

The experiments with ultrasound were carried out using a cylindrical ultrasonic bath (Bandelin Sonorex RK 106, Germany) working at a constant frequency (35 kHz) and power (480 W). In order to investigate the effect of ultrasound on the flocculation process and to observe whether the ultrasound was causing floc breakage, the ultrasonic application was performed for 10 min before the settlement process starts. The suspension was stirred with a glass bar gently during the ultrasonic application to prevent the suspension to settle. The mechanic stirring was not preferred to avoid further floc breakage. The ultrasonic application method is shown in Figure 3.

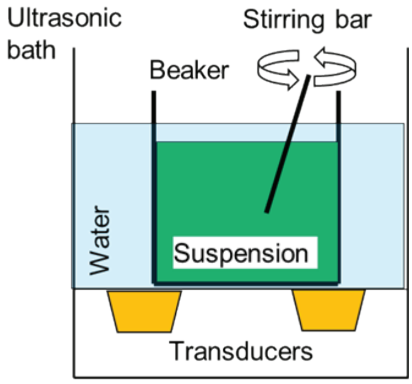

Figure 3. The ultrasonic application method.

During the flocculation experiments, a 5 cm^3 sample was taken from the top of the suspension using a Pasteur pipette and the turbidity measurements were performed with a turbid meter (Aquafast-II, Thermo Scientific, USA) with respect to settling time.

3. Results and Discussion

The settling rate [33] and the turbidity of the residual suspension [34,35] are important indicators of the success of the flocculation process. The settling rate of the Ağıldere and Hisarcık samples at various solid-in pulp ratios is seen in Figure 4a and b, respectively in the absence of flocculant. Figure 4 shows that the Ağıldere sample settled in a shorter time than the Hisarcık sample. While the maximum settling rate was observed between 1-3 min with the Ağıldere sample, the settling rate of the Hisarcık sample was the highest between 1-10 min. The maximum settling rate was obtained as 17 cm/min at 1 min and 10 cm/min at 8 min for Ağıldere and Hisarcık samples at 3% solid-in-pulp ratio, respectively. Furthermore, it is obvious in Figure 4 that the flocculation process becomes more difficult with an increase in the solid-in-pulp ratio and therefore the settling rates decreased. This can be related to the increase in the clay content of the suspension and hence the change in its rheological properties [36]. It is known from the literature that the adsorbed flocculants per solid amount decreased with the increase in the solid-in-pulp ratio. In addition, the particle-reagent collision probability is low in crowded colloidal systems [37]. Therefore, it has an important role in flocculation efficiency [38,39]. However, it is also a fact that when the solid content of the system decreased, the flocculation capacity will also decrease. Therefore, no solid-in-pulp ratios below 3% were used in this study considering the capacity of the flocculation process. It is also seen in Figure 4 that the settling rate did not change significantly after 60 min for both samples. Therefore, it was decided to perform flocculation experiments for up to 60 min for further studies.

The results of the flocculation experiments in the presence of flocculants along with the results of the turbidity measurements for the Ağıldere sample are seen in Figure 5. It is seen in Figure 5a-c that since the use of flocculant caused the re-stabilization of the particles

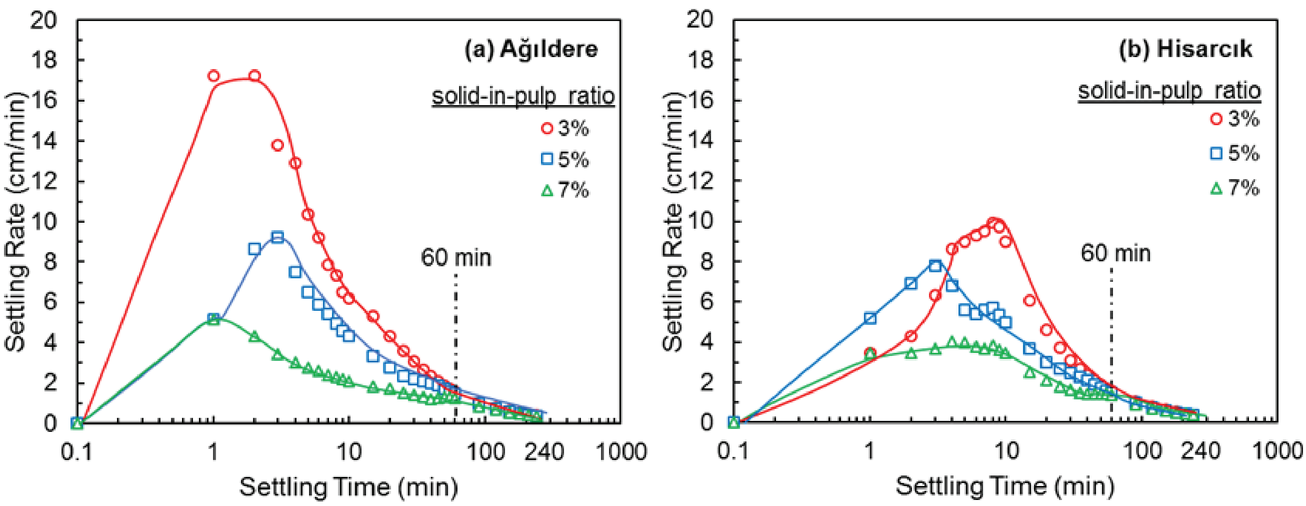

Figure 4. Settling rate of Ağıldere (a) and Hisarcık (b) samples at various solid-in-pulp ratios in the absence of flocculant.

[40,41], flocculant addition decelerated the settling of the Ağıldere sample. For instance, at 1 min settling time, while the settling rate was 17 cm/min without flocculant, it sharply decreased to 3 cm/min with anionic flocculant at 67 g/t while the settlement process did not begin in the presence of cationic and non-ionic flocculants. Although the settling rate increased with flocculant dosage, it is a fact that flocculants were not useful for the settlement of the Ağıldere sample. In parallel, the results of the turbidity measurements given in Figure 5(d-f) showed that more muddy suspensions were obtained at the end of 60 min settling time in the presence of flocculant. The difference in the turbidity of the suspension increased with flocculant dosage and reaches 617 NTU, 318 NTU, and 223 NTU, for anionic, non-ionic, and cationic flocculants at 200 g/t, respectively, while it was 171 NTU in the absence of flocculant.

The results of the flocculation experiments in the presence of flocculants along with the results of the turbidity measurements for the Hisarcık sample are given in Figure 6.

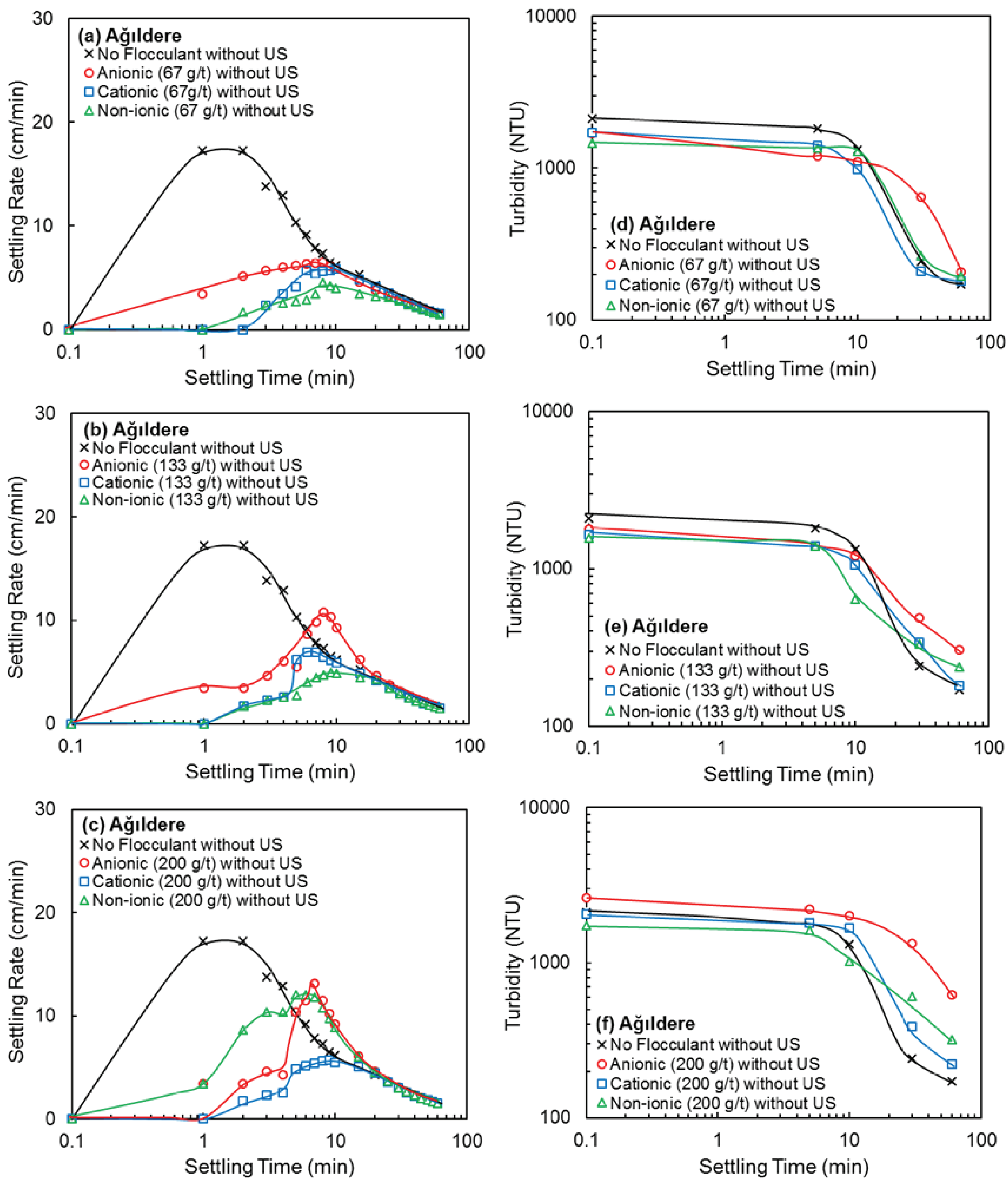

Figure 5. Settling rate (a-c) and turbidity (d-f) of the Ağıldere sample related to flocculant type and dosage.

Figure 6a-c indicates that contrary to the Ağıldere sample, the settling rate increased significantly in the presence of flocculant for the Hisarcık sample. While the settling rate was 3 cm/min in the absence of flocculant, it increased to 52 cm/min, 62 cm/min, and 69 cm/min at 1 min in the presence of 67 g/t non-ionic, cationic, and anionic flocculant, respectively. The maximum settling rate was obtained as 83 cm/min at 200 g/t anionic flocculant at 1 min. It is also clear in Figure 6d-f that the use of flocculant decreased the turbidity of the suspension, considerably related to the flocculant type [42,43].

It is seen from the results of the flocculation experiments that the effect of the flocculant type on the flocculation of the Hisarcık sample can be generally written as anionic > cationic > non-ionic > no-flocculant. Considering that the tailings had negative zeta potentials, it can be said that the interaction between the particle surfaces and flocculant molecules was chemical rather than physical.

In the light of the flocculation experiments at various dosages, the ultrasound application was applied at 67 g/t flocculant consideration considering the efficiency

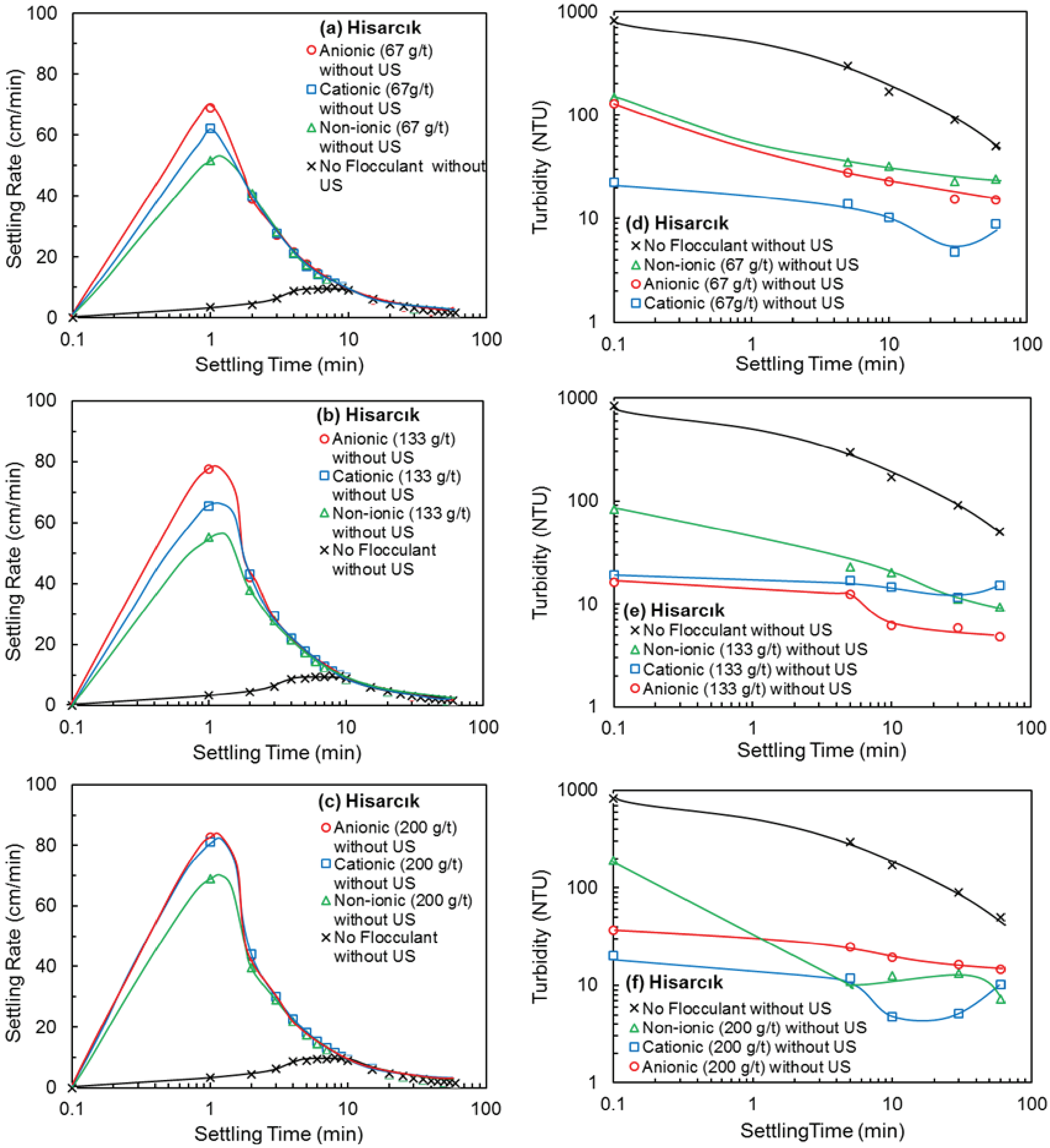

Figure 6. Settling rate (a-c) and turbidity (d-f) of the Hisarcık sample related to flocculant type and dosage.

and cost factors. The effect of the ultrasound application on the results of the settling rate and turbidity is given in Figure 7 for the Ağıldere sample. It is seen in Figure 7a-d that the use of ultrasound decreased the settling rate of the Ağıldere sample, significantly because of the floc breakage. For instance, while the settling rate was 17% at 1 min settling time in the absence of flocculant without ultrasound, it decreased to 2% with ultrasound. This trend did not change in the presence of flocculant. In several previous studies, it was also reported that ultrasound could be detrimental to the flocculation process related to the application conditions [44-46]. On the other hand, it is seen in Figure 7e-h that lower turbidity values were obtained with ultrasound in most experiments because of the formation of a more compact sediment bed in the presence of ultrasound.

The results of the settling rate and turbidity measurements without and with ultrasound for the Hisarcık

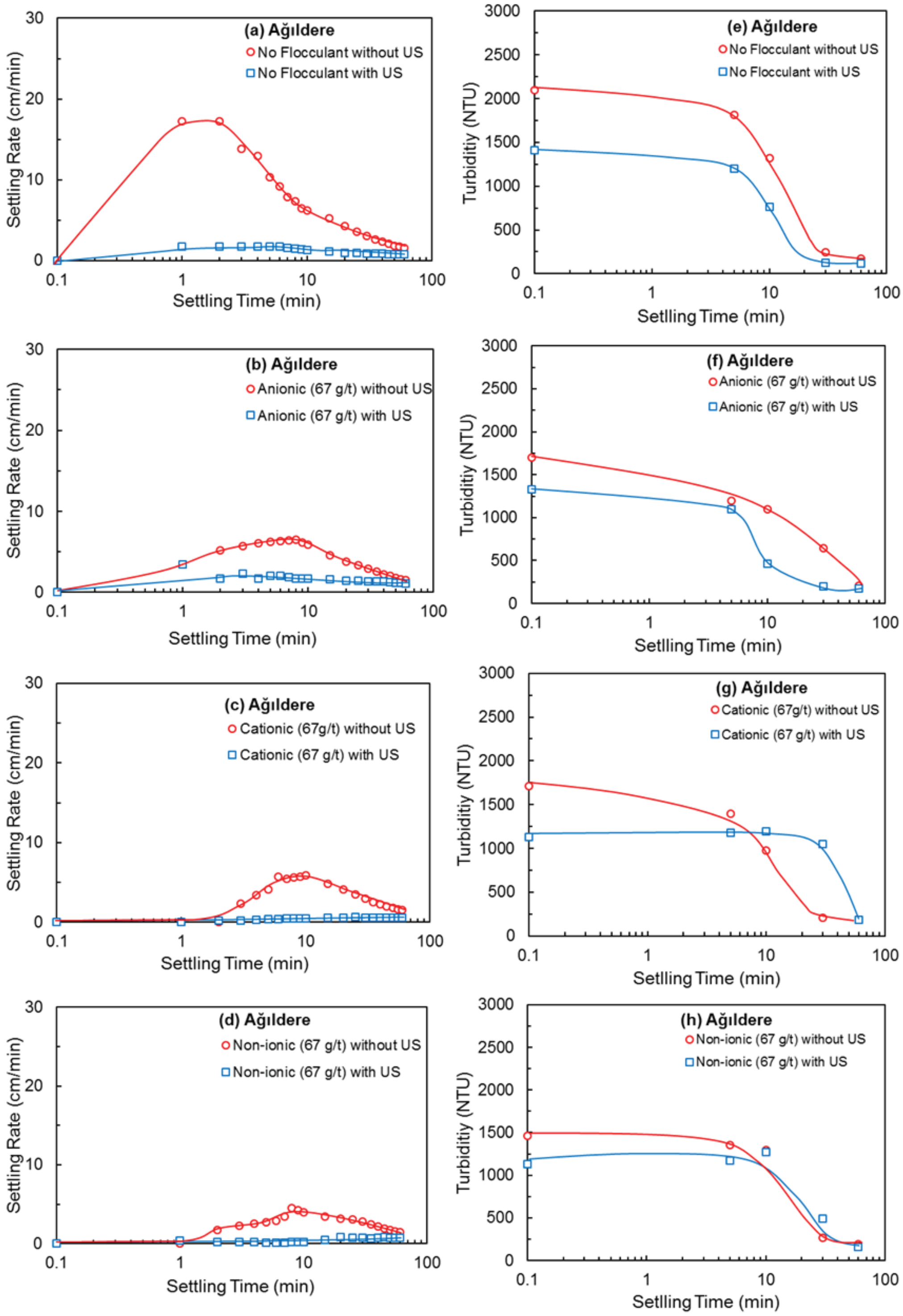

Figure 7. Settling rate (a-d) and turbidity (e-h) of the Ağıldere sample related to flocculant type without and with ultrasound.

sample are given in Figure 8. Similar to the Ağıldere sample, the results of the experiments for the Hisarcık sample seen in Figure 8 show that lower settling rate values were obtained with ultrasound at shorter settling times. At longer settling times, the settling rates became equal without and with ultrasound. However, higher turbidity values were obtained with ultrasound. Although the use of flocculant increased the settling rate, the trend between the samples without and with ultrasound did not change. For instance, while the settling rate was 69 cm/min without ultrasound, it was only 14 cm/min with ultrasound in the presence of 67 g/t anionic flocculant.

Height of the sediment bed of Ağıldere and Hisarcık samples without and with ultrasound at 60 min is given

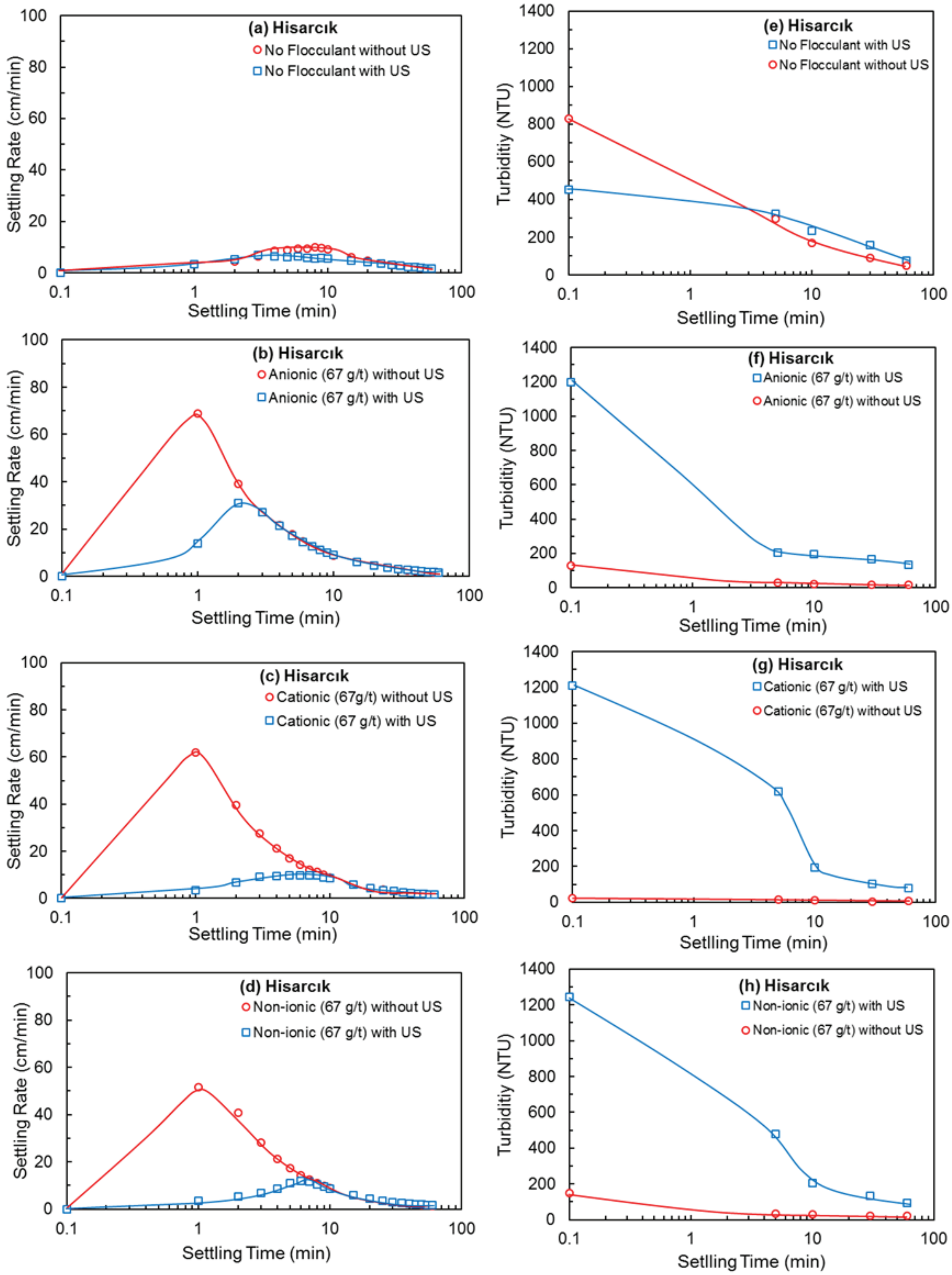

Figure 8. Settling rate (a-d) and turbidity (e-h) of the Hisarcık sample related to flocculant type without and with ultrasound.

in Figure 9. Figure 9a shows that while higher sediment bed heights were obtained with ultrasound with the Ağıldere sample, ultrasound decreased the sediment bed heights of the Hisarcık sample as seen in Figure 9b. The positive effect of ultrasound on the sediment bed height was mostly originated from allowing closer packing of the particles [47]. Meanwhile, there are some additional effects of ultrasound including the enhancement of emulsification and dispersion processes [17,48], as well as increasing the polymer adsorption onto clay particles [49], facilitation of the migration of moisture through channels created by wave propagation [24]. Furthermore, the cavitation bubbles formed at the solid surfaces can help the separation of solid and liquid via forming gas/liquid interfaces with much lower surface energy compared to solid/liquid surfaces [23]. Furthermore, Videla et al. [50] stated that ultrasound can favor the effects of flocculants and increasing their performance. They compared the longitudinal and transverse ultrasonic radiation in flocculation. They stated that acoustic longitudinal radiation served better than transverse radiation to improve the sedimentation rate. Furthermore, they investigate the effect of frequency. Their results showed that the sedimentation rate improved as the frequency decreased, and therefore, ultrasound at different frequencies could be used in the flocculation process for optimization purposes. On the other hand, the detrimental effects of ultrasound on the flocculation of boron tailings observed in this study could be related to the floc breakage and inefficient agglomeration process in the presence of ultrasound in accordance with Riera-Franco de Sarabia et al. [51]. Moreover, it is also a fact that cavitation bubbles collapse asymmetrically in the presence of solid particles because of the asymmetric distribution of the pressure around the bubble near a solid particle. The asymmetric collapse of the cavitation bubbles causes the formation of micro-jets and shock waves

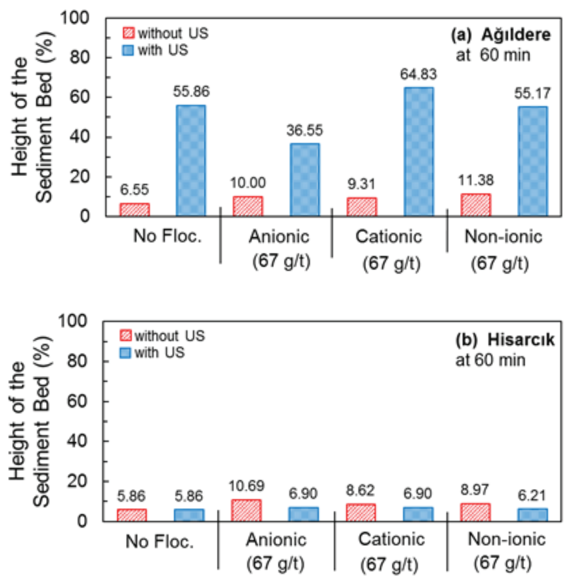

Figure 9. Height of the sediment bed for Ağıldere (a) and Hisarcık (b) samples.

[21,52,53]. These shock waves could remove the clay minerals on boron particles which are very fine and very difficult to settle. These fine clay particles could be responsible for the decrease in the settling rate and increase in the turbidity of the suspension.

4. Conclusions

In this study, the effect of ultrasound on the flocculation of the boron tailings from Ağıldere and Hisarcık regions of Turkey in the presence of anionic, cationic, and non-ionic flocculants was investigated in detail. The results showed that the decrease in the solid-in-pulp ratio increased the settling rate of both samples. It was observed that the Ağıldere sample could be settled in free settling conditions and flocculant addition harmed the settling process. On the other hand, there was a significant increase in the settling rate of the Hisarcık sample in the presence of flocculants with a considerable decrease in the turbidity of the suspension. The difference between the flocculation behaviors of the two samples was originated from the differences in their chemical compositions. The most effective flocculant types for the Hisarcık sample can be ordered as anionic, cationic, and non-ionic, respectively. In this study, ultrasound was also used as a supporting application for flocculation. The results indicated that although the use of ultrasound had a negative effect on the settling rate of both samples mostly caused by the floc breakage, since ultrasound allowed closer packing of the particles, lower sediment bed heights were obtained for the Hisarcık sample in the presence of ultrasound application.

Acknowledgements

This study was supported by the Research Fund of İstanbul University, project number: FBA-2017-25533.

References

[1] Çırak, M. (2010). *Flocculation behavior of two different clay samples from Kirka tincal deposit* [M. Sc. Thesis, Middle East Technical University]. Council of Higher Education Thesis Center (Thesis Number 269092).

[2] Çırak, M., & Hoşten, Ç. (2015). Characterization of clay rock samples of a borax ore in relation to their problematical flocculation behavior. *Powder Technology, 284*, 452-458.

[3] Yang, Y., Wu, A., Klein, B., & Wang, H. (2019). Effect of primary flocculant type on a two-step flocculation process on iron ore fine tailings under alkaline environment. *Minerals Engineering, 132*, 14-21.

[4] Ding, C., Xie, A., Yan, Z., Li, X., Zhang, H., Tang, N., & Wang, X. (2021). Treatment of water-based ink wastewater by a novel magnetic flocculant of boron-containing polysilicic acid ferric and zinc sulfate. *Journal of Water Process Engineering, 40*.

[5] Çırak, M., & Hoşten, Ç. (2017). Optimization of coagulation-flocculation process for treatment of a colloidal suspension containing dolomite/clay/borax. *Interna-*

tional Journal of Mineral Processing, 159, 30-41.

[6] Şimşek, B., Taş, E., & Sabah, E. (2019). Modeling and optimization of the flocculation process of polydisperse travertine suspension employing an eco-friendly hybrid flocculant. *Arabian Journal of Geosciences, 12*(24), 1-11.

[7] Sabah, E., & Yeşilkaya, L. (2000). Evaluation of the settling behaviour of Kirka borax concentrator tailings using different type of polymers. *Ore Dressing, 2000*(3), 1-12.

[8] Eti Mine. (2021). *Bor Sektör Raporu* [*Boron Sector Report*]. The Ministry of Energy and Natural Resources. https://www.etimaden.gov.tr/storage/2021/Bor_Sektor_Raporu_2020.pdf

[9] Savaş, M. (2016). Recovery of colemanite from tailing using a Knelson concentrator. *Physicochemical Problems of Mineral Processing, 52*(2), 1036-1047.

[10] Özkan, Ş. G., & Acar, A. (2004). Investigation of impact of water type on borate ore flotation. *Water Research, 38*(7), 1773-1778.

[11] Özdemir, O., & Çelik, M. S. (2010). Surface Properties and Flotation Characteristics of Boron Minerals. *The Open Mineral Processing Journal, 3*(1), 2-13.

[12] Arslan, V., & Bayat, O. (2016). Kolemanit cevherinden oksalik asit liçi ile borik asit eldesi [Production of boric acid from colemanite ore by oxalic acid leaching]. *Journal of Underground Resources, 5*(10), 11-20.

[13] Çelik, M. S., Batar, T., Akın, Y., & Arslan, F. (1998). Upgrading schemes for boron minerals through calcination. *Mining, Metallurgy & Exploration, 15*(1), 53-56.

[14] Eskibalcı, M. F., & Özkan, Ş. G. (2012). An investigation of effect of microwave energy on electrostatic separation of colemanite and ulexite. *Minerals Engineering, 31*, 90-97.

[15] Uçbeyiay, H., & Özkan, A. (2014). Two-stage shear flocculation for enrichment of fine boron ore containing colemanite. *Separation and Purification Technology, 132*, 302-308.

[16] Acarkan, N., Kökkılıç, O., Baştürkçü, H., & Sirkeci, A. A. (2018). Precipitation of boron from waste water of Kirka borax plant. *Recycling and Sustainable Development, 11*(1), 21-26.

[17] Güngören, C., Özdemir, O., Wang, X., Özkan, Ş. G., & Miller, J. D. (2019, Apr). Effect of ultrasound on bubble-particle interaction in quartz-amine flotation system. *Ultrasonics Sonochemistry, 52*, 446-454.

[18] Özkan, Ş. G. (2018). A review of simultaneous ultrasound-assisted coal flotation. *Journal of Mining and Environment, 9*(3), 679-689.

[19] Ambedkar, B., Chintala, T. N., Nagarajan, R., & Jayanti, S. (2011). Feasibility of using ultrasound-assisted process for sulfur and ash removal from coal. *Chemical Engineering and Processing: Process Intensification, 50*(3), 236-246.

[20] Mason, T. J., Collings, A., & Sumel, A. (2004). Sonic and ultrasonic removal of chemical contaminants from soil in the laboratory and on a large scale. *Ultrasonics Sonochemistry, 11*(3-4), 205-210.

[21] Suslick, K. S., Didenko, Y., Fang, M. M., Hyeon, T., Kolbeck, K. J., McNamara III, W. B., ... & Wong, M. (1999). Acoustic cavitation and its chemical consequences. *Philosophical Transactions of the Royal Society of London. Series A: Mathematical, Physical and Engineering Sciences, 357*(1751), 335-353.

[22] Singh, B. P. (1999). Ultrasonically assisted rapid solid-liquid separation of fine clean coal particles. *Minerals Engineering, 12*(4), 437-443.

[23] Önal, G., Özer, M., & Arslan, F. (2003). Sedimentation of clay in ultrasonic medium. *Minerals Engineering, 16*(2), 129-134.

[24] Burat, F., Sirkeci, A. A., & Önal, G. (2014). Improved fine coal dewatering by ultrasonic pretreatment and dewatering aids. *Mineral Processing and Extractive Metallurgy Review, 36*(2), 129-135.

[25] Özkul, C., Çiftçi, E., Tokel, S., & Savaş, M. (2017). Boron as an exploration tool for terrestrial borate deposits: A soil geochemical study in Neogene Emet-Hisarcık basin where the world largest borate deposits occur (Kütahya-western Turkey). *Journal of Geochemical Exploration*, 173, 31-51.

[26] Helvacı, C. (2017). Borate deposits: An overview and future forecast with regard to mineral deposits. *Journal of Boron, 2*(2), 59-70.

[27] Koçak, İ., & Koç, Ş. (2018). Geochemical characteristics of The Emet (Espey-Hisarcik) borate deposits, Kütahya, Turkey. *Journal of African Earth Sciences, 142*, 52-63.

[28] Yücel, M. (2018). *Bor Atıklarının Çöktürülmesi* [Settlement of Boron Tailings]. [B.Sc. Thesis, Istanbul University].

[29] Garip, Ş. (2015). *Bor Atıklarının Geri Dönüşümüne Yönelik Karakterizasyon Çalışmaları* [Characterization Studies for Recycling of Boron Wastes]. [B.Sc. Thesis, Istanbul University].

[30] Helvacı, C., & Alonso, R. N. (2000). Borate Deposits of Turkey and Argentina; A Summary and Geological Comparison. *Turkish Journal of Earth Sciences, 9*(1), 1-27.

[31] Addai-Mensah, J., Yeap, K. Y., & McFarlane, A. J. (2007). The influential role of pulp chemistry, flocculant structure type and shear rate on dewaterability of kaolinite and smectite clay dispersions under couette Taylor flow conditions. *Powder Technology, 179*(1-2), 79-83.

[32] Castillo, C., Ihle, C. F., & Jeldres, R. I. (2019). Chemometric optimisation of a copper sulphide tailings flocculation process in the presence of clays. *Minerals, 9*(10), 582.

[33] Ye, L., Manning, A. J., & Hsu, T. J. (2020). Oil-mineral flocculation and settling velocity in saline water. *Water Research, 173*, 115569.

[34] Ersoy, B., Tosun, İ., Günay, A., & Dikmen, S. (2009). Turbidity removal from wastewaters of natural stone processing by coagulation/flocculation methods. *CLEAN - Soil, Air, Water, 37*(3), 225-232.

[35] Arulmathi, P., Jeyaprabha, C., Sivasankar, P., & Rajkumar, V. (2019). Treatment of textile wastewater by coagulation–flocculation process using gossypium herbaceum and polyaniline coagulants. *CLEAN - Soil, Air, Water, 47*(7), 1800464.

[36] Karapınar, N. (2019). Flocculation behavior of borax clayey tailings in mono- and dual- flocculant systems: effect of tailings slurry characteristics and polyDAD-

MAC type. *Global Journal of Earth Science and Engineering, 6*(1), 9-15.

[37] Birdi, K. S. (2015). *Handbook of Surface and Colloid Chemistry*. CRC press. ISBN 1466596686.

[38] Kurşun, İ., İpekoğlu, B., Çelik, M. A., & Kaytaz, Y. (2000). Flocculation and adsorption-desorption mechanism of polymers on albite. *In Developments in Mineral Processing* (Vol. 13, pp. C5-24). Elsevier.

[39] Winterwerp, J. C. (2002). On the flocculation and settling velocity of estuarine mud. *Continental Shelf Research, 22*(9), 1339–1360.

[40] Abu Hassan, M. A., Hui, L. S., & Noor, Z. Z. (2009). Removal of boron from industrial wastewater by chitosan via chemical precipitation. *Journal of Chemical and Natural Resources Engineering, 4*(1), 1-11.

[41] Weber Jr., W. J. (1972). *Physicochemical Processes for W ater Quality Control*. John Wiley and Sons. ISBN 0471924350.

[42] Chong, M. F., Lee, K. P., Chieng, H. J., & Ramli, I. I. S. B. (2009). Removal of boron from ceramic industry wastewater by adsorption-flocculation mechanism using palm oil mill boiler (POMB) bottom ash and polymer. *Water Research, 43*(13), 3326-3334.

[43] Zarei Mahmudabadi, T., Ebrahimi, A. A., Ehrampoush, M. H., & Eslami, H. (2021). Investigating the effect of coagulation and flocculation - adsorption process on boron removal from industrial wastewater (Case study: Ceramic tile industry). *Journal of Rafsanjan University of Medical Sciences, 19*(10), 1015-1034.

[44] Du, J., McLoughlin, R., & Smart, R. S. C. (2014). Improving thickener bed density by ultrasonic treatment. International *Journal of Mineral Processing, 133*, 91-96.

[45] Zhu, L., Lyu, W., Yang, P., & Wang, Z. (2020). Effect of ultrasound on the flocculation-sedimentation and thickening of unclassified tailings. *Ultrasonics Sonochemistry, 66*, 104984.

[46] Zhao, Y., Meng, L., & Shen, X. (2020). Study on ultrasonic-electrochemical treatment for difficult-to-settle slime water. *Ultrasonics Sonochemistry, 64*, 104978.

[47] Smythe, M. C., & Wakeman, R. J. (2000). The use of acoustic fields as a filtration and dewatering aid. *Ultrasonics, 38*(1-8), 657–661.

[48] Kowalski, W., & Kowalska, E. (1978). The ultrasonic activation of non-polar collectors in the flotation of hydrophobic minerals. *Ultrasonics, 16*(2), 84-86.

[49] Aldrich, C., & Feng, D. (1999). Effect of ultrasonic preconditioning of pulp on the flotation of sulphide ores. *Minerals Engineering, 12*(6), 701-707.

[50] Videla, A., Faúndez, D., Meneses, J., Gaete, L., & Vargas, Y. (2020). Enhancement of the sedimentation rate of copper tailings by application of acoustic fields. *Minerals Engineering, 146*, 106096.

[51] de Sarabia, E. R. F., Gallego-Juarez, J. A., Rodriguez-Corral, G., Elvira-Segura, L., & Gonzalez-Gomez, I. (2000). Application of high-power ultrasound to enhance fluid/solid particle separation processes. *Ultrasonics, 38*(1-8), 642-646.

[52] Ambedkar, B., Nagarajan, R., & Jayanti, S. (2011). Ultrasonic coal-wash for de-sulfurization. *Ultrasonics Sonochemistry, 18*(3), 718-726.

[53] Özkan, Ş. G., & Güngören, C. (2012). Enhancement of colemanite flotation by ultrasonic pre-treatment. *Physicochemical Problems of Mineral Processing, 48*(2), 455-462.

YAZAR KILAVUZU

1. KAPSAM

Bor Dergisi, bor alanında aşağıda nitelikleri açıklanmış makaleleri Türkçe ve İngilizce olarak kabul etmektedir.

Araştırma Makalesi: Orijinal bir araştırmayı bulgu ve sonuçlarıyla yansıtan yazılardır. Çalışmanın özgün ve mutlaka uluslararası bilime katkısı olmalıdır.

Tarama Makalesi: Yeterli sayıda bilimsel makaleyi tarayıp, konuyu bugünkü bilgi ve teknoloji düzeyinde özetleyen, değerlendirme yapan ve bulguları karşılaştırarak yorumlayan yazılardır.

Her makale, konusu ile ilgili en az iki hakeme gönderilerek şekil, içerik, özgün değer, uluslararası literatüre ve bilime/teknolojiye katkı bakımından incelettirilir. Hakem görüşlerinde belirtilen eksikler tamamlandıktan sonra, dergide yayınlanabilecek nitelikteki yazılar, son baskı formatına getirilir ve yazarlardan makalenin son halinin onayı alınır. Dergide basıldığı haliyle makale içinde bulunabilecek hataların sorumluluğu yazarlara aittir.

Kabul edilen makaleler, ücretsiz olarak dergi internet sayfasında (online) ve basılı şekilde yayınlanmaktadır.

2. BAŞVURU FORMLARI

Makale; Kapak Sayfası, Makale Kontrol Listesi Formu, Makale Metni, Telif Hakkı Devir Formu ve Benzerlik Oran Dosyası olmak üzere beş ayrı formdan oluşmalıdır. Başvurularda iletişimde bulunulacak yazar ve diğer yazarların iletişim bilgileri (adres, e-posta, cep ve sabit telefon no) kapak sayfasında verilmelidir.

3. GÖNDERİ KONTROL LİSTESİ

Başvuru sürecinde yazarlar gönderilerinin aşağıdaki listede bulunan tüm maddelere uygunluğunu kontrol etmelidirler, bu rehbere uymayan başvurular değerlendirmeye alınmayacaktır.

1. Gönderilecek makale daha önceden yayınlanmadı ve/veya yayımlanmak üzere herhangi bir dergiye sunulmadı.
2. Makale Microsoft Office Word 2010 ve üzeri bir kelime işlemci ile hazırlandı.
3. Makale A4 sayfasında, kenar boşlukları, üstbilgi ve altbilgi boşlukları ve satır aralığı dergi formatına uygun olarak ayarlandı.
4. Ana başlıklar ve alt başlıklar İngilizceleriyle birlikte dergi formatına uygun olarak düzenlendi.
5. Tablolar dergi formatına uygun olarak hazırlandı, metin içerisinde bahsedildi, makalenin metin bölümüne yerleştirildi.
6. Şekiller dergi formatına uygun olarak hazırlandı, metin içerisinde bahsedildi, makalenin metin bölümüne yerleştirildi.
7. Eşitlik ve Reaksiyon numaralandırmaları sıralı olarak dergi formatına uygun olarak verildi.
8. Orijinal şekiller bütünüyle yazım kurallarına uygun hazırlandı.
9. Şekil boyutları formata uygun olacak biçimde düzenlendi.
10. Metin içinde şekiller ardışık numaralandı.
11. Kaynaklar yazım kurallarına uygun yazıldı.
12. Kaynaklar metin içinde ardışık sıralandı.
13. Kaynaklar metin sonunda, metin içinde verildiği sırada listelendi.
14. Türkçe makale başlığı/Özet/Anahtar kelimeler/Bölüm başlıkları/Tablo ve Şekil adlandırmaları ile İngilizce makale başlığı/Özet/Anahtar kelimeler/Bölüm başlıkları/Tablo ve Şekil adlandırmalarının birbirleri aynı olduğu kontrol edildi.
15. "Kapak Sayfası" oluşturuldu.
16. Telif Hakkı Devir Formu imzalandı ve gönderildi.
17. Muhtemel yazım hataları kelime işlemcinin "Yazım ve Dilbilgisi" denetimi ile kontrol edildi.
18. "Editöre Not" alanına makalenin özgün yönü ve makalenin bilime somut katkısı yazıldı.

4. TELİF HAKLARI

Makalelerin telif hakkı devri, dergi internet sayfasında sunulan Telif Hakkı Devir Formu doldurulup imzalanmak suretiyle alınır. Form imzalandıktan sonra "ek dosyaları yükle" bölümünde PDF olarak yüklenmelidir. Bu formu göndermeyen yazarların makaleleri basılamaz.

5. GİZLİLİK BEYANI

Bu dergi sitesindeki isimler ve elektronik posta adresleri bu derginin belirtilen amaçları doğrultusunda kullanılacaktır ve diğer amaçlar veya başka bir bölüm için kullanılmayacaktır.

YAZIM KURALLARI

GENEL BİLGİ

Makale; Kapak Sayfası, Makale Kontrol Listesi Formu, Makale Metni, Telif Hakkı Devir Formu ve Benzerlik Oran Dosyası olmak üzere beş ayrı formdan oluşmalıdır. Başvurularda iletişimde bulunulacak yazar ve diğer yazarların iletişim bilgileri (adres, e-posta, cep ve sabit telefon no) kapak sayfasında verilmelidir.

KAPAK SAYFASI

Başvuru esnasında yazar isimleri ayrı bir dosya olarak yüklenen Kapak Sayfası hazırlanmalı ve online olarak dergimizin internet sayfasına ayrı bir dosya olarak yüklenmelidir. İlk başvuru esnasında yazarları sadece dergi editörlerimiz görebilecektir.

Makalenin başlığının ilk harfi büyük ve diğerleri küçük harflerle sayfaya ortalı olarak yazılmalıdır. Başlık metne uygun, kısa ve açık olmalıdır. Başlığın altına, makalenin yazar ya da yazarlarının adı, soyadı, e-posta adresleri, posta adresleri, posta kodu ve ORCID numaraları yazılmalıdır.

İngilizce makale başlığı: Makaleyi kapsayıcı ve anlaşılır bir başlık kullanılmalıdır. Başlık büyük harfle başlamalı ve diğer tüm harfleri küçük yazı karakterinde yazılmalıdır. Başlık, gerektiğinde standart kısaltmalarla birlikte en çok 15 kelimeden oluşmalıdır.

Türkçe makale başlığı: İngilizce makale başlığıyla uyumlu olmalıdır.

Yazar adları ve adres bilgileri: Yazar adlarının ve soyadlarının ilk harfleri büyük diğer tüm harfleri küçük olacak şekilde yazılmalıdır. Çalışmanın yürütülmüş olduğu yer yazar isimlerinden sonra gelmelidir. Yazarı ve çalışmanın yürütüldüğü yeri ilişkilendirebilmek amacıyla yazarın soyadından sonra ve çalışmanın yürütülmüş olduğu yerden önce üstsimge (1, 2, 3 vb.) ile numaralandırılmalıdır. Sorumlu yazar, soyadından sonra " * " simgesi ile belirtilmelidir. Adres bilgileri içerisinde çalışmanın yürütüldüğü yer, şehir, posta kodu ve ülke adı yer almalıdır. Adres bilgilerinden sonraki satıra her bir yazarın e-posta adresi yazar isimlerinin sırasına uygun olarak verilmelidir.

Özet: Ana metne atıf yapmadan makalenin konusu anlaşılır bir şekilde özetlemelidir. Özet 220 kelimeyi geçmemelidir. Standart olmayan kısaltmalar ilk kullanıldığında tam olarak yazılmalıdır.

Anahtar Kelimeler: Özetten hemen sonra gelmelidir. En fazla 5 anahtar kelime, harf sırasıyla verilmelidir. Anahtar Kelimeler konuyu açıklayıcı kelimelerden seçilmelidir. Her bir anahtar kelime "," ile ayrılmalıdır. Anahtar kelimeler cümle içermemelidir

Abstract: Özette verilen metnin İngilizceye çevrilmesiyle oluşturulmalıdır. Ondalıklı sayılar kullanılıyorsa bu sayıların Türkçe Özette " , " İngilizce özette " . " olmasına dikkat edilmelidir.

Key Words: İngilizce özetten sonra verilmelidir. Türkçe anahtar kelimelerle uyumlu olmalıdır. Konu ile ilgili en çok 5 anahtar kelime alfabetik olarak yazılmalıdır.

MAKALE KONTROL LİSTESİ FORMU

Makalenin metin bölümünün dergi yazım kurallarına uygunluğunun kabul edildiğini gösteren formdur. Başvurular yapılmadan önce Makale Kontrol Formunun doldurulması gerekmektedir. Kontrol formu makalenin ilk sayfası olarak verilmelidir. Dergi formatına uygun olmayan veya kontrol listesi doldurulmamış olan başvurulan değerlendirilmeye alınmayacaktır.

MAKALE METNİ

Makale Kontrol Listesi Formundan hemen sonra Makale Metni başlamalıdır. Makaleler aşağıda verilen detaylar göz önünü alınarak hazırlanmalıdır.

- Makalenin metin bölümü Times New Roman 12 punto Yazı Tipi karakterinde, Microsoft Office Word 2010 ve üzeri bir kelime işlemci ile hazırlanması ve Microsoft Office Word'un Yazım ve Dilbilgisi bölümünden yazım hatalarının kontrol edilmesi ve düzeltilmesi gerekmektedir.
- Makale tek sütun halinde mümkün olduğunca yalın olarak, 2,5 cm kenar boşlukları kullanılarak A4 sayfasında oluşturulmalıdır.
- Makale düzenlenirken sayfa düzeninin değiştirilmemesi gerekmektedir.
- Satır aralıkları 1,5 olarak ayarlanmalı ve paragraflar arasında bir satır boşluk bırakılmalıdır. Paragraflar öncesi veya sonrasında otomatik aralık bırakılmamalıdır.
- Sayfa geçişlerinde bölüm sonları eklenmemeli ve tüm Makale tek bir bölümden oluşmalıdır.
- Tüm başlıkların yanında İngilizce karşılıkları parantez içerisinde yazılmalıdır.
- Makale metni referanslar dahil araştırma makaleleri için 14.000 kelimeyi tarama makaleleri için ise 22.000 kelimeyi geçmemelidir.
- Tablolar ve Şekiller Dergimizin istemiş olduğu formata uygun olarak hazırlanmadır.
- Makale metni, ana başlıklarla bölümlere ayrılmalı ve her bölüm başlığı numaralandırılmalıdır. Numaralandırma işlemleri ana bölümler için 1.'den başlamalı ve tüm ana başlıklar (Özet, Teşekkür, Kaynaklar ve Ekler bölümleri hariç) için devam etmelidir. İkincil başlıklar ana bölüm numaralandırmasına uygun olarak 1.1., 1.2., 1.3., ... şeklinde devam etmelidir. Üçüncü başlıklar ikinci başlıklara uygun olarak 1.1.1., 1.1.2., 1.1.3., ... şeklinde devam etmelidir.

Örnek bir makale formatı aşağıda verilmiştir:

Kapak sayfası
1. Giriş (Introduction)
2. Malzemeler ve Yöntemler (Materials and Methods)
3. Sonuçlar ve Tartışma (Results and Discussion)
4. Sonuçlar (Conclusions)
5. Simgeler (Symbols)
Teşekkür (Acknowledgment)
Kaynaklar (References)
Ekler (Appendices)

1. Giriş (Introduction)
Detaylı bir literatür özeti, çalışmanın amacını ve kurulmuş olan hipotezi içermelidir. Kaynaklar toplu olarak ve aralıklı verilmemeli (örnek [1-5] veya [1, 2, 3, 5, 8]), her kaynağın çalışmaya katkısı irdelenmeli ve metin içerisinde belirtilmelidir.

2. Malzemeler ve Yöntemler (Materials and Methods)
Yürütülmüş olan çalışma deneysel bir çalışma ise deney prosedürü/metodu anlaşılır bir şekilde açıklanmalıdır. Teorik bir çalışma yürütülmüşse teorik metodu detaylı bir şekilde verilmelidir. Yapılan çalışmada kullanılan metot daha önce yayınlanmış bir metot ise diğer çalışmaya atıf yapılarak bu çalışmanın diğer çalışmadan farklı belirtilmelidir.

3. Sonuçlar ve Tartışma (Results and Discussion)
Elde edilen verilen açık ve öz bir şekilde verilmelidir. Elde edilen tüm veriler literatür ile karşılaştırılmalıdır.

4. Sonuçlar (Conclusions)
Elde edilen verilen açık ve öz bir şekilde verilmelidir. Elde edilen tüm veriler literatür ile karşılaştırılmalıdır.

5. Simgeler (Symbols)
Makalede kullanılan simgeler açıklamalarıyla birlikte alfabetik sıraya uygun olarak düzenli bir şekilde verilmelidir. Kullanılan diğer simgeler alfabetik sıralamadan sonra gelebilir. Gerektiğinde “Yunan Harfleri”, “Alt İndis” gibi alt başlıklar kullanılabilir.

Teşekkür (Acknowledgment)
Makalenin sonunda ve kaynaklar bölümünden önce verilir.

Kaynaklar (References)
- Basılmış kaynakların DOI ve ISBN numarası belirtilmelidir.
- İnternet sitesi adresleri (URL) kaynak olarak verilmemelidir. Ancak metin içerisinde verinin geçtiği yerde veriden sonra belirtilebilir.
- Kaynaklar listesi metin içerisinden kullanılma sırasına uygun olarak numaralandırılmalıdır.
- Kaynaklar, “APA Publication Manual, Seventh Edition” kurallarına uygun olarak hazırlanmalıdır.
- Kaynaklar İngilizce olarak hazırlanmalıdır. Türkçe kaynakların İngilizce karşılıkları köşeli parantez içerisinde belirtilmelidir.

Kaynaklar için örneklere *https://apastyle.apa.org/style-grammar-guidelines/references/examples* adresinden ulaşılabilir.

Kaynaklar için örnekler aşağıda verilmiştir:

- Kaynak bir makale ise: Yazarın soyadı, Adının baş harfi. (Yıl). Makalenin tam başlığı. *Derginin Tam Adı, Cilt no* (Sayı no), makalenin başlangıç ve bitiş sayfa no.

Uysal, İ., Yilmaz, B., Evis, & Z. (2020). Boron doped hydroxyapatites in biomedical applications. *Journal of Boron, 5*(4), 192-201.

- Kaynak yazarı verilen bir kitap ise: Yazarın soyadı, Adının baş harfi. (Yıl). *Kitabın Adı*. (cilt no, varsa editörü). Yayınevinin adı. ISBN veya DOI numarası.

Yünlü, K. (2019). *Bor: Bileşikleri, Sentez Yöntemleri, Özellikleri, Uygulamaları*. [Boron: Its Compounds, Synthesis Methods, Properties and Applications] (2nd Ed.). Aydili Advertising Agency. ISBN 978-605-5310-93-6.

- Kaynak editörü verilen bir kitap ise: Editörün soyadı, Adının baş harfi (Eds.). (Yıl). *Kitabın Adı*. (cilt no). Yayınevinin adı. ISBN veya DOI numarası.

Korkmaz, M. (Eds.). (2020). *Bor ve İnsan Sağlığı [Boron and Human Health]*. Kuban Printing and Publishing. ISBN 978-605-9516-69-3.

- Kaynak kitaptan bir bölüm ise: Bölüm yazarının soyadı, Adının baş harfi. (Yıl). Kitabın Adı. In bölüm editörünün Soyadı, Adının baş harfi (Eds.), *Bölümün Adı* (Varsa cilt no, alıntılanan sayfalar). Yayınevinin adı.

Hakkı, S., & Nielsen, F., N. (2020). Boron and Human Health., Anti-Inflammatory and Anti-Microbial Potentials of Boron in *Medicine and Dentistry* (pp. 67-82). Nobel Academical Publishing, Education, Consultancy Ltd.

- Kaynak basılmış tez ise: Yazarın soyadı, Adının baş harfi. (Yıl). *Tez Başlığı* [Tezin kategorisi, Üniversite]. Tezin kayıtlı olduğu arşiv. Varsa tezin bağlantısı.

Akbaba, S. (2018). *Biopolymer modified polypropylene mesh for hernia treatment* [M. Sc. thesis, Middle East Technical University]. Council of Higher Education Thesis Center (Thesis Number 527833).

- Kaynak kongreden alınmış bir tebliğ ise: Yazarın soyadı, Adının baş harfi. (Yıl). Tebliğin adı. *Kongrenin Adı*, Yapıldığı yer, Tebliğin başlangıç ve bitiş sayfa no.

Akbaba, S., Atila, D., Tezcaner, T., & Tezcaner A. (2018). BİOMED2018-TR *23. Biyomedikal Bilim ve Teknoloji Sempozyumu [BIOMED2018-TR 23rd Biomedical Science and Technology Symposium]*, Turkey, p. 43.

Ekler (Appendices)
Makaledeki ekler EK A (Appendix A), EK B (Appendix B) ve EK C (Appendix C) vb. olarak adlandırılmalıdır. Ekler içerisindeki denklem numaralandırmaları A1, A2, A3 vb. olarak, Tablo ve Şekil numaralandırmaları Tablo A1, Tablo A2, Şekil A1, Şekil A2 vb. olarak adlandırılmalıdır.

Diğer Hususlar

Eşitlik Numaraları: Metin içerisinde eşitlikler Eş. 1, Eş. 2

şeklinde verilmelidir. Eşitlik numaralandırmaları parantez içerisinde (1), (2), (3) vb. olarak, reaksiyon numaralandırmaları (R1), (R2), (R3) vb. olarak numaralandırılmalıdırlar.

Birimler: Metin, şekil ve tablo içerisinde SI birim sistemi kullanılmalıdır.

Şekiller ve Tablolar:

- Tablo içermeyen bütün görüntüler (fotoğraf, çizim, diyagram, grafik, harita vs.) şekil olarak belirtilir.
- Tablo ve şekiller metin içinde geçişlerine göre numaralandırılmalı, bütün tablo ve şekiller ilgili paragraftan hemen sonra verilmelidir. Tablo ve şekillerin her birinin metin içerisinde bahsedildiğinden emin olunmalıdır.
- Tablo başlıkları tablonun üstüne ve şekil başlıkları şeklin altına konulmalıdır. Tabloların ve Şekillerin Türkçe başlıklarından sonra İngilizce başlıkları parantez içerisinde verilmelidir.
- Makaleye eklenecek şekiller (fotoğraf, çizim, diyagram, grafik, harita vs.) mutlaka yüksek çözünürlükte (300dpi veya üstü) olmalıdır. Kabul edilen görüntü formatları jpeg, png, tiff, bmp, eps, wmf, emf veya pdf'dir. Dosya boyutları 1 Mb'tı geçmemelidir.
- Boyutlandırma işlemi orijinal veri üzerinde yapılmalıdır. Eksen başlıkları, etiketlendirme ve açıklamaları (metin kutusu, oklar, üste resim vb. şekilde) Word içerisinde yapılmamalıdır. Grafik, Word belgesine tek bir öge halinde eklenmelidir
- Tablolar resim olarak verilmemelidir. Büyük tabloların tek bir sayfaya sığması tercih edilir. Şekillerde el yazısı kullanılmamalıdır. Renkli fotoğraflar kabul edilebilir ancak baskı siyah-beyaz formata olacaktır. Grafiklerin siyah-beyaz baskıda belirgin olabilmesi için uygun simgelerin kullanılmasına özen gösterilmelidir.

Yapısal Diyagramlar ve Matematiksel Denklemler: Molekül yapılarının yanı sıra matematiksel denklemler metin içinde ait oldukları yerde çizilmiş veya yazılmış olmalı ve ayrı bir satırda gösterilmelidir. Bu molekül yapıları veya matematiksel denklemler sağ yanında ve parantez içinde numaralandırılarak daha sonraki kullanımlarda bu numaralara atıf yapılmalıdır.
Eşitlikler ve denklemler için MS Word Equation Editor fonksiyonu, simgeler için ise MS Word'de Insert/Symbol fonksiyonu kullanılmalıdır.

TELİF HAKKI DEVİR FORMU

Yazıların telif hakkı devri, dergi internet sayfasında sunulan form doldurulup imzalanmak suretiyle alınır. İmzalı Telif Hakkı Devir Formunu göndermeyen yazarların yayınları değerlendirmeye alınmaz.

BENZERLİK ORAN DOSYASI

Makalenizin referanslar bölümü dahil Tam Metni "iThenticate" veya "Turnitin" programları ile taranmalıdır. İlgili programdan alacağınız benzerlik oranı sonucunun PDF formatında sistemimize yüklenilmesi gerekmektedir.

AUTHOR'S GUIDE

1. SCOPE

Journal of Boron; accepts articles in the field of boron, whose qualifications are explained below, in Turkish and English.

Research Article: These are articles that reflect an original research with its findings and results. The study must be original and must contribute to international science.

Scan Article: These are articles that scan a sufficient number of scientific articles, summarize the subject at the current knowledge and technology level, evaluate and compare the findings.

Each article is sent to at least two referees on its subject and has it examined in terms of form, content, original value, contribution to international literature and science / technology. After the deficiencies stated in the referee opinions are completed, the articles that can be published in the journal are brought to the final print format and the approval of the final version of the article is obtained from the authors. The responsibility of the errors that may be found in the article as it is printed in the journal belongs to the authors.

Accepted articles are published free of charge on the journal's website (online) and in print.

2. APPLICATION FORMS

It should consist of five separate forms: Cover Page of Article, Article Checklist Form, Article Text, Copyright Form and Similarity Ratio File. Contact information (address, e-mail, mobile and fixed phone number) of the author and other authors to be contacted during the applications must be given on the cover page.

3. SUBMISSION CHECKLIST

During the application process, authors must check the compliance of their submissions with all the items in the list below, applications that do not comply with this guideline will not be evaluated.

1. The article to be sent has not been published before and/or has not been submitted to any journal for publication.
2. The article was prepared using Microsoft Office Word 2010 or higher word processor.
3. Margins, header and footer spacing and line spacing on the A4 page of the article have been adjusted according to the journal format.
4. Main headings and sub-headings were arranged in accordance with the journal format, together with their English translations.
5. The tables were prepared in accordance with the journal format, they were mentioned in the text and placed in the text section of the work.
6. Figures were prepared in accordance with the journal format, they were mentioned in the text, and placed in the text section of the work.
7. Equation and Reaction numbers were given in order in accordance with the journal format.
8. Original figures were prepared entirely in accordance with the spelling rules.
9. Figure sizes are arranged to fit the format.
10. Figures in the text are numbered consecutively.
11. References are written according to the spelling rules.
12. References are listed consecutively in the text.
13. References are listed at the end of the text, in the order given in the text.
14. It was checked that Turkish Article Title / Abstract / Keywords / Section Titles / Table and Figure titles and English Article Title / Abstract / Keywords / Section Titles / Table and Figure titles are the same.
15. The "Cover Page" containing the title of the work, the names of the authors and contact information was created.
16. The Copyright Form was signed and sent.
17. Possible spelling errors were checked with the word processor's "Spelling and Grammar" check.
18. The original aspect of the article and its concrete contribution to science are written in the "Note to the Editor" field.

4. COPYRIGHTS

The copyright transfer of the articles is taken by filling and signing the Copyright Transfer Form presented on the journal website. After the form is signed, it should be uploaded as PDF in the "upload additional files" section. Works of authors who do not submit this form cannot be published.

5. PRIVACY NOTICE

Names and e-mail addresses on this journal site will be used in line with the stated purposes of this journal and will not be used for other purposes or any other section.

WRITING RULES

GENERAL INFORMATION
An atricle is composed of 5 individual forms which are cover page, article checklist form, article manuscript, copyright transfer form and plagiarism score file. Contact information (address, e-mail address and phone number) of the corresponding author must be given in cover letter.

COVER PAGE
A cover page must be prepared and submitted to journal's webpage as an individual file. Author information will be visibe only to journal editors during initial application.

Title of the article must start with a capital letter and centered to the page. The title must be brief, clear and appropriate for the manuscript. Name, surname, e-mail, affiliation, postal code, city and ORCID number of author(s) must be given below the title.

Title of the article in English: An inclusive and understandable title must be used. The title must start with a capital letter and the rest must be lowercase. The title must be no longer than 15 words including required standard abbreviations.

Title of the article in Turkish: Must be in concorcance with the Turkish title.

Author Names and Address Information: Authors' names and surnames must start with a capital letter. Author names are followed by the institution where the author is affiliated. Uppercase numbers must be used in order to relate the author to the institution. Corresonding author must be denoted with the asterisk sign " * ", after their surname. Address information must include institution, city, postal code and country name. E-mail address must be added after the adddress line for all authors, according to author order.

Abstract: Topic of the article must be summarized without citing the article. An abstrat must not exceed 220 words. Non-standard abbreviations must be explained when used for the first time.

Keywords: Must be placed after abstract. Maximum 5 words must be given with alphabetical order. Keywords must be chosen from explanatory words about the topic. Every keyword must be separated from each other with " , ". Keywords must not include full sentences.

Abstract in English: Must be formed by translating the text in abstract. If decimal are used, " , " must be used for Turkish abstract and " . " must be used for English numbers.

Keywords in English: Must be placed after Abstract in English. Must be in concordance with Turkish keywords. Maximum of 5 words must be written with the alphabetical order, about the topic.

ARTICLE CHECKLIST FORM
It is the form that shows approval of the article manuscript to the journal's writing rules. Article Checklist Form must be filled before submission. Article Checklist Form must be given as the first page of the monuscript. Applications that are not in accordance with the journal's format or submitted without Article Checklist Form will not be evaluated.

ARTICLE MANUSCRIPT
Article Manuscript must be placed after Article Checklist Form. Article manuscript must be prepared by considering details given below.

- Article manuscript must be prepared with Times New Roman font and 12 font size by using Microsoft Office Word 2010 or later version word processor. Misspelings and grammatical errors must be checked and corrected by using Microsoft Office Word's proofing errors section.
- Article manuscript mus be prepared in A4 size page with 2.5 cm margins from each side, as a single column.
- Page order must not be changed when aricle is rewieved.
- Line and paragraph spacing must be set to 1.5 and there must be 1 line space between paragraphs. There must be no automatic line spacing before and after paragraphs.
- There must be no page breaks between pages and whole manuscript must consist of a single section.
- In case the article is in Turkish, translation of all headings must be given in parantheses.
- The manuscript must not exceed 14,000 words for research articles and 22,000 for review articles including references.
- Tables and figures must be prepared according to the journal's requirements.
- The manuscript must be divided into main sections and each section must be numbered. Numbering must start from 1 and go on for all main sections (Except for Abstract, Acknowledgements, References and Appendices sections). Secondary headings must be numbered as 1.1., 1.2., 1.3., etc. in concordance with main headings. Tertiarty headings must be numbered as 1.1.1., 1.1.2., 1.1.3., etc. in concordance with secondary headings.

Manuscript format sample is given below:

Cover page
1. Introduction
2. Materials and Methods
3. Results and Discussion
4. Conclusions
5. Symbols
Acknowledgments
References
Appendices

1. Introduction
Must include detailed literature review, purpose and hypothesis of the conducted study. Contribution of a reference must be examined and placed individually in the manuscript, must not be given collectively.

2. Materials and methods
If the manuscript is for a research article, experimental methods must be explained in an understandible and detailed manner. Theoretical approach must be explained in detail, if a theoretical study was conducted. If the method that was used is already published, related source must be cited and differences must be pointed.

3. Results and discussion
Obtained data must be presented clearly. Data interpretation and literature comparison must be done.

4. Conclusions
Main conclusions of the conducted study must be given birefly.

5. Symbols
Symbols that are used in the manuscript must be given with an alphabeticl order. Other symbols can be given after the alphabetical order. Greek letters and subscripts can be used, if required.

Acknowledgment
Acknowledgements is given after the manuscript and before the references.

References
- DOI or ISBN numbers of published sources must be given.
- Webpages (URL) must not be used as a reference. They can be used only in manuscript after data.
- References must be numbered with the same order as mentioned in the manuscript.
- References must be prepared according to "APA Publication Manual, Seventh Edition" rules.
- References must be prepared in English. English translation of Turkish sources must be denoted with square brackets.

Sample references can be found from the URL address *https://apastyle.apa.org/style-grammar-guidelines/references/examples*

- If the source is an article: Author's Last Name, Initial of Author's First Name. (Year). Article's full title. *Journal's Full Title, Volume number* (Issue number), Page numbers.

Uysal, İ., Yilmaz, B., Evis, & Z. (2020). Boron doped hydroxyapatites in biomedical applications. *Journal of Boron, 5*(4), 192-201.

- If the source is a book with authork: Author's Last Name, Initial of Author's First Name. (Year). *Book's Name*. (Volume number, Editor, if present). Publisher. ISBN or DOI number.

Yünlü, K. (2019). *Bor: Bileşikleri, Sentez Yöntemleri, Özellikleri, Uygulamaları. [Boron: Its Compounds, Synthesis Methods, Properties and Applications]* (2nd Ed.). Aydili Advertising Agency. ISBN 978-605-5310-93-6.

- If the source is a book with editor: Editor's Last Name, Initial of Editor's First Name (Eds.). (Year). *Book's Name*. (Volume number). Publisher. ISBN or DOI number.

Korkmaz, M. (Eds.). (2020). *Bor ve İnsan Sağlığı [Boron and Human Health].* Kuban Printing and Publishing. ISBN 978-605-9516-69-3.

- If the source is a chapter from a book: Chapter Author's Last Name, Initial of Chapter Author's First Name. (Year). Book's Name. In Last Name of Chapter's Editor, First Name of Chapter's Editor (Eds.), *Chapter's Name* (Volume nıumber if present, Pages). Publisher.

Hakkı, S., & Nielsen, F., N. (2020). Boron and Human Health., *Anti-Inflammatory and Anti-Microbial Potentials of Boron in Medicine and Dentistry* (pp. 67-82). Nobel Academical Publishing, Education, Consultancy Ltd.

- If the source is a published thesis: Author's Last Name, Initial of Author's First Name. (Year). *Thesis title* [Thesis category, University]. Archieve that the thesis is registered (Thesis Number). Link to the thesis, if present.

Akbaba, S. (2018). *Biopolymer modified polypropylene mesh for hernia treatment* [M. Sc. thesis, Middle East Technical University]. Council of Higher Education Thesis Center (Thesis Number 527833).

- If the source is from a conference proceeding: Author's Last Name, Initial of Author's First Name. (Year). Name of the proceeding. *Name of the Conference*, Place of the Conference, Proceeding page numbers.

Akbaba, S., Atila, D., Tezcaner, T., & Tezcaner A. (2018). BİOMED2018-TR 23. *Biyomedikal Bilim ve Teknoloji Sempozyumu [*BIOMED2018-TR *23rd Biomedical Science and Technology Symposium]*, Turkey, p. 43.

Appendices
Appendices in the manuscript must be named as AP A (Appendix A), AP B (Appendix B) and AP C (Appendix C) etc. Equation numbering within the appendix must be as A1, A2, A3 etc., whereas Table and Figure numbering must follow as Table A1, Table A2, Figure A1, Figure A2 etc.

Other Issues

Equality Numbers: Equations in the manuscript must be given as Eq. 1, Eq. 2. Equations must be numbered in brackets as (1), (2), (3), etc., and reaction numbers as (R1), (R2), (R3), etc.

Units: The SI unit system must be used in the text, figures and tables.

Figures and Tables:
- All images (photographs, drawings, diagrams, graphs, maps, etc.) that do not contain tables are considered as figures.
- Each table and figure must be numbered according to their transition in the text, and all tables and figures must be given right after mentioned paragraph in manuscript. It must be made sure that each table and figure was mentioned in the text.
- Table captions must be placed above the table and figure captions must be placed under the figure. Table and figure captions must also be noted in English and given in parentheses if the manuscript is in Turkish.
- Figures (photograph, drawing, diagram, graphic, map, etc.) to be added to the article must be at high resolution (300dpi or higher). Accepted image formats are jpeg, png, tiff, bmp, eps, wmf, emf or pdf. File sizes must not exceed 1 Mb.
- The sizing process must be done on the original data. Axis titles, labelling and explanations (such as text box, arrows, picture on top, etc.) must not be added with Word. The plot must be added to the Word document as a single element.
- Tables must not be added as pictures. Large tables are preferred to be fit in a single page. Handwriting must never be used in figures. Although colorized figures are acceptable, printing will be done in black-white for-

mat. Appropriate symbols must be used in order for figures to be prominent in black-white printing.

Structural Diagrams and Mathematical Equations: Mathematical equations as well as molecular structures must be drawn or written where they belong in the text and displayed on a separate line. These molecular structures or mathematical equations must be numbered on the right side and in parentheses for later referring.

MS Word Equation Editor function must be used for equations, and Insert/Symbol function in MS Word for symbols.

COPYRIGHT FORM

Copyright transfer of the articles is taken by filling and signing the form presented on the journal website. The publications of the authors who do not send the signed Copyright Form will not be evaluated.

SIMILARITY RATIO FILE

The manuscript, excluding the references section, must be scanned using the "iThenticate" or "Turnitin" programs. The similarity ratio result received from the relevant program must be uploaded to system in PDF format. It is expected that similarity ratio is not more than 10%.

BOR DERGİSİ
JOURNAL OF BORON
https://dergipark.org.tr/boron

İÇİNDEKİLER/CONTENTS

TENMAK Bor Araştırma Enstitüsü

Dumlupınar Bulvarı (Eskişehir Yolu 7. km), No:166, D Blok, 06530, Ankara
Tel: (0312) 201 36 00
Faks: (0312) 219 80 55
e-mail: boren.journal@tenmak.gov.tr
web:https://dergipark.org.tr/boron